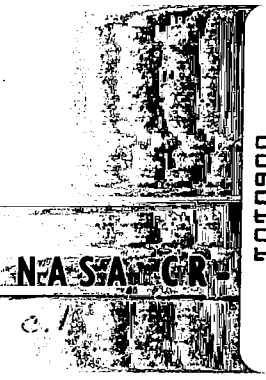

NASA CONTRACTOR REPORT

NASA CR-892

DEVELOPMENT OF A PROTOTYPE PLASTIC SPACE ERECTABLE SATELLITE

by Vincent F. D'Agostino and Preston Keusch

Prepared by
RAI RESEARCH CORPORATION
Long Island City, N.Y.
for Goddard Space Flight Center

NATIONAL AERONAUTICS AND SPACE ADMINISTRATION • WASHINGTON, D. C. • SEPTEMBER 1967

NASA CR-892

DEVELOPMENT OF A PROTOTYPE PLASTIC SPACE ERECTABLE SATELLITE

By Vincent F. D'Agostino and Preston Keusch

Prepared under Contract No. NAS 5-3923 by
RAI RESEARCH CORPORATION
Long Island City, N.Y.

for Goddard Space Flight Center

NATIONAL AERONAUTICS AND SPACE ADMINISTRATION

For sale by the Clearinghouse for Federal Scientific and Technical Information
Springfield, Virginia 22151 – CFSTI price $3.00

TABLE OF CONTENTS

TABLE OF CONTENTS (Continued)

TABLE OF CONTENTS (Continued)

LIST OF TABLES

LIST OF TABLES (Continued)

LIST OF ILLUSTRATIONS

LIST OF ILLUSTRATIONS (Continued)

LIST OF ILLUSTRATIONS (Continued)

LIST OF ILLUSTRATIONS (Continued)

ABSTRACT

This report describes the work done and conclusions resulting in the development of procedures and data for construction of a prototype space erectable plastic passive communications satellite of spherical design with a diameter of 425 ft. using the plastic memory effect. Research under this contract has resulted in the development of a crosslinked polyethylene metal laminate weighing 1.58×10^{-3} lbs./ft.^{2} (resulting in a satellite weight of 896.6 lbs.) and capable of withstanding solar pressures when fabricated into a sphere with a 425 ft. diameter. Experimental data and theoretical calculation indicate that a 0.30 mil perforated polyethylene film electrolessly plated with 15×10^{-6} inches of copper on both sides would be satisfactory to withstand buckling pressures within the weight conditions specified.

Prototype items were constructed and delivered following a detailed testing program on the various materials used in construction. Additionally, the procedures necessary for the scale-up and production of a 425 foot diameter spherical passive communications satellite were investigated in this study. Recommendations for construction are detailed in this report. The results of the testing program and the building of the deliverable items (cap section, cylinders and flat sections) show that the crosslinked polyethylene copper laminate film developed under this contract is satisfactory for building large, self-erectable satellites. Although it was not possible to conclusively demonstrate the plastic memory effect, in a 1-g field, on thin polyethylene (sub-mil) film models, the memory effect has been demonstrated on a 15 mil

polyethylene mesh. Other tests (not using models) and based on firm theoretical grounds substantiate the existence of the memory effect in thin film polyethylene.

It is recommended that an experimental 0-g deployment study be undertaken to conclusively demonstrate the plastic memory effect on thin polyethylene film in the absence of a gravitational field. Another area requiring investigation to complete the goals of the overall program is a thermal control study, since it was not included in the scope of this program.

1.0 INTRODUCTION

1.1 General

The scope of this contract and the sequence of the investigations undertaken during this program are presented in this section. The objective of this program was to develop a polyethylene film with an area weight of less than 1.72×10^{-3} lbs./ft.^{2} which was capable of withstanding five times solar buckling pressure when fabricated with a sphere of 425 ft. diameter. This program is a change in emphasis from the initial program NASr-78 which was primarily concerned with an investigation of the mechanism of the memory phenomenon and the memory forces. In addition to the development of a light-weight film the material developed here was also required to act as a reflector of RF frequency (90-95% reflectance at 8-9 GHz frequencies). The material must, therefore, receive a metal coating and exhibit a resistance of less than 2 ohms/square.

Included in the scope of this investigation was a continuing clarification of the mechanism of the memory phenomenon. All these objectives have been accomplished.

The materials investigated under this contract included polyethylene meshes and films of various densities and thicknesses. The film materials were laminated by electroless plating with various thicknesses of copper and buckling pressure calculations were undertaken to determine the proper laminate thickness necessary to withstand five times solar pressure. Results showed that a laminate of 0.30 mil polyethylene and 30×10^{-6} in. (15×10^{-6} in. on both sides of the film) of copper met the weight and strength qualifications. Studies were then performed on film perforation and film extraction as a means of decreasing

the film weight. Studies eliminated the possibility of lowering the weight of film by extraction. It was found, however, that the film could be perforated to 40% open area while retaining its required physical resistance to solar buckling pressure.

Upon completion of the above-mentioned studies a production study program was undertaken to produce a perforated polyethylene film laminated with copper. The steps in the production program were as follows:

1. Film extrusion (blown film).
2. Irradiation of the extruded film.
3. Heat treatment (annealing) of the irradiated film.
4. Perforation of the annealed film.
5. Electroless plating.

A detailed experimental testing program was subsequently undertaken on the laminated material. Results showed that the production material was suitable for the construction of a large passive communications satellite.

As part of the overall program a number of deliverable items were constructed to be used for radio-frequency tests by NASA. The items constructed and delivered were as follows:

1. A 24 ft. chord diameter spherical cap section of 212 ft. radius of curvature (mesh).
2. Seven cylinders 7.5 in. diameter x 1 ft. length (mesh and film).
3. Six flat sections (4' x 6') (mesh and film).

With the completion of the deliverable items and the testing program, recommendations and procedures for the scale-up, production and packaging of full size passive communications satellites were determined. These included a determination of

the five steps listed above plus:

6. Cutting of gore sections.

7. Ultrasonic bonding.

8. Packaging.

The final phase of this program was a study of the memory forces in thin film as a means of clarifying the mechanism of the memory phenomenon. Difficulty was encountered in demonstrating the memory effect on thin gauge polyethylene models since gravitational and air circulation forces both exceeded the memory force and acted to resist its effect. After evaluation of numerous methods it was shown that the memory effect could be observed for heavy mesh material. The transition of the observation of the memory phenomenon to thin film was finally shown by use of tensile test data above the crystalline melting point (T_m) of the polyethylene. This procedure which conclusively proves the existence of the memory effect on thin gauge film is based on a firm theoretical background developed for rubber elasticity. The results obtained prove the existence of memory in a "1-g" environment. Extrapolation to a 0-g environment cannot be rigorously proven but since the removal of gravity forces should not change the elastomeric forces it is intuitively concluded that this system will operate in a 0-g environment.

1.2 History

1.2.1 Memory Effect Background

The memory effect induced in polyethylene by irradiation of plastic with either beta or gamma radiation was first noted by Charlesby[1] in his book, "Atomic Radiation and Polymers" wherein he describes the memory phenomenon as

"an interesting and often amusing property of lightly irradiated polyethylene". He notes further that the memory phenomenon "relies on the fact that on irradiation a crosslinked network is formed with a definite equilibrium state. When other constraints such as crystallinity or external stresses are removed, the polymer will return to the same molecular arrangement it had during radiation". The memory effect will be discussed more fully in a subsequent section of this report.

The application of this plastic memory effect to the development of a space structure was first proposed by R A I in 1961. This resulted in a preliminary study of the phenomenon under contract to the National Aeronautics and Space Administration. The scope of work under this contract, although empirical in nature, was directed toward an investigation of the mechanism of the memory phenomenon to permit adaptation of the process to development of erectable space structures. To this end the following was investigated:

1. The magnitude of the restoration forces exerted by irradiated sheet material (40 mils) during the process of restoration to the undeformed state.

2. The degree of completeness with which memory occurs as a function of the T_m (i.e., the crystalline melt temperature of the polymer).

3. The conditions required to change the minimum restoration temperature at which complete restoration could be effected were also studied by an evaluation of polyethylene and copolymers of polyethylene.

The emphasis of this effort was, therefore, a study of all the factors noted above on sheet and to a limited extent

on mesh material. A summary of results of this study is given below. By degree of restoration referred to below is meant the extent of recovery of a deformed article to its original configuration. The "NT" deformation term refers to deformation of a sample of crosslinked polyethylene at a temperature below the melt temperature of the crystalline melting point. At this stage the polyethylene is Non-Transparent. The T deformation refers to deforming a polyethylene sample after it has been heated above its crystalline melting point (T_m). At this temperature the plastic is Transparent.

The results from contract NASr-78 on degree of restoration and the restoration were as follows:

1.2.1.1 Degree of Restoration

a. The deformation conditions were found to have no effect on the degree of restoration. Complete restoration occurs under a variety of deformation conditions if the restoration temperature is above the crystalline melting point of the polymer.

b. The restoration conditions are of major importance in controlling the degree of restoration of deformed polyethylene. For restoration to be complete, the polyethylene must be heated to transparency (i.e., above its normal T_m). For high density polyethylene, this temperature is ca. 130-135°C.; for low density, the required temperature is ca. 105°C. Polyethylene copolymers containing 15% or more ethyl acrylate or vinyl acetate were found to require lower minimum restoration temperatures than the homopolymers since their T_m values were lower. Thus, the various acrylate and acetate copolymers studied restored at temperatures of 65-90°C.

c. Unirradiated and irradiated polyethylene behave very similarly at deformation temperatures below T_m. Above T_m, unirradiated polyethylene melts and flows and, thus, memory cannot be observed.

d. Radiation dose does not control the degree of restoration above the minimal dose of ca. 5-10 Mrads for a polyethylene of $\overline{M}_w$ of at least 70,000.

e. Polyethylene density affects the degree of restoration only insofar as it affects the normal crystalline melting point of the polymer (see paragraph c above). Low density grades restore the completion at lower temperatures than high density grades.

f. Initial molecular weight, above a certain minimum, is not a factor in controlling the degree of restoration; however, this is closely related to the radiation dose (see paragraph d above). A 10 Mrad dose to a polyethylene of $\overline{M}_w$ of ca. 70,000 gives complete restoration.

g. Storage of NT deformed specimens at -78°C. will prevent creep which is common at ambient temperatures and retarded at -15°C.

h. Moulding and extrusion-induced stresses and strains in polyethylene complicate the memory effect studied on this project. Such complications can, however, be minimized by annealing techniques.

i. Vexar polyethylene mesh behaves exactly similar to polyethylene sheet as regards the memory effect.

j. The acrylate and acetate copolymers of polyethylene exhibit the memory effect as does polyethylene.

1.2.1.2 Restoration Force

a. Deformation conditions greatly influence the restoration force. NT deformed polyethylene has much greater restoration forces than T deformed polyethylene.

b. The restoring force increases with radiation dose for both T and NT deformed polyethylene.

c. The restoring force for NT deformed polyethylene increases with increasing polymer density and T_m.

d. The restoring force increases with increasing molecular weight (as measured under T deformation conditions).

e. The restoring force is proportional to the square of the polyethylene thickness for NT deformed polyethylene over the 20-60 mil thickness range.

f. Quenching and moulding conditions do not appear to affect the restoring force.

g. The presence of ZnO or $CaSiO_3$ fillers in the polyethylene prior to irradiation lowers the restoring force.

The results of the original effort (contract NASr-78) describes the memory force in plastics at various temperatures in terms of both a plastic (NT) and elastic (T) memory. It is noted from these results that the complete restoration of an irradiated article to its undeformed configuration is observed only above the T_m when the total memory force is due only to an elastic memory. It is for this reason that the work under the current contract was only concerned with T deformation, i.e., memory above the crystalline melting temperature, where complete restoration is observed.

The prime emphasis of the current contract was directed toward a study of materials for development of

engineering data for design purposes. This data has been developed and is given in subsequent sections of this report.

1.2.2 Memory Phenomenon in Polyethylene

Prior to a discussion of the research conducted under Contract NAS5-3923, a description of the memory phenomenon and the current theory of how it functions will be given.

The observed memory effect in polyethylene is composed of both a plastic and an elastic memory. The plastic memory is observed below the crystalline melting point of the polymer under investigation while the elastic memory is observed above the crystalline melting point. The elastic memory is only observed when the polymer in question is crosslinked, i.e., has a three-dimensional character. All thermoplastics, in the engineering sense, may show a plastic memory which is due to crystal forces induced during moulding or extrusion processes but they will not show an elastic memory since on heating above their crystalline melting point (T_m) the polymers will exhibit flow characteristics and, therefore, lose their moulded forms. An additional disadvantage of the induced plastic memory was noted previously. The restoration of deformed articles via the plastic memory force (i.e., NT deformation) was shown to be incomplete and dependent on the temperature. The closer the restoration temperature approached the T_m of the polyethylene, the more complete was the degree of restoration. The plastic memory force was shown to be a relatively strong force which decreases with increasing temperature. At the T_m of the plastic the plastic memory force is zero. Additionally, it was noted that an article below its T_m will offer an increasing resistance to folding as the temperature is increased and if

folded significantly below its T_m will not retain its packaged configuration during storage.

The development of space erectable structures can be accomplished with excellent precision by taking advantage of the elastic memory force. The operational steps in the development of the memory force in plastics are accomplished as follows:

1. A thermoplastic (polyethylene) having a crystalline structure is irradiated in a predetermined configuration. The irradiation is conducted using either beta or gamma radiation.

2. The irradiated object is then heated above its crystalline melting point (T_m) and in this state it is folded and packaged.

3. The folded or packaged object is allowed to cool permitting the crystal structure to develop. This configuration is then retained indefinitely by virtue of the crystal forces.

4. Upon reheating the object above its crystalline melting point, it will return to the configuration it had during irradiation.

Investigation of this phenomenon under the current contract has confirmed that the "memory" or restoration force is an elastic force and further, that it can be measured by a determination of the modulus of elasticity (E) above the crystalline melting point (T_m) of the plastic. This finding shows that the memory force is in reality an elastic force and that the memory phenomenon is due to polyethylene (or other thermoplastic) exhibiting elastomeric properties above the crystalline melting point, which now permits a rigorous determination of the magnitude of the restoration forces in

very thin film.

In unirradiated thermoplastics, i.e., linear polymers, once the T_m is exceeded the plastic exhibits permanent flow properties and the memory phenomenon is not observed. Irradiation of a thermoplastic, however, causes the development of crosslinks in the thermoplastic thereby changing the linear structure to a three-dimensional network. Radiation in effect vulcanizes the plastic and makes it an elastomer. The elastomeric properties, however, are not observed at temperatures below T_m because the crystalline force is much greater than the memory force. When the crystalline force is eliminated by exceeding the crystalline melting point, the memory force is observed.

From the theory of rubber elasticity the modulus of a rubber material is given by:

$$E = 3vkT \quad \text{(ref. 2)} \qquad (1)$$

where k = Boltsman constant
T = absolute temperature (above T_m).
v = number of chains per unit volume

$$= \frac{\rho N}{M_c}\left[1 - \frac{2M_c}{M_n}\right]$$

ρ = density
N = Avagadro's number
M_c = Molecular weight between crosslinks
M_n = Number average molecular weight of chain

Using this expression, the parameters involved in the development of the memory force can be investigated. This will be discussed more fully in Section 5.0 of this report.

The M_c noted above can be determined by application of the Flory equation:

$$v^{5/3} = (0.5 - \mu)M_c/\rho_v \quad \text{(ref. 3)} \qquad (2)$$

where μ = polymer solvent interaction parameter
v = molar volume of the solvent
ρ = density
M_c = molecular weight between crosslinks.

The results of our studies show that the memory phenomenon observed in polyethylene is part of the general phenomenon of elastomeric recovery of rubber. It also indicated that the memory effect observed in polyethylene via application of radiation crosslinking should be evident in other crystalline polymers. The memory observed in polyethylene can be thought of as due to the same forces as the elastic forces studied in rubber. In the case of rubber, the crystal structure is not evident at room temperature because the T_m of rubber is well below room temperature. If a rubber ball is deformed under load and then cooled with dry ice and acetone the deformed state is "set" in the rubber. As long as the temperature is kept below the crystalline melting point of the crystal structure developed in the rubber by the low temperature, the ball will maintain its deformed configuration. On removing the dry-ice acetone environment and warming the ball to room temperature, the crystals melt and the deformed ball returns to its original configuration. This observation of the memory phenomenon in rubber is the same phenomenon we observe in polyethylene, the only difference being a shift in the temperature scale at which the phenomenon is observed.

The results of this theory also indicate that the memory effect can be induced in other plastics provided that (1) the plastic has a crystal structure, (2) the plastic can be crosslinked by either chemical or radiation means, and (3) the crosslinks do not degrade when heated to the crystalline

melting point of the polymer.

To substantiate the above, polypropylene was irradiated and shown to exhibit a memory. Further, a copolymer of polyethylene-ethyl acrylate was crosslinked by chemical means and showed to exhibit a memory. These findings were observed only once and development of the memory effect via chemical crosslinking would require a full research program. It would be an extremely fruitful area of research since other plastics such as nylon, polyimides, polysulfones, polycarbonates, etc. and other structural polymers can be given an elastomeric character by crosslinking them. These materials should then exhibit this elastomeric character at their respective T_m values.

1.2.3 Background on Materials Selection

With the mechanism of the plastic memory effect established, a search was undertaken to find a polyethylene material that could be used to construct a 425 ft. diameter spherical passive communications satellite. The main requirements specified for the satellite are that it weigh less than 1000 lbs., have a surface resistance of less than 2 ohms/sq. for required radio-frequency characteristics and be able to resist buckling from solar pressure. These requirements then necessitate the material to be light in weight, capable of being metallized and to have reasonable strength. For this work it was necessary that the material be polyethylene since its memory effect was thoroughly investigated.

The first material investigated was 8 - 14 mil polyethylene monofilament. It was expected that the monofilament could be woven into a fabric and that the satellite would then be constructed from this fabric. The use of a monofilament was

quickly eliminated in the course of testing due to its poor dimensional stability. In the course of a memory cycle a material must be heated to initiate restoration. It was found that upon heating the monofilament shrunk considerably in its longitudinal direction due to residual stresses induced in the strand during processing. The results of the shrinkage tests are shown in Table 1 below.

Table 1

Dimensional Stability of Polyethylene Monofilament with Respect to Heat Treatment

	l_i (cm.)	l_f (cm.)	$\Delta l/l_i$ (%)	d_i (mils)	d_f (mils)	$\Delta d/d_i$
LDPE[1]						
Unannealed	23.80	2.55	-89	8.8	27.0	107
Ann. & Irr.	12.45	4.15	-67	12.0	20.7	73
Irr. & Ann.	12.35	4.10	-67	12.2	21.1	74
HDPE[2]						
Unannealed	24.25	1.40	-94	13.4	61.2	257
Ann. & Irr.	19.05	3.90	-80	13.2	34.2	159
Irr. & Ann.	21.65	3.25	-85	13.4	35.1	162

[1]Vectra low density polyethylene

[2]Vectra high density polyethylene

l_i = initial length
l_f = final length
d_i = initial diameter
d_f = final diameter

It can additionally be seen from the above table that even crosslinking the material before heating does not eliminate the shrinkage sufficiently to warrant further evaluation of this material.

The next material investigated was a commercially available polyethylene mesh. The mesh, Rexwell MX 44 and MX 46 was manufactured by the Rexall Drug & Chemical Co. In Rexall's manufacturing process cross-strands are molded perpendicular to continuously extruded longitudinal strands. Manifestly, the incorporation of extruded and molded filaments into a mesh structure may be expected to give rise to anisotropic physical properties. Although the mesh was too heavy (area weight of 39.6×10^{-3} lb./ft.^{2} compared to an area weight of 1.72×10^{-3} lb./ft.^{2} required for a 1000 lb. weight) for the construction of the actual satellite, it did possess many of the properties that the design specifications called for and was therefore used in an initial testing program to investigate the feasibility of the following three operations (to be detailed in a later section discussing the production scheme): (1) metallization, (2) irradiation (commercial scale), and (3) bonding, necessary for the satellite fabrication using any polyethylene material. The salient features of the Rexwell mesh are presented in Tables 2 and 3 below.

Table 2

Dimensional Stability of Rexwell Mesh

Operation Performed on Mesh	Dimensional Changes (%) Length (Parallel to ED)	Dimensional Changes (%) Width (Perpendicular to ED)	Thickness (mil)
Annealing*	-2.5 ± 0.2	-2.2 ± 0.9	+3.4 ± 1.6
Irradiation of annealed stock			
16.6 Mrads	0.0	-0.6 ± 0.7	0.0
34.5 Mrads	0.0	-0.6 ± 0.8	0.0
48.8 Mrads	0.0	-1.1 ± 0.7	0.0
Heat Treatment of annealed, irradiated stock			
16.6 Mrads	-2.2	-5.0	+6.1
34.5 Mrads	-1.3	-3.3	+4.9
48.8 Mrads	-0.9	-3.3	+2.5
Heat Treatment of unannealed, irradiated stock			
15 Mrads	-4.4	-4.8	+8.0

*Temperature: 125°C.
Time: 3 hrs.

Table 3

Properties of Processed Rexwell Mesh
(MX 44 Thickness = 28 mils
Density = 0.96 gm./cc.
T_m = 140°C.)

Direction (degrees)	Area Weight ($lb./ft.^2 \times 10^{-3}$)	F_y (lbs.)	ϵ_y (%)	E ($psi \times 10^3$)	G ($lb.\frac{in.}{in.^2} \times 10^{-5}$)	R_{sq} (Ω/sq.)
Unprocessed Mesh						
0	39.6	10.9±0.5	7.0±0.8	72±8	996±131	-
45	39.6	12.0±0.4	27.7±3.8		1248±317	-
90	39.6	14.0±0.8	8.4±1.4	59±7	2316±667	-
Irradiated (15 Mrad)						
0	39.6	11.7±0.6	7.2±1.2	66±9	1464±199	-
45	39.6	11.9±0.3	25.0±1.5		1548±204	-
90	39.6	15.6±1.4	7.2±1.8	70±14	2660±808	-
Irradiated-Heat Treated Mesh (145°C., 2 hrs.)						
0		12.9±1.2	7.5±1.7	80±20	1608±133	-
45		13.1±2.0	42.0±2.0		1728±126	-
90		18.8±1.7	9.2±3.0	69±25	3740±432	-
Irradiated-Heat Treated-Plated Mesh						
0	41.2	15.7±0.7	5.0±0	123±6	1891±395	0.52±0.19
45	41.2	13.0±0.3	40.0±0		2419±329	
90	41.2	19.4±0.9	7.5±1.7	81±18	4973±870	0.70±0.25

Table 3 (Continued)

Direction (degrees)	Area Weight ($lb./ft.^2 \times 10^{-3}$)	F_y (lbs.)	ϵ_y (%)	E ($psi \times 10^3$)	G ($lb.\frac{in.^2}{in.}$)	R_{sq} (Ω/sq.)
Irradiated-Heat Treated-Plated-Bonded Mesh*						
0		8.6 ± 1.0	4.6 ± 0.5	75 ± 17	-	-
90		15.9 ± 0.6	7.0 ± 2.0	77 ± 22	-	-
Irradiated Heat Treated-Plated-Bonded Mesh**						
0		8.8 ± 2.9	4.0 ± 0.3	95 ± 19	-	>10 <150
90		15.3 ± 2.3	5.0 ± 1.0	86 ± 13	-	>10 <300

*Copper removed from bonded area with nitric acid.

**Copper not removed from bonded area.
Instron Tensile test: strain rate 2 in./min., ambient temperature. Flexural rigidity determined by Standard ASTM D 1388-551. (Tensile Test see Appendix I, Flexural Rigidity Tests see Appendix IV)

Legend:
F_y = Yield force (highest force in linear portion of stress strain curve per inch of material).
ϵ_y = Yield strain (strain corresponding to yield force).
E = Modulus of elasticity.
G = Flexural rigidity.
R_{sq} = Surface resistance.

From the results of the mesh testing program as summarized in Tables 2 and 3 and Figure 1 it has been concluded that: (1) polyethylene can be suitably metallized for radio-frequency characteristics by a commercially available* electroless plating process. A maximum resistance of 2 ohms/sq. is specified. The experimental results give a resistance of 0.5-0.7 ohms/sq. (2) Commercial irradiation equipment can satisfactorily irradiate the polyethylene mesh without degrading it. In fact, a small increase in strength is realized after irradiation. (3) The irradiated mesh which is crosslinked can be adequately ultrasonically bonded. It can be seen that on the average the plated, bonded mesh is as strong as the unbonded material.

It is also important to note that the metallized mesh is approximately twice as rigid as the unprocessed mesh. This consideration is of importance in establishing a required rigidity to withstand solar pressures. Since only 10×10^{-6} in. of copper was able to increase the rigidity of an unplated mesh it means that small thicknesses of copper can replace large thicknesses of polyethylene to achieve an improved rigidity at a lower total weight.

Table 3 and Figure 2, photomicrograph D additionally show that electrical continuity across an ultrasonic bond is not maintained. It seems that the ultrasonic welding action cracks the copper near the bond causing a loss of continuity. If electrical continuity is desirable across the bonds, on the satellite, it will be necessary to coat the bonds with a small amount of a conductive lacquer.

*The Enthone electroless copper plating process which is detailed in Section 4.1.5.1.

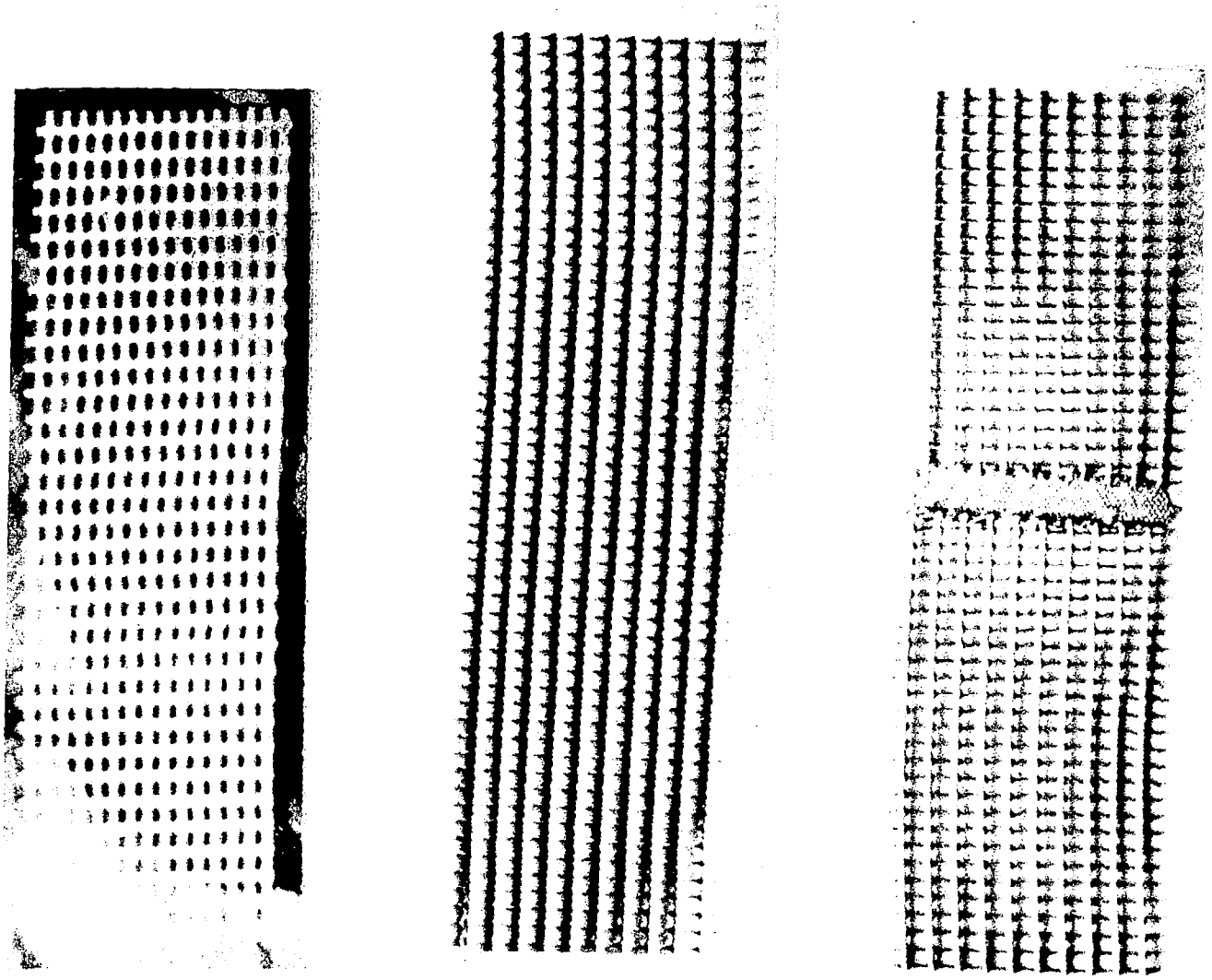

A B C

Figure 1 PHOTOGRAPHS OF REXWELL POLYETHYLENE MESH (1.9x)

A) Unprocessed
B) Electrolessly Plated (10 x 10^{-6} in. Copper)
C) Plated Bonded

Figure 2 PHOTOMICROGRAPHS OF REXWELL MX-44 PLATED MESH (200X)

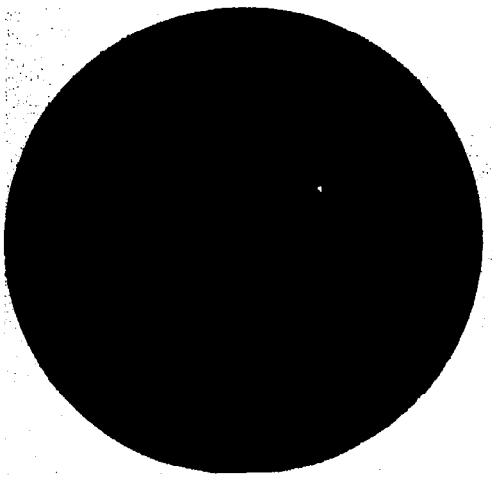

A
PLATED-UNTOUCHED

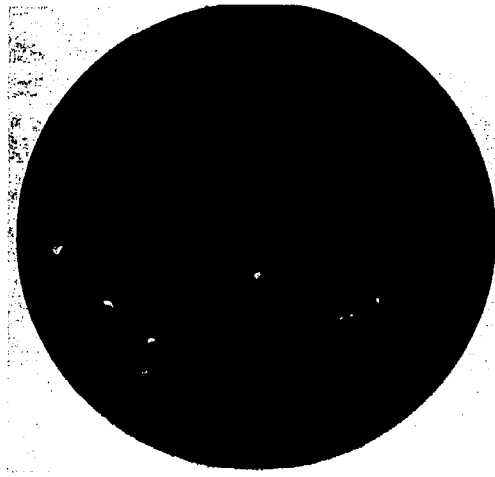

B
PLATED-PULLED TO LOSS OF CONTINUITY

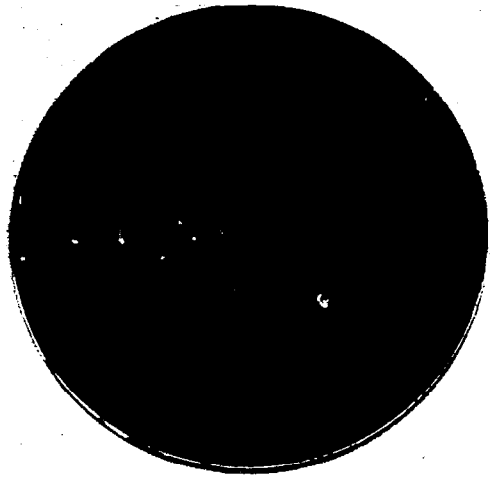

C
BEND RADIUS-PULLED TO LOSS OF CONTINUITY

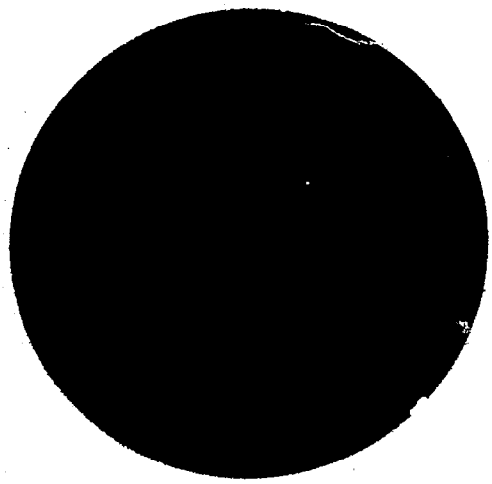

D
PLATED-BONDED (AT BOND)

E
PLATED-BONDED AT LOSS OF CONTINUITY
(AT BOND)

The final material investigated was polyethylene film. The type of film looked for was one that could be produced in various thicknesses, all of which were less than 1 mil and biaxially oriented. Ordinary polyethylene film is uniaxially oriented and has poorer physical properties in the direction perpendicular to extrusion than in the direction of extrusion. Thus, a biaxially oriented polyethylene film was custom-made to meet the above conditions. The film is a biaxially oriented, intermediate density polyethylene film manufactured by Sea Space Systems, Inc., Torrance, California. Due to scheduling and procurement problems, mainly based on funding and time limitations, it was decided to use this 1 mil, intermediate density biaxially oriented polyethylene film* for the construction of the deliverable items and for preparing samples for the testing program. The properties of the film are listed in Table 4.

A research and design study later showed that a 0.30 mil film would be adequate for the satellite in question. Results show that the intermediate density polyethylene film possessed superior strength compared to a similar low density film and that this material was also a superior acceptor of an electroless copper plate. Following this testing, fabrication of test models was initiated using the 1 mil material. It should be kept in mind that 0.30 mil material would be used in the actual fabrication of the 425 foot diameter passive communications satellite. It must be noted that test results obtained on the 1 mil material can be safely extrapolated to an 0.30 mil material since both materials would be made out of the same

*From hereon in called "PE 12"

Table 4

Physical Properties of Sea Space Intermediate Density, 1 Mil, Biaxially Oriented Polyethylene Film (PE 12)

Direction (degrees)	σ_y (psi x 10^3)	σ_u (psi x 10^3)	E (psi x 10^3)	T_m (°C.)	ρ (gms./cc.)	M_n
0	0.94 ± 0.03*	2.35 ± 0.13	29.2 ± 2.2			
45	0.87 ± 0.04	2.00 ± 0.11	26.2 ± 1.5	116.5**	0.931***	16,000
90	0.94 ± 0.04	1.65 ± 0.07	33.2 ± 3.2			

σ_y = Yield Stress

σ_u = Ultimate Stress

E = Modulus of Elasticity

T_m = Crystalline Melting Point

ρ = density

M_n = Number Average Molecular Weight

* All tensile tests performed on a Table Model Instron with a strain rate of 2 in./min., 5 lbs. full scale load. Full tensile testing procedures discussed in Appendix I.

** The average result of three crystalline melting tests presented in Appendix II.

*** The average of the density given by the manufacturer and tests run on density gradient apparatus described in Appendix III.

resin and would have the same processing history and the only difference would be in thickness.

Sea Space's biaxially oriented polyethylene films are produced in a cylindrical extruder with an annular tube of polyethylene film emerging from the dies. The tube is blown with air from the inside creating a pressure in the tube. The complete details of the production of biaxially oriented film is spelled out in detail in another NASA report.[4] The biaxial orientation results from the fact that internal pressure produces membrane stresses in the film in the radial direction (transverse direction, 90° direction). This is in addition to the usual stresses created in the machine direction (extrusion direction, 0° direction) due to the fact that the film is being drawn out of the extruder under stress.

2.0 MATERIAL PROPERTIES DEVELOPMENT PROGRAM

Prior to specifying the required properties of the film to be used in construction of the 425 foot diameter satellite the three areas indicated below were critically investigated.

1. Extraction Study - This study was undertaken in an attempt to decrease the weight of crosslinked polyethylene film to be used for construction of the sphere without detracting from the film's physical properties. To this end the low weight fractions of crosslinked polyethylene were extracted with a suitable solvent to lower the area weight of the crosslinked film.

2. Development of a Laminate - Calculations and preliminary tests indicated that the stiffness of copper metallized polyethylene film increases dramatically with the addition of a small weight fraction of a copper plate to the total film weight. The effects of varying the thickness of copper metallized to varying thicknesses of polyethylene were therefore critically investigated to obtain a laminate of low weight and high stiffness.

3. Perforation Study - The deployment of a space structure via the memory effect has a distinct advantage over deployment mechanisms using inflatants. This advantage is due to the ability of deploying film which is perforated. The use of perforated film is two-fold, it decreases the effect of solar pressure, and materially decreases the weight of the deployed sphere. Therefore, because of the importance of perforation a thorough study was conducted on the effect of perforation on laminate weight, stiffness and electrical resistance.

2.1 Extraction Study

The primary goal of the extraction study was to develop a polyethylene film with an E/ρ value higher than currently

available. To this end, polyethylene film was irradiated to from 5 - 75 Mrads using beta radiation to impart varying degrees of crosslinking. It was subsequently extracted in a suitable solvent.

The modulus of elasticity, E, and density, ρ, of the extracted film were then measured and compared with unextracted and unirradiated material. Test results showed that the crosslinked, extracted polyethylene did not improve the strength sufficiently, to realize any significant increase in E/ρ. Additional work incidental to the extraction study yielded valuable information regarding minimum radiation dosage required for crosslinking and the effect of dosage on the strength of extracted polyethylene.

2.1.1 Variation of Strength with Dose

Instron tensiles have been determined on samples of 1 mil standard density polyethylene film irradiated to from 5 to 75 Mrads. The results, see Table 5, indicate only modest changes in E. In fact, in some cases a slight decrease with dose in the 0° direction is observed.

2.1.2 Solvent Tests

Samples of unirradiated polyethylene were extracted for one day in the various solvents at $100^{\circ}C. \pm 2^{\circ}C.$ The results of these tests are listed in Table 6 below.

These results indicate that solvents with little or no polarity are the best solvents for extracting polyethylene which is itself mainly a saturated substance. The solution of the polyethylene at $100^{\circ}C. \pm 2^{\circ}C.$ by the first three solvents indicate that they are very acceptable solvents for polyethylene extractions. Xylene was used in all subsequent extraction experiments.

Table 5

Effect of Radiation* Dose on the Strength** of 1 Mil Standard Density Sea Space Polyethylene Film

Dose (Mrads)	0 degrees Modulus of Elasticity, E (psi x 10^{+3})	90 degrees Modulus of Elasticity, E (psi x 10^{+3})
0	26.3 ± 2.9	20.4 ± 4.9
5	23.8 ± 1.7	38.6 ± 1.3
10	23.8 ± 1.6	31.7 ± 1.9
15	31	40
20	25.5 ± 1.7	35.1 ± 2.1
30	18.5 ± 1.7	26.5 ± 2.2
40	30.7 ± 0.9	35.5 ± 0.4
50	24.3 ± 1.2	36.6 ± 1.0
60	29.8 ± 1.6	39.4 ± 2.5
70	23.5 ± 1.0	27.8 ± 1.1
75	22.4 ± 1.0	29.0 ± 0.3

* Irradiated in Nitrogen, Heat Treated in Nitrogen

** Determined by Instron Tensile Test.
Strain rate: 2.0 in./min.
Temperature: room temperature

Table 6

Extraction Efficiency of Various Solvents on Polyethylene

Solvent	Type	% Extracted*
Decalin	Unsaturated	99.23
Tetralin	Saturated	99.19
Xylene	Aromatic	99.08
O-Dichlorobenzene	Aromatic-Polar	83.74
Butyric acid	Polar	4.92
Dimethyl formamide	Polar	0.98
Dimethyl sulfoxide	Polar	-0.19

* % Extracted = % dissolved

2.1.3 Extraction

The low molecular weight fractions in the irradiated polyethylene film samples were extracted in xylene at 100°C. over 4 days. The 4-day time was selected since other studies at these laboratories[5] indicate this would insure complete extraction of uncrosslinked material. In addition, the anti-oxidant n-beta-phenylnaphthylamine was added to each solvent to retard oxidation of the polyethylene during extraction.

2.1.4 Gel Fractions

As part of the extraction study and in general for all irradiation crosslinking done in the contract it was necessary to know at what doses crosslinking occurred. The most effective way of determining the effect of irradiation on the crosslinking of a polymer is to determine its gel fractions, i.e.,

$$\frac{\text{weight of non-extractible material}}{\text{weight of unextracted material}} = \frac{\text{wt. gel}}{\text{wt. sol}}$$

The gel fractions obtained after extraction of samples irradiated to various doses are plotted in Figure 3. It can be seen from the curve that pronounced gelation (crosslinking) occurs after 10 Mrads of irradiation. This result gives further verification that a dose of 15 Mrads is satisfactory for sufficient crosslinking. The curve furthermore shows that at ca. 75 Mrads the materials approach a constant maximum gel of 85%.

2.1.5 Strength Dose Variations of Extracted Material

Tensiles have been determined on samples of 1 mil standard density polyethylene film given various doses of irradiation and were then extracted. The resulting tensile tests obtained on samples parallel to the extrusion (i.e., 0° direction) are given in Table 7 and in Figure 4.

Figure 3 GEL FRACTIONS OF IRRADIATED POLYETHYLENE FOR VARYING RADIATION DOSES

Irradiation: Nitrogen Atmosphere
Heat Treatment: Nitrogen, 100°C.
Samples Aged Approximately 1 Month After Irradiation

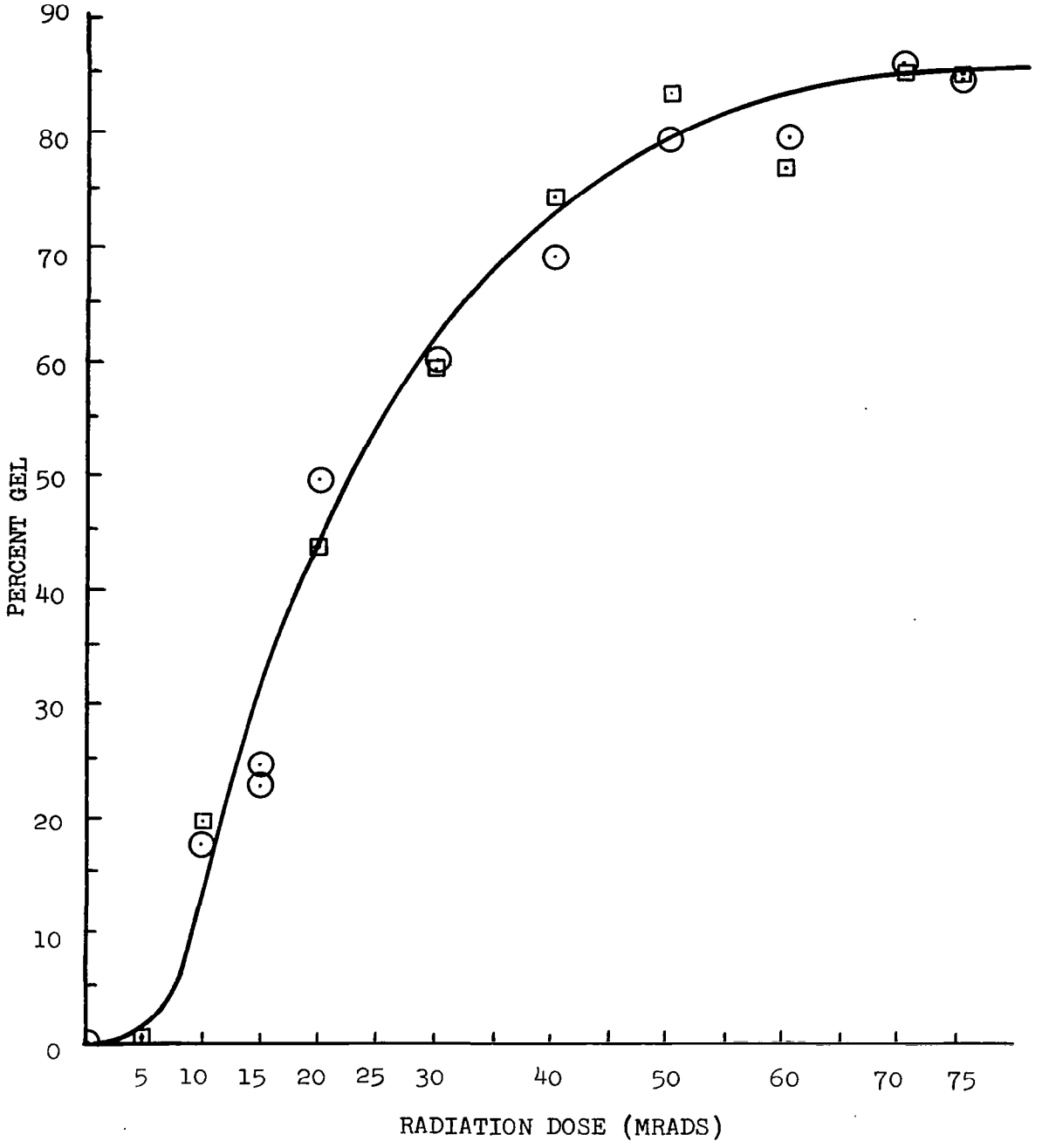

Table 7

Effect of Complete Extraction* on Strength of 1 Mil Standard Density Sea Space Polyethylene Film Given Various Doses of Radiation**

Dose (Mrads)	Modulus of Elasticity, E (psi x 10^3)
0	0
5	0
10	0
15	3.76
20	5.85
30	24.3
40	26.3
50	19.5
60	24.0
70	18.9
75	20.2

* Extracted in xylene at 100°C. for 4 days with 0.1% n-beta-phenylnaphthylamine

** Irradiated in Nitrogen, Heat Treated in Nitrogen, 100°C.

It is seen that there is some increase in strength over untreated film. The fact that the strength has not increased significantly can be attributed to some degradation occurring during irradiation and during extraction.

2.1.6 Densities of Extracted Polyethylene Film

The densities of crosslinked-extracted standard density (0.92 gm./cc.) Sea Space polyethylene film, hereinafter called "PE 11" were determined using the density gradient apparatus described in Appendix III. The film samples were irradiated to from 5 to 75 Mrads and were extracted in xylene at 100°C. The values of the new densities of the extracted material are given in Table 8 below.

It can be seen from the results of this experiment

Figure 4 EFFECT OF COMPLETE EXTRACTION ON STRENGTH OF 1 MIL STANDARD DENSITY SEA SPACE POLYETHYLENE FILM GIVEN VARIOUS LOSES OF RADIATION

Irradiated in Nitrogen
Heat Treated in Nitrogen, 100°C.
Extracted in Xylene at 100°C. for 4 days with 0.1% n-beta-phenylnaphthylamine

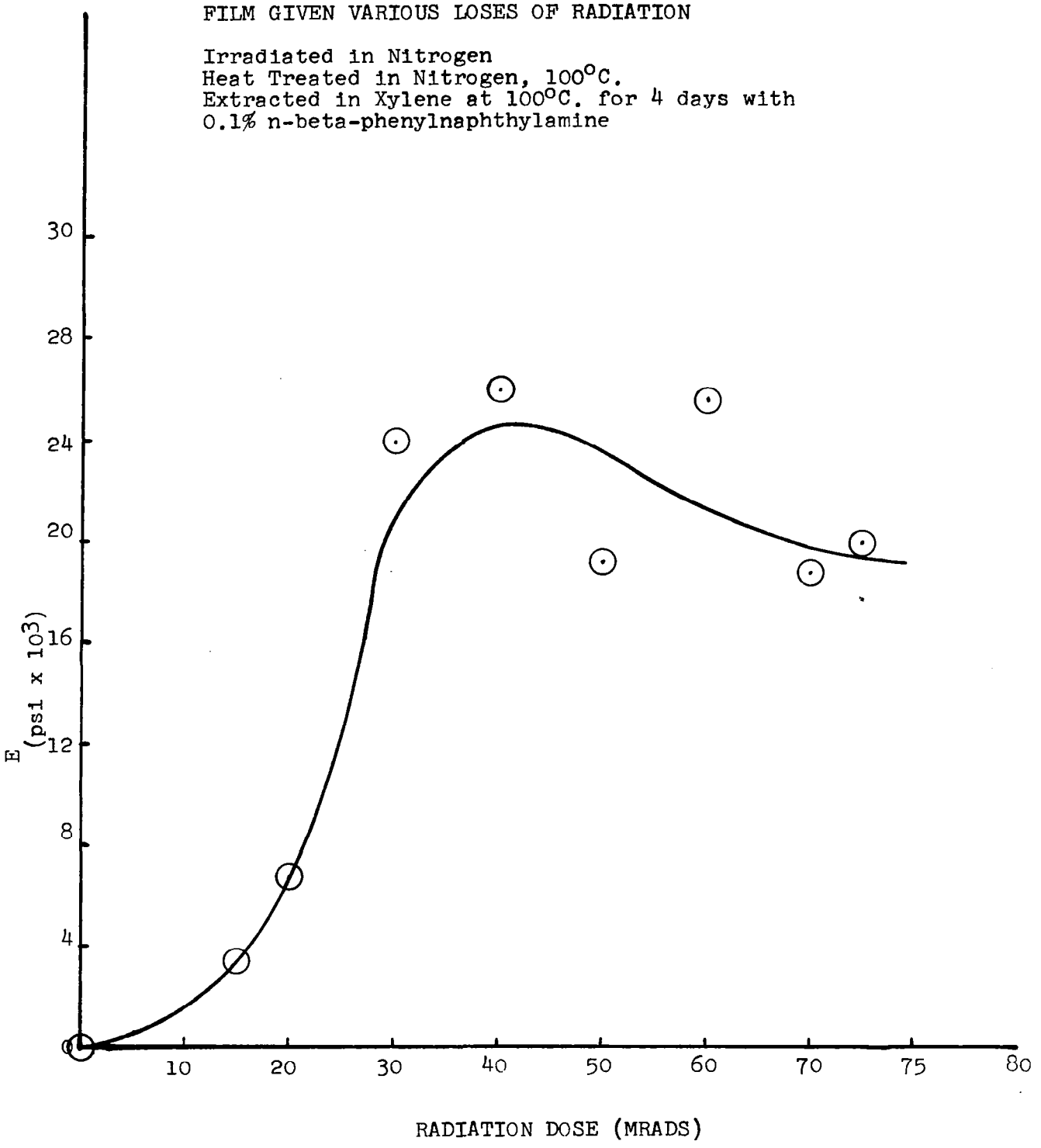

that an extraction technique does not lower the density of the polymer and in fact increases it somewhat. The increase is probably due to further alignment and collapsing of the molecular chains. It is believed, from the results of these tests, that extraction will not lower the density of irradiated polyethylene film.

Table 8

Densities of Extracted-Crosslinked PE 11

Dose (Mrads)	ρ(gm./cc.)
0(Unextracted)	0.920
10	0.941
15	0.943
50	0.932
60	0.932
70	0.932
75	0.932

2.1.7 Results of Extraction Program

It is seen from Figure 4 that the strength of extracted, crosslinked polyethylene does not increase very much above that of untreated polyethylene. In fact, in some instances it actually decreases. Additionally, it was found that the densities of the extracted material did not decrease, see Table 8. With these results it can be concluded that irradiation-extraction treatments do not increase E/ρ.

2.2 Development of Laminate

To determine the specifications of the film to be used to construct the satellite, it was necessary to establish the proper film density and type and the metal thickness that would result in a laminate low in weight and sufficiently rigid to withstand five times solar pressure when fabricated as a

425 ft. diameter sphere. The program proceeded by electrolessly plating a complete thickness range of polyethylene films to a given metal thickness and then determining if (a) the laminate was low in area weight, and (b) if the sphere made from this laminate could withstand five times solar pressure. It was found after considerable trial and error that a 15×10^{-6} in. coat of copper on both sides of polyethylene film was necessary so that a thin polyethylene film (for low weight) could be used.

2.2.1 Flexural Rigidities of Metallized Polyethylene Film

In an effort to lower the required thickness of the polyethylene-metal laminate, experiments were run where both sides of thin polyethylene film were plated. Polyethylene films of various densities and thicknesses were electrolessly plated with copper in thicknesses from 5×10^{-6} to 15×10^{-6} inches on both sides. Flexural rigidities of the plated films were determined using the Standard ASTM D 1388-55T Beam Cantilever Test for flexural rigidity by measuring the length of overhang. The ASTM beam cantilever test is a test designed to measure the flexural rigidities of films and fabrics. It has been successfully used to measure flexural rigidities of similar thin film laminates before and has been proven to be an accurate test.[6,7] A description of the experimental procedures used to measure flexural rigidities is given in Appendix IV.

Flexural rigidities, $G^L(t)$ were calculated as follows:

$$G^L(t) = W_A\left(\frac{l_F}{2}\right)^3 \qquad (3)$$

where l_F = length of overhang of plated film

W_A = area weight of plated film

= area weight of film + area weight of deposited copper film

= (density of the film)(thickness of film) + (density of copper)(thickness of copper film)

$= \rho_F t + \rho_{cu} t_{cu}$

where

ρ_{cu} = 8.9 gm./cc.

ρ_F = 0.920 gm./cc., 0.931 gm./cc.

For a number of test samples:

$$\hat{G}^L(t) = \sqrt{\bar{G}_0(t)\ \bar{G}_{90}(t)} \qquad (4)$$

where $\bar{G}_0^L$ = average flexural rigidity in 0° direction

$\bar{G}_{90}^L$ = average flexural rigidity in 90° direction

2.2.2 Flexural Rigidities of PE 11 (Plated) Type Films

Standard density (0.920) polyethylene films, ranging in thickness from 0.15 mil to 4 mils, were electrolessly copper plated to a depth of either 5×10^{-6} or 10×10^{-6} inches on both sides. Lengths of overhang were determined and the flexural rigidities were calculated.

The results are given in Table 9 below and are plotted in Figure 5, curves A and B.

2.2.3 Flexural Rigidities of PE 12 (Plated) Films

Samples of PE 12 film (0.931) plated with 5×10^{-6} inches or 10×10^{-6} inches of copper were tested for flexural rigidity. It was found that the higher density plated film gives a considerably higher flexural rigidity as compared to the

Table 9

Flexural Rigidity as a Function of Film Thickness with Electroless Plating Time as a Parameter

t (mil)	5 Minute Plate			10 Minute Plate		
	$\bar{G}_0$ lb.in.x10^{-6}*	$\bar{G}_{90}$ lb.in.x10^{-6}*	$\hat{G}$ lb.in.x10^{-6}*	$\bar{G}_0$ lb.in.x10^{-6}*	$\bar{G}_{90}$ lb.in.x10^{-6}*	$\hat{G}$ lb.in.x10^{-6}*
0.15	1.293	1.635	1.45	1.341	1.010	1.16
0.21	1.442	0.967	1.18	1.460	1.007	1.21
0.30	2.566	1.837	2.17	2.385	2.464	2.42
0.55	3.911	3.174	3.52	3.819	8.572	5.72
1.00	18.686	24.937	21.58	37.89	18.26	26.30
2.85	146.8	168.7	157.5	247.9	339.2	299.0
4.00	678.4	702	689.9	929.6	743.7	831.0

*lb.in. = lb.in.^{2}/in. since samples are 1 inch wide

plated standard density film. In addition to the higher density material, having a higher modulus of elasticity, it also gives a surface that is more receptive to the metallization process. This is evident from Figure 5 where the flexural rigidities of the plated PE 12 are compared with the flexural rigidities of the plated 1-mil PE 11.

2.2.4 Flexural Rigidities of Plated PE 12 Film over the Complete Range of Film Thicknesses

The necessity of a stiff film at low area weight prompted the use of PE 12 as the base material. It was plated to a depth of 15 x 10^{-6} in. on each side. The flexural rigidity thickness curve for this laminate was then constructed. Use was made of the flexural rigidity of plated 1 mil PE 12 to give the displacement above the low density curves. Its contour was determined using the low density curves. The "limiting" points for the flexural rigidities were experimentally determined. For the upper point a 2-mil laminate of PE 12 plated to a 15 x 10^{-6} inch depth on each side was used while the lower point was determined using a 0.15 mil PE 11 film plated to 15 x 10^{-6} in. thickness on each side. PE 11 film could be used for the lower point because the type of polyethylene film becomes less important as the polyethylene film thickness becomes very small, since it only contributes a small fraction of the flexural rigidity of the laminate. This is shown in curve D of Figure 5, where the flexural rigidity of unplated, standard density film is plotted vs. thickness using the beam cantilever test data (listed in Table 10). The final flexural rigidity-thickness curve constructed from the three data points and the contour of the 5 x 10^{-6} and 10 x 10^{-6} in. thickness curve is given

Figure 5 EXPERIMENTAL FLEXURAL RIGIDITIES

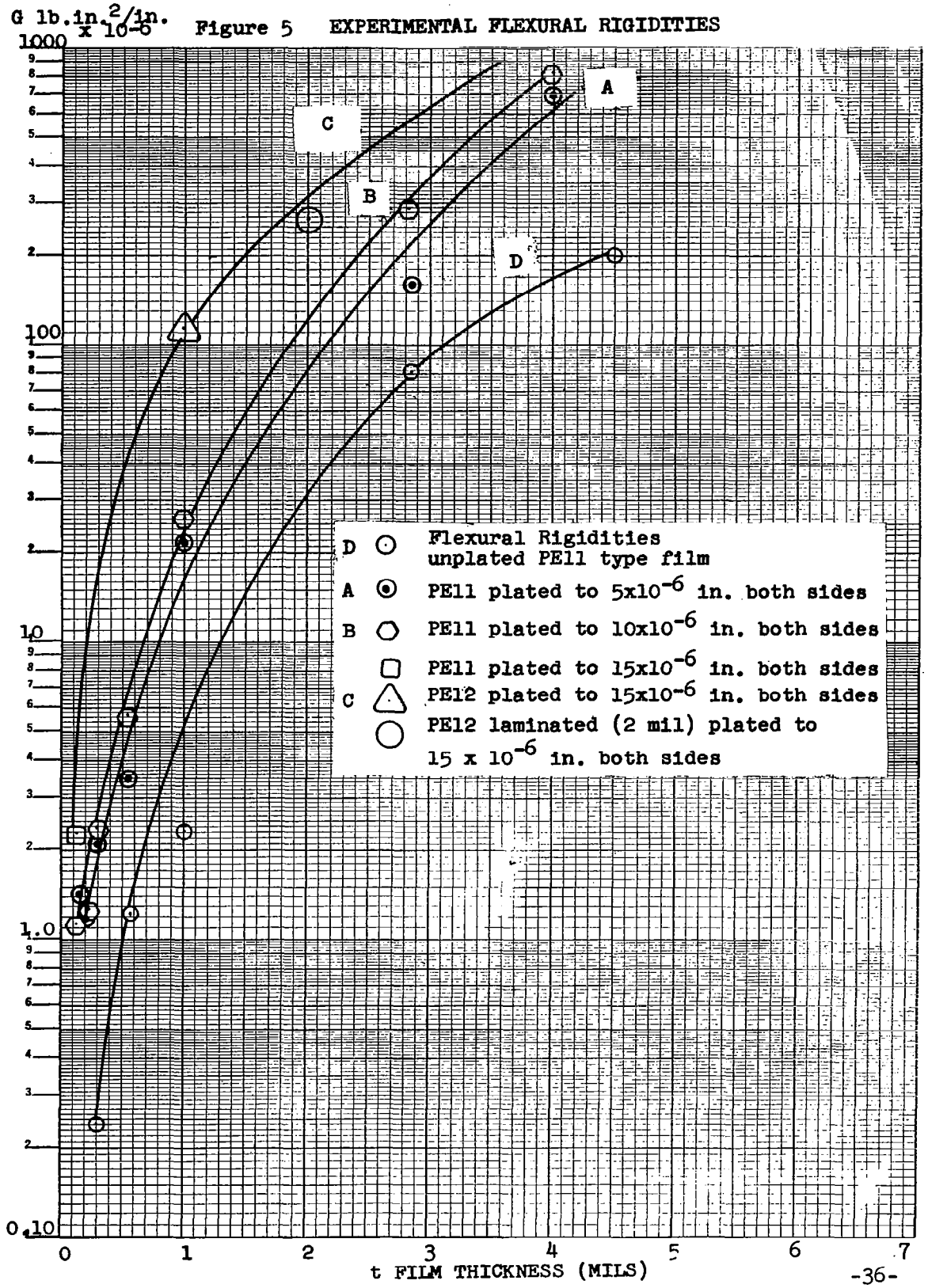

in Figure 5, curve C. The extrapolated flexural rigidities given by curve C will be used to determine the polyethylene thickness needed to withstand five-times solar pressure, and to determine the satellite weight. The calculation is carried out in Section 3.2.2 to follow.

Table 10

Flexural Rigidity of Unplated PE 11 vs. Thickness

t (mil)	G^* (lb.in.^{2}/in. x 10^{-6})
0.15	No reading obtainable
0.21	0.0567
0.30	0.2431
0.55	1.226
1.0	2.30
2.85	81.714
4.5	196.155

* Arithmetic mean reported

2.3 Perforations

In order to test the effects of perforation (fraction open area) on flexural rigidity and resistance of metallized film a perforation study was initiated. Samples of polyethylene film were perforated to 10, 20 and 40% open area using small perforation dies made at NASA, GSFC. The die patterns are shown in Figures 6 and 7, and Table 11. A staggered circular arrangement has been chosen because it is known that a staggered pattern has been found to possess more rigidity than a pattern of uniform rows.[8] It should be additionally pointed out that staggered hexagons give higher rigidity than staggered circles,[9]

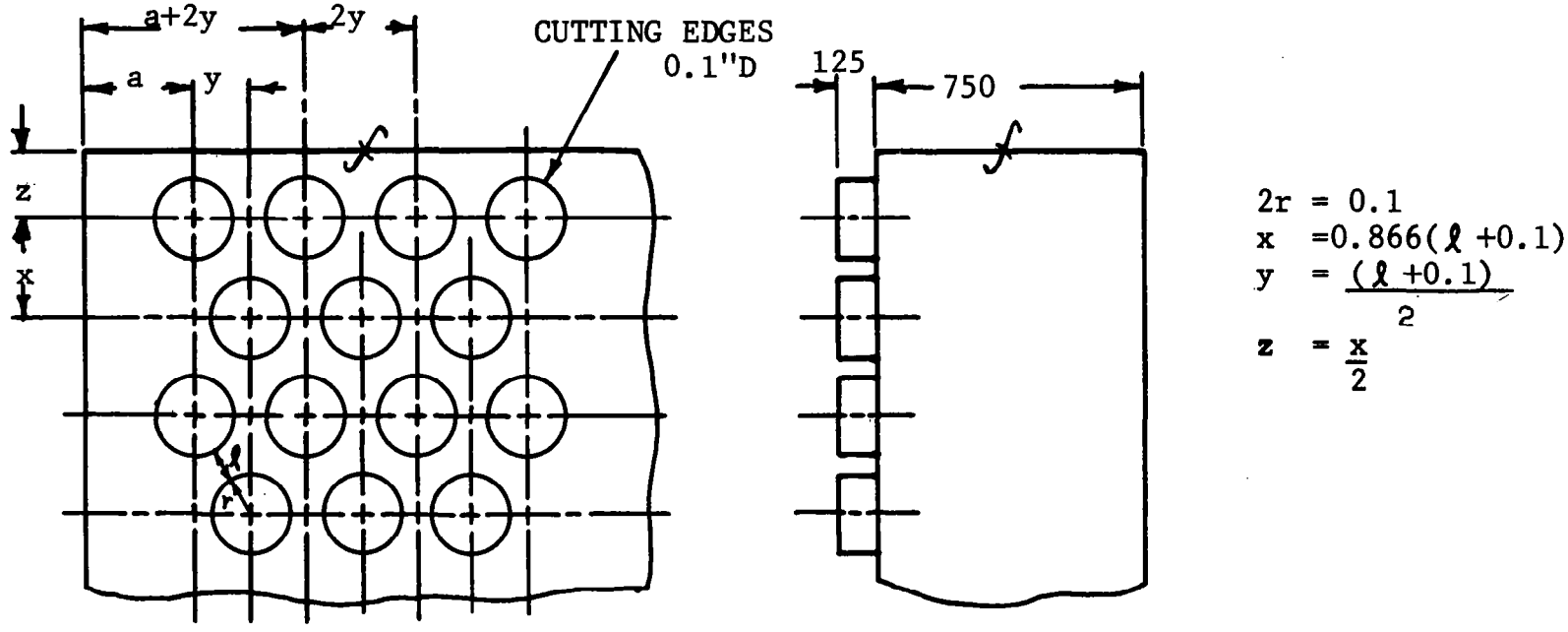

Figure 6 PERFORATOR-DIE PATTERN, DETAIL 1
(Dimensions in Table 11)

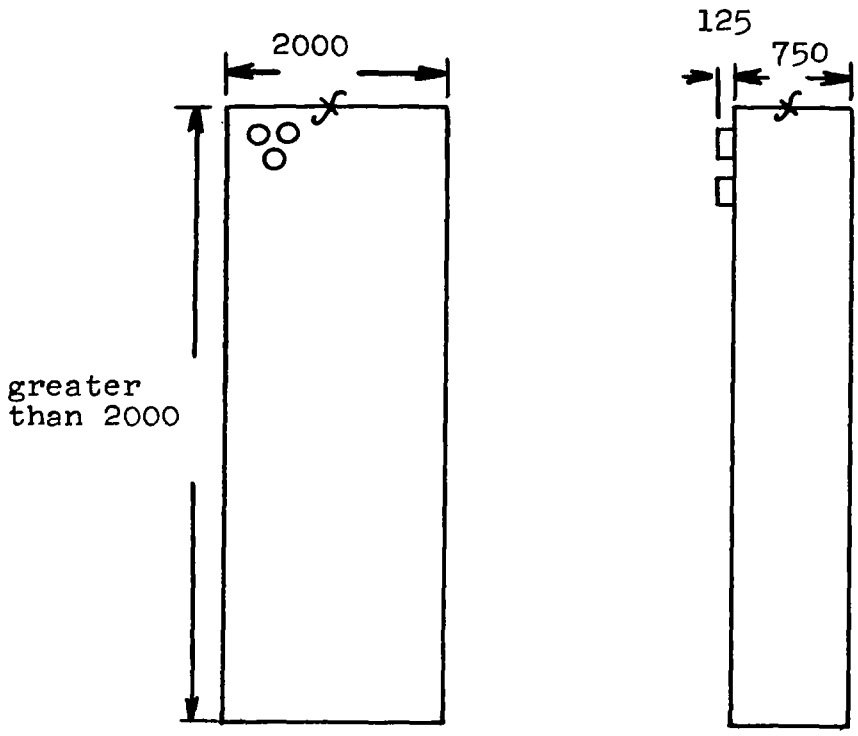

Figure 7 PERFORATOR DIE PATTERN, DETAIL 2

however, it was found in the design study to follow that staggered circles are quite adequate for the goals of the project. It was found that flexural rigidity and electrical resistance were significantly better if the film was perforated before metallization. Tests were run both ways. All samples were made from 0.30 mil standard density polyethylene film metallized with 15 x 10^{-6} in. of copper on both sides. This particular laminate configuration was chosen, since this configuration was found to be able to withstand five times solar pressure using a buckling pressure-thickness calculation which is presented in Section 3.0 to follow.

Table 11

Perforator Dimensions

F_v	l	x	y	z	n_R	a
0.10	0.2012	0.2608	0.1506	0.1304	6	0.2470
0.20	0.1129	0.1844	0.1066	0.0922	7	0.3613
0.30	0.0739	0.1506	0.0870	0.0753	9	0.3044
0.40	0.0506	0.1304	0.0753	0.0652	10	0.3223
0.50	0.0347	0.1167	0.0674	0.0584	11	0.3264

2.3.1 Flexural Rigidity of Perforated Film

The flexural rigidities of perforated film were measured in the same way unperforated film was measured see Section 2.2.1. The only difference is that equations (3) and (4) are modified as follows:

$$G^L(t,F_v) = (1-F_v)W_A \quad \frac{1F}{2}^3 \qquad (5)$$

and

$$\hat{G}^L(t,F_v) = (1-F_v)\sqrt{\bar{G}_0^L(t,F_v)\bar{G}_{90}^L(t,F_v)} \qquad (6)$$

The results of the study for plating, then perforating and perforating, then plating are listed in Table 12 and plotted in Figure 8.

2.3.2 Electrical Resistance of Perforated Film

Electrical surface resistances (in ohms/sq.) were measured across samples of perforated, metallized film and metallized perforated film. The resistances reported were the average of resistances measured in two directions according to the following diagram:

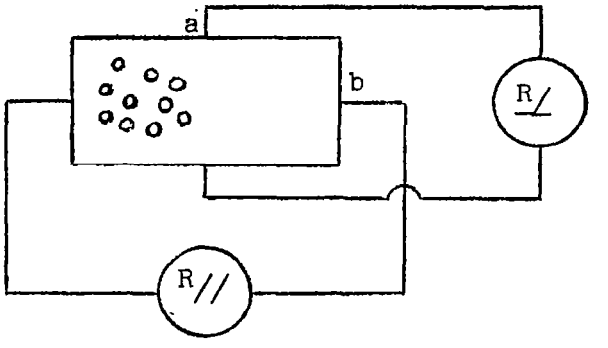

where $\bar{R}_{sq} = \frac{1}{2}\left[R_{//}\frac{b}{a} + R_{/}\frac{a}{b} \right] = \frac{1}{2}\left[R_0 + R_{90}\right]$ (7)

Table 12

Effect of Perforation on 0.30 Mil Plated Standard Density Polyethylene Film

Percent Open Area	$\overline{G}_0$ (lb.in. x 10^{-6})	$\overline{G}_{90}$ (lb.in. x 10^{-6})	$\hat{G}$(lb.in. x 10^{-6})
Plated for 15 Minutes then Perforated			
0	13.476	12.206	12.826
10	7.501	10.680	9.618
20	4.921	6.430	5.625
40	4.510	4.831	4.667
50	0.835	0.899	0.866
Perforated and then Plated for 15 Minutes			
0	13.476	12.206	12.826
10	9.487	5.773	7.403
20	11.162	7.138	8.926
40	5.532	12.498	8.315

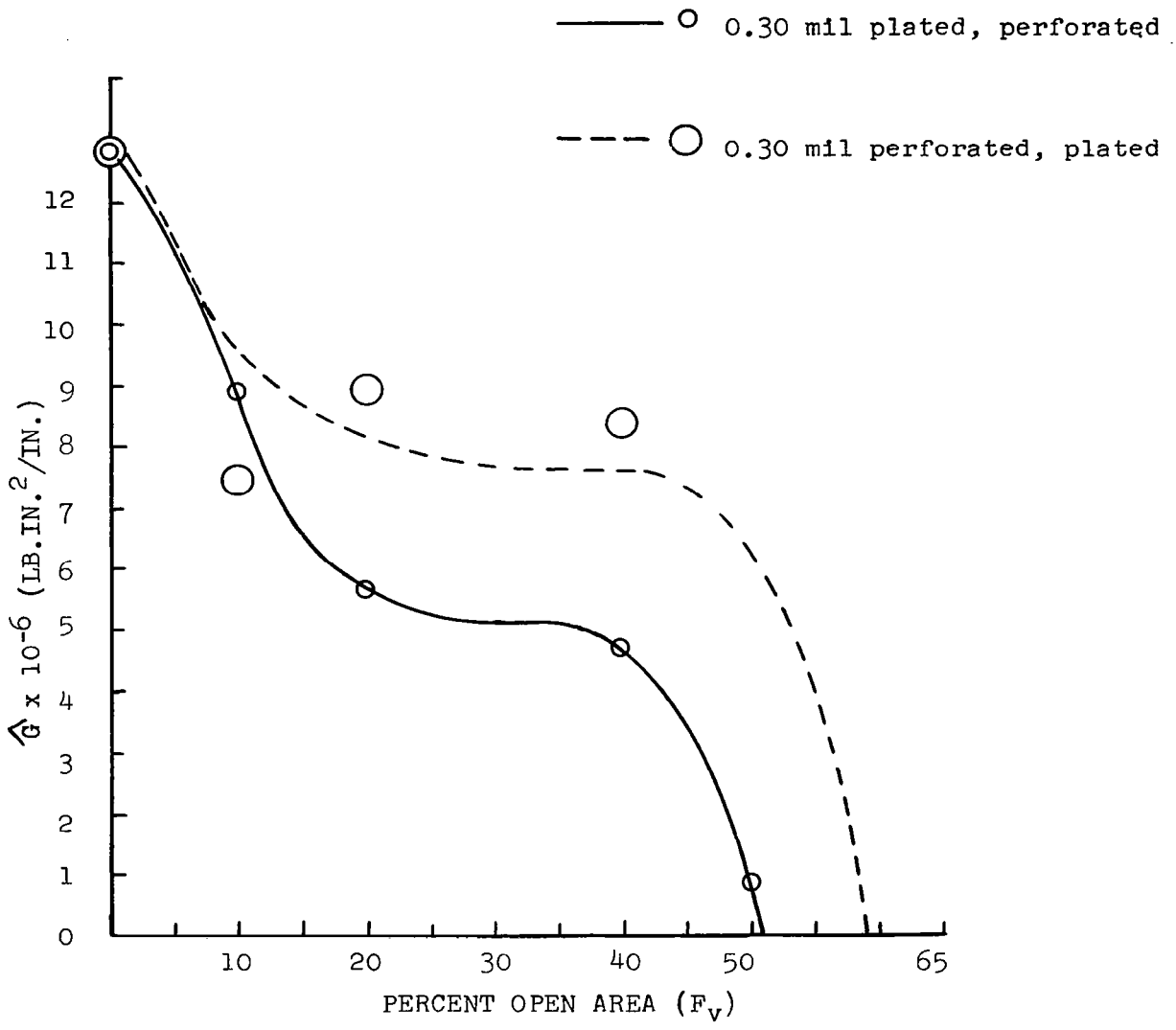

Figure 8 FLEXURAL RIGIDITY OF PERFORATED 0.30 MIL STANDARD DENSITY POLYETHYLENE FILM VS. PERCENT OPEN AREA

(Plated to 15 x 10^{-6} inches on both sides)

The results of the resistance measurements are tabulated in Tables 13 and 14 below.

Table 13

Resistance of Plated (15×10^{-6} in. Cu) Perforated, Standard Density Polyethylene Film

Percent Open Area	Sample Size	$R_{//}$ (ohms)	$R_{\perp}$ (ohms)	$\overline{R}_{sq}$ (ohms/sq.)
0	3x5			0.275*
10	2x5	2.05	0.25	0.72
20	2x5	2.32	0.59	1.19
40	2x5	15.40	3.81	7.85
50	2x5	281.00	634.00	1090.8

* Average of resistance values from each sample before perforation (the sample size was 3x5).

Table 14

Resistance of Perforated-Plated (15×10^{-6} in. Cu) Standard Density Polyethylene Film

Percent Open Area	Sample Size	Run 1 $R_{//}$ (ohms)	Run 1 $R_{\perp}$ (ohms)	Run 2 $R_{//}$ (ohms)	Run 2 $R_{\perp}$ (ohms)	$\overline{R}_{sq}$ (ohms/sq.)
0						2.75*
10	3x3	0.6	0.6	0.65	0.6	0.61
20	3x3	0.6	0.6	0.6	0.6	0.6
40	3x2(run 1) 2x2(run 2)	1.2	0.4	0.8	0.8	0.8

* Since the film was perforated first, the resistance value for 0% open area from Table 13 is used.

2.3.3 Conclusions on Perforation Tests

It can be seen from the perforation tests summarized in Figures 8 and 9 that metallizing the material after perforation as opposed to before perforation results in a material with considerably better properties. Apparently the perforation procedure distorts and stresses the circular boundaries it punches out. This may be seen from the bottom photomicrographs of Figure 56 in Section 6.1.

If the copper is applied before perforation, it along with the plastic is distorted and cracked when perforated. If the copper is applied after perforation it is unharmed and even corrects some of the distortion and weak spots in the plastic around the hole boundary by filling in small tears and cracks. Since there are no additional problems involved in electroless metallization of perforated film as opposed to a non-perforated film it was decided to metallize after perforation. The flexural rigidity of the laminate decreases with perforation. This is shown in Figure 8, Curve B, which is further used in the perforation optimization study to follow in Section 3.0.

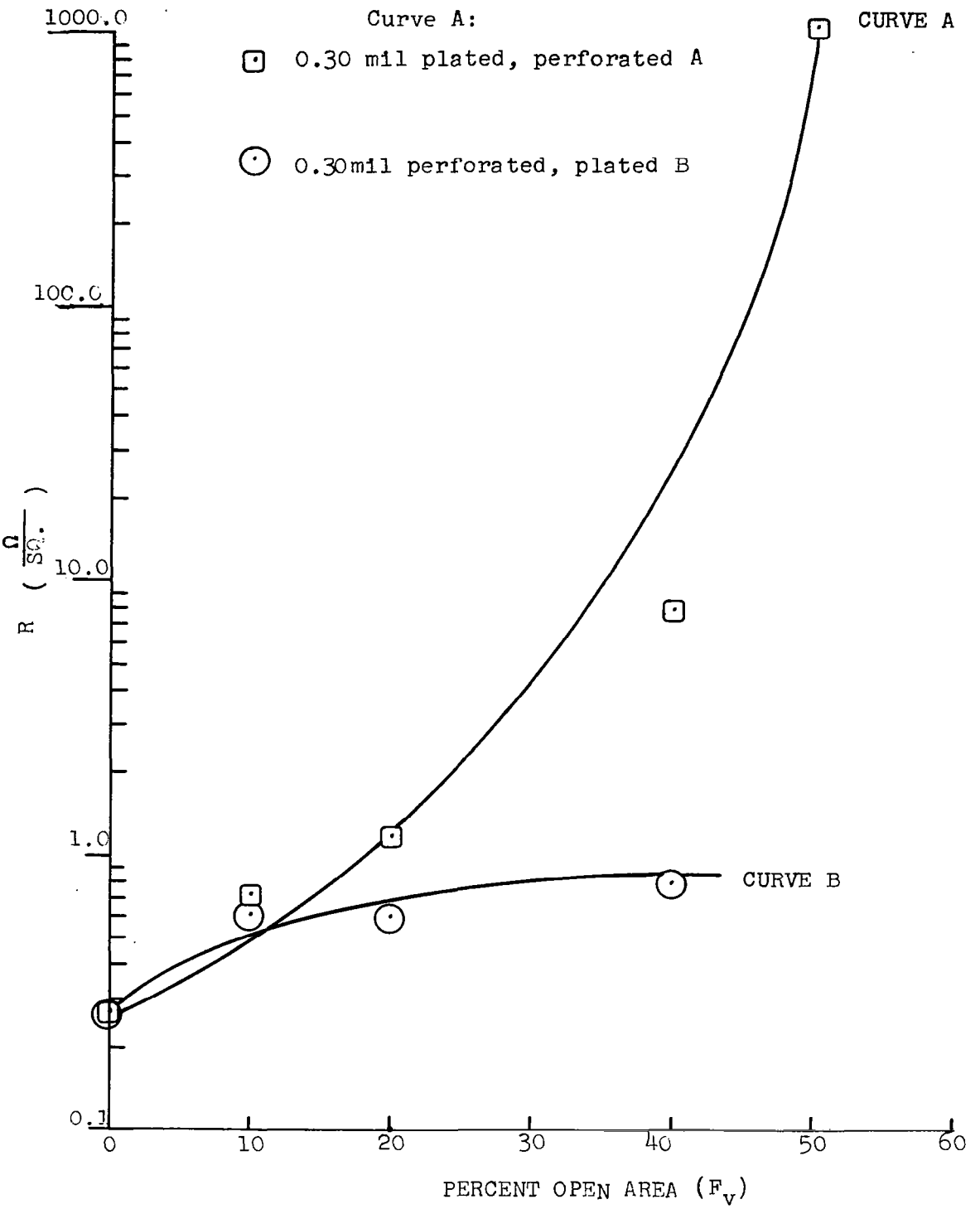

Figure 9 RESISTANCE (Ω/SQ.) OF PERFORATED 0.30 MIL STANDARD DENSITY POLYETHYLENE FILM VS. PERCENT OPEN AREA
(Plated to 15 x 10^{-6} in. Cu on both sides)

3.0 BUCKLING PRESSURE - THICKNESS STUDY

A literature search, an experimental program and calculations for the design of a 425 foot diameter sphere capable of withstanding a buckling pressure of five times solar pressure ($P_s = 1.3 \times 10^{-9}$ psi) were completed during this investigation. The total weight of the proposed sphere is less than 1000 lbs. The design which follows is based on the application of a thin polyethylene film as the material of construction. This material has been irradiated and contains a memory. The design study has been divided into three stages. The first stage was concerned with developing an equation which would yield a critical buckling pressure - thickness relationship for the configuration under study. In the second stage the equations developed during the first stage were modified to account for the effects of the applied copper laminates. Finally, in the third stage the experimentally determined effects of perforations were included in the equations and the satellite weight was optimized with respect to fraction open area.

3.1 Theoretical Equation

The classical equation derived for determining the critical buckling pressure as a function of thickness, t, of a thin spherical shell is given as follows:[10,11]

$$P_{cr} = \frac{2Et}{R(1-\nu^2)} \left[\left(\frac{1-\nu^2}{3} \right)^{\frac{1}{2}} \frac{t}{R} - \frac{\nu}{2} \frac{t^2}{R^2} \right] \qquad (8)$$

where E = the modulus of elasticity
v = Poisson's ratio
R = Radius of sphere

For a large sphere with a thin shell

$$\frac{t^2}{R^2} \rightarrow 0$$

So equation (8) may be simplified as follows:

$$P_{cr} = \frac{2\,Et^2}{R^2\, 3^{\frac{1}{2}}(1 - v^2)^{\frac{1}{2}}}$$

or

$$t = 3^{\frac{1}{4}}(1-v^2)^{\frac{1}{4}} R \left(\frac{P_{cr}}{2E}\right)^{\frac{1}{2}} \qquad (9)$$

In equation (9) if the following values are chosen:

$$E = 20 \times 10^3 \text{ psi}$$

$$P_{cr} = 5(1.3 \times 10^{-9} \text{ psi})$$

$$R = 2550 \text{ inches}$$

$$v = 0.50$$

t is found to equal 0.104 mil.

It is found that the classical buckling pressure equation yields low values when the $\frac{t}{R}$ ratio is less than 10^{-3}. Summaries of the inaccuracy of using theoretical buckling pressure equations for large thin shelled spheres are given in Theory of Elastic Stability and Formulas for Stress and Strain. They are, respectively, as follows:

> "Experiments with thin spherical shells subjected to uniform external pressure show that buckling occurs at pressures much smaller than that given by equation (8)...." (ref. 12)

> "Because of the greater likelihood of serious geometrical irregularities, and their greater relative effect, the critical stresses actually developed by such members usually fall short of the theoretical values by a wider margin than in the case of bars..... The critical stresses or loads indicated by any one of the theoretical formulas should, therefore, be regarded as an upper limit, approached more or less closely according to the closeness with which the actual shape of the member approximates the geometrical form assumed ....."

Rourk additionally states that this discrepancy continues to increase with the thinness of the material.[13]

3.2 Spherical Cap Models

Since the theoretical approach is inaccurate for small $\frac{t}{R}$ ratios, equations have been used based upon models of spherical cap sections with small $\frac{t}{R}$ ratios. The methods used in the following sections will separately compare required thicknesses based on two models. One model is a uniformly loaded cap section, the other model is a point loaded cap section. For comparison the calculations have been performed without a material correction factor as well as with one.

3.2.1 No Material Correction Factor

3.2.1.1 Uniformly Loaded Cap Section

Articles by Reiss,[14] and Reiss, Greenburg and Keller[15] dealing with the buckling of uniformly loaded spherical cap sections of small curvature, determine critical buckling pressures for spherical caps of various geometries. The results given in the articles and which are plotted as $\frac{P_{cr}}{t^2}$ in Figure 10 were determined both numerically and experimentally. The critical buckling pressure is given in non-dimensional form:

$$P_{crr}(\rho) = \frac{P_{cr}}{2\,Ek^{\frac{1}{2}}\left(\frac{t}{R}\right)^2}$$

or

$$\frac{P_{cr}}{t^2} = \frac{2\,Ek^{\frac{1}{2}}}{R^2} P_{crr}(\rho) = U(\rho) \qquad (10)$$

Figure 10 THE FUNCTION $U(\rho) = \frac{P_{cr}}{t^2}$

$$U(\rho) = \frac{2Ek^{\frac{1}{2}}}{R^2} P_{crr}(\rho)$$

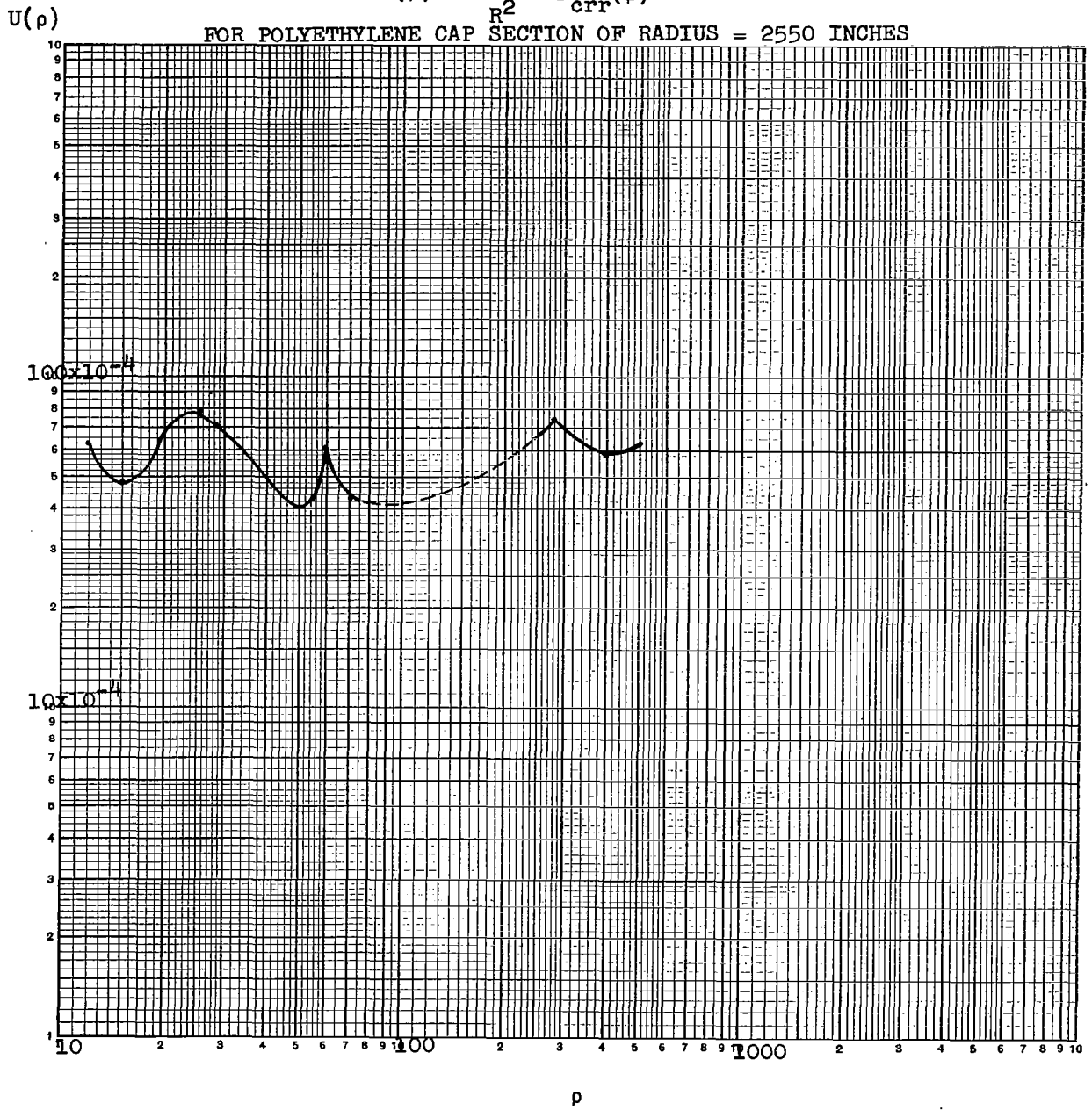

where $P_{crr}(\rho)$ = non-dimensional buckling pressure

P_{cr} = actual buckling pressure (= 6.5×10^{-9} psi)

$k = \frac{2}{3}(1 - v^2)$ (=0.50)

v = Poisson's ratio (=0.50)

t = film thickness

R = radius of spherical cap (=2550 inches)

E = modulus of elasticity (= 20×10^3 psi)

The non-dimensional buckling pressure P_{crr} is plotted against a non-dimensional geometrical parameter defined as

$$\rho = 2k^{-\frac{1}{2}} \frac{r^2}{R} \frac{1}{t} \qquad (11)$$

where r is equal to the radius of deformation, see Figure 11 .

It is convenient to plot P_{cr}/t^2 against ρ for all modes of deformation (caps with different geometrical parameters deform in different ways[16]). The results are given in Figure 10. It can be seen from this curve that P_{cr}/t^2 varies between 40×10^{-4} and 80×10^{-4}. For a critical buckling pressure of 6.5×10^{-9} psi this range corresponds to a thickness ranging from 0.902×10^{-3} in. to 1.275×10^{-3} in.

3.2.1.2 Point Loaded Cap Section

A point loaded spherical cap model has been used for the following reasons. A point loaded force gives a more severe test than a uniformly distributed force (a pressure). The point loaded model will thereby give the designer an additional factor of safety when the thickness is determined. Furthermore, a point load results in a "dimple like" failure which is the type of deformation observed in the buckling of thin spherical shells.[17]

In a text by Biezeno and Grammel[18] critical buckling

pressures have been theoretically determined for spherical cap sections of various geometries. The results are given in terms of a loading parameter (μ) versus a geometrical parameter (λ). They are defined respectively as follows:

$$\mu = \frac{RF_{cr}}{Et^3} \tag{12}$$

$$\lambda = \frac{r^4}{t^2R^2} \tag{13}$$

where F_{cr} = critical buckling force.

If P_{cr} is concentrated as a force, F_{cr}, at a point on the center spherical cap, then

$$F_{cr} = \pi r^2 P_{cr} \tag{14}$$

This transformation is shown in Figure 11.

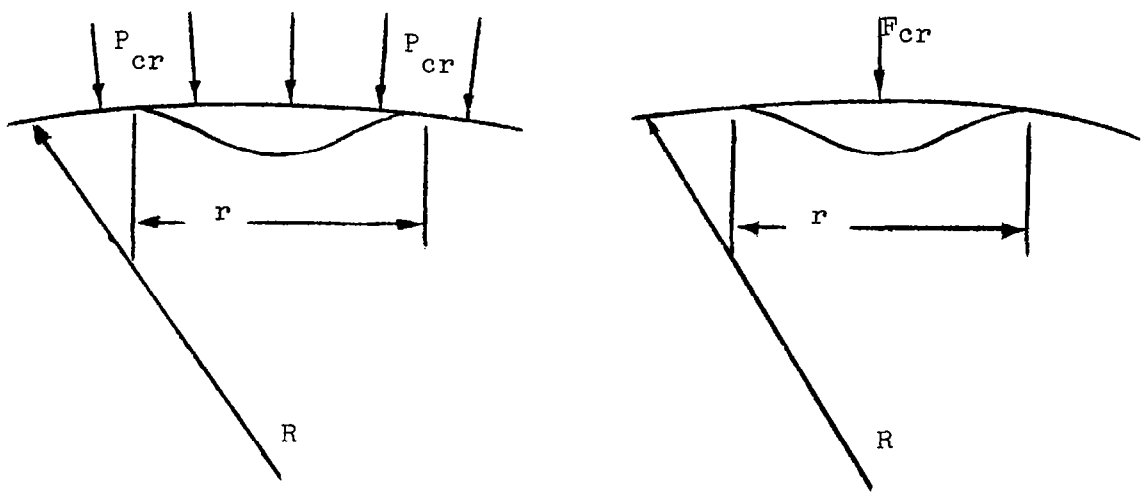

Figure 11 : TRANSFORMATION FROM DISTRIBUTED LOAD TO POINT LOAD

From the graph of μ and λ in Engineering Dynamics,[18] μ may be represented by the equation:

$$\mu = \sqrt{0.093(\lambda + 11.5)} - 0.94 \approx 1 \times 10^{-2}\lambda + 1 \qquad (15)$$

It should be noted that at $\lambda > 500$ the approximation of equation (15) gives a high value of μ which will provide an additional factor of safety for the designer. If equations (11) - (15) are used to solve for P_{cr} in terms of ρ and t the following equation is obtained:

$$P_{cr} = \frac{2E}{\pi R^2 k^{\frac{1}{2}}} \left[\frac{10^{-2}k}{4}\rho + \frac{1}{\rho} \right] t^2$$

$$\text{or} \quad \frac{P_{cr}}{t^2} = F(\rho) \qquad (16)$$

where $F(\rho) = \frac{2E}{\pi R^2 k^{\frac{1}{2}}} \left[\frac{10^{-2}k}{4}\rho + \frac{1}{\rho} \right]$

$F(\rho) = \frac{P_{cr}}{t^2}$ was then plotted versus ρ, see Figure 12. Since the value of the geometrical parameter is not known for this system, the value of ρ which gives the minimum $F(\rho)$ was chosen. In this way, the maximum value of t will be obtained. The result is as follows at $\rho = 30$, $\frac{P_{cr}}{t^2}$ is a minimum. At the minimum $\frac{P_{cr}}{t^2}$, t is found by solving equation (16); the result is 1.85×10^{-3} inches.

3.2.2 Calculation with Material Correction Factor

The above calculations have not taken into account the added resistance to buckling due to the thin copper laminations on the polyethylene film. If equation (12) is combined with equation (14) it is seen that P_{cr} is proportional to Et^3. This suggests that P_{cr} is proportional to the

Figure 12 THE FUNCTION $F(\rho)$ (POLYETHYLENE)

$$F(\rho) = \frac{2\,E}{\pi\,R^2\,k^{\frac{1}{2}}}\left(\frac{10^{-2k\rho}}{4} + \frac{1}{\rho}\right)$$

$E = 20 \times 10^3$
$R = 2550$ INCHES
$k = 0.50$

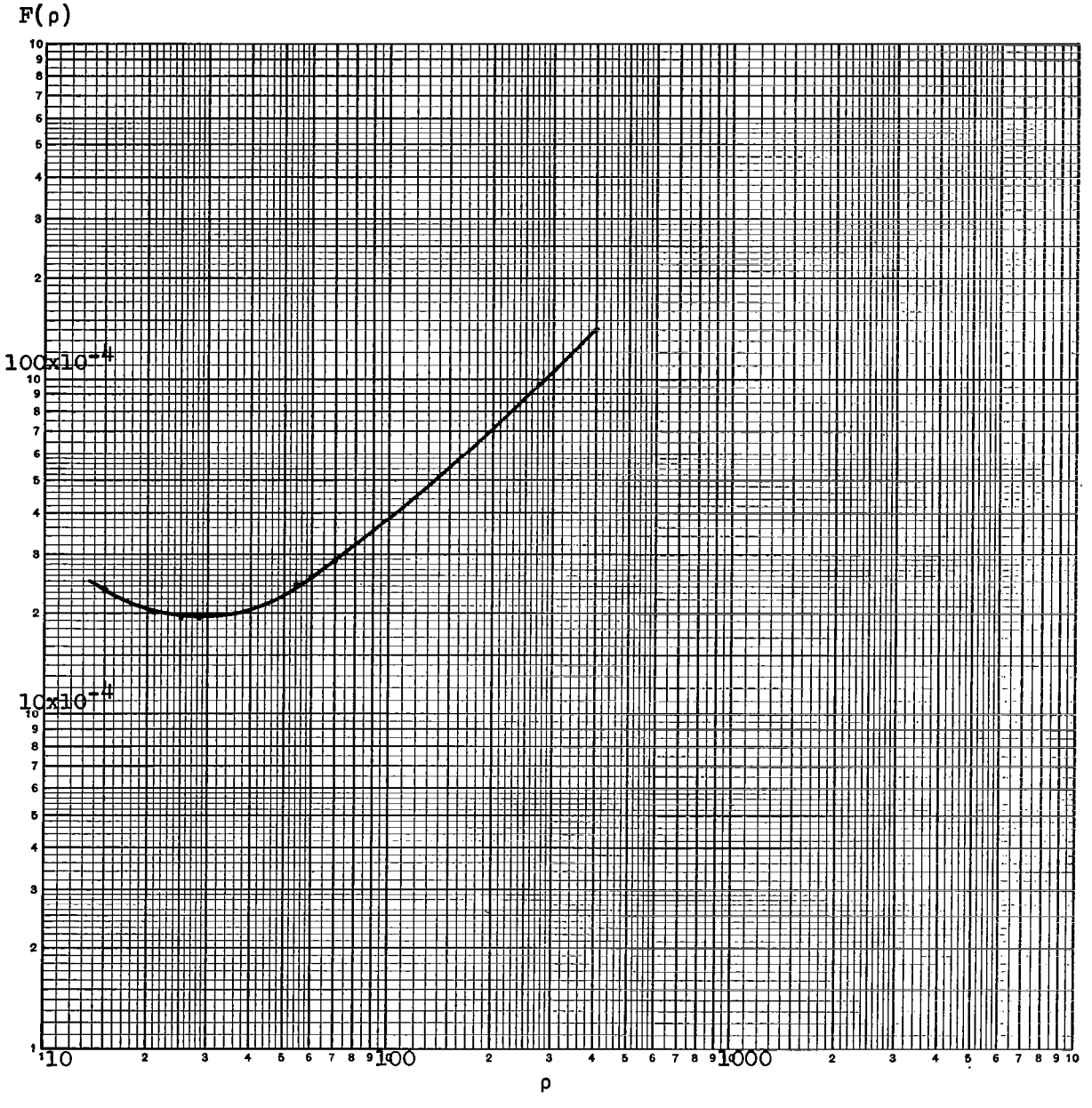

flexural rigidity $\hat{G}^L(t)$ of the laminated film since $\hat{G}^L(t) \propto EI \propto Et^3$. An experimental flexural rigidity used as a correction factor additionally will correct for any imperfections in the film (such as microscopic cracks) since the imperfections will be reflected in the experiment. It also suggests that the actual P_{cr} is proportional to the ratio of the actual laminate flexural rigidity to the flexural rigidity of the unlaminated film ($\hat{G}^L(t)/\frac{1}{12} Et^3$). It is in this way that the above buckling pressure equations have been corrected for the effect of the increased resistance to buckling by the added thickness of copper.

It was assumed for a thin film laminate of copper and polyethylene that increasing the copper thickness a small amount and decreasing the polyethylene thickness a large amount can still increase the rigidity of the laminate. This is so because of a very high modulus of elasticity of the copper compared to the polyethylene. Various combinations of thicknesses of polyethylene and copper ranging from 0.15-1.5 mil and 5×10^{-6} - 15×10^{-6} in. respectively were therefore investigated (see Section 2.2). It was found that after considerable trial and error (Section 2.2.3) that 15×10^{-6} in. of copper was necessary to achieve sufficient flexural rigidities to withstand calculated solar buckling pressures and still be within design weight limitation. For the above reasons the experimental flexural rigidity curve of Figure 5 has been used in the correction factor in the following calculations.

3.2.2.1 Uniformly Loaded Cap Section

If the critical buckling pressure in equation (10)

is corrected for rigidity using the factor

$$\frac{\hat{G}^L(t)}{\frac{1}{12}Et^3}$$

the following equation results

$$P_{cr} = \frac{\hat{G}^L(t)}{\frac{1}{12}Et^3}\, U(\rho)t^2$$

or $$H(t) = \frac{U(\rho)}{E\, P_{cr}} \qquad (17)$$

where $$H(t) = \frac{t}{\hat{G}^L(t)}$$

Solutions to equation (17) can be found using Figures 10 and 13 . The solutions are only obtainable at critical buckling pressures greater than 6.5×10^{-9}. Table 15 below indicates the solutions for maximum and minimum $U(\rho)$ at the closest buckling pressures to the 6.5×10^{-9} psi specified.

Table 15

Solutions to Equation (17)

	$U(\rho)$	max $H(t)$	P_{cr}	t
minimum	40×10^{-4}	62.5	38.4×10^{-9}	0.15×10^{-3}
maximum	80×10^{-4}	62.5	76.8×10^{-9}	0.15×10^{-3}

The results presented in the table above indicate that a film thickness of 0.15×10^{-3} in. can withstand critical buckling pressures of ca. 6 to 12 times the required pressure. This means in effect that the 0.15×10^{-3} in. thick film can well withstand $P_{cr} = 6.5 \times 10^{-9}$ psi of pressure or a film thickness of less than 0.15×10^{-3} in. can withstand $P_{cr} = 6.5 \times 10^{-9}$ psi.

Figure 13 THE FUNCTION $H(t) = \frac{t}{\hat{G}^L(t)}$

where $\hat{G}^L(t)$ is the flexural rigidity of the laminated film given in Figure 5 curve C.

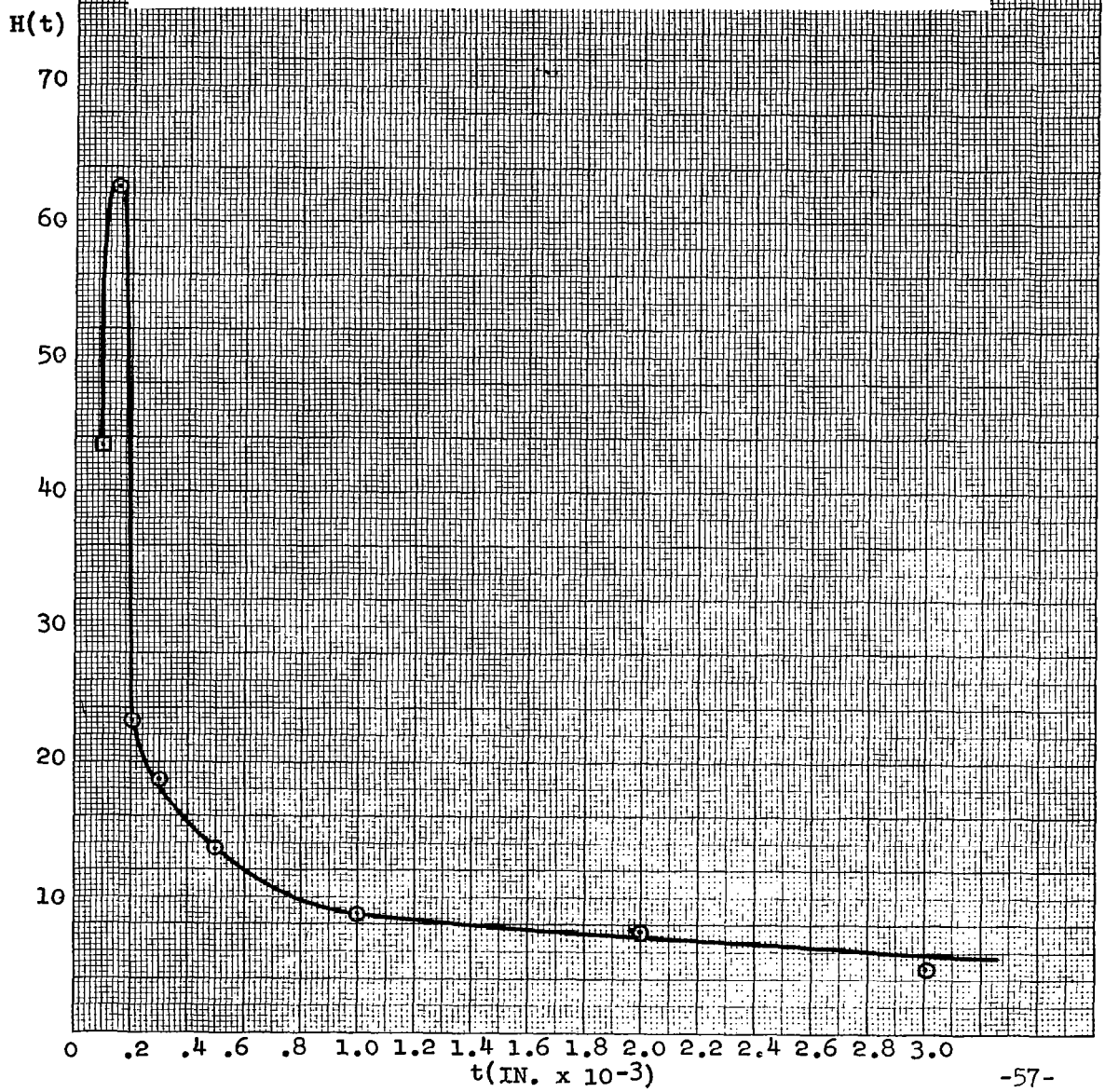

3.2.2.2 Point Loaded Cap Section

An approach-using a point loaded cap section as a model-believed to be conservative for design purposes, has been used to determine the composite film thickness that will withstand the specified buckling pressure of five-times solar pressure. The approach consists of modifying equation (16) the basic buckling pressure equation for the effect of small film thickness and the effect of metallic laminates. The method used corrects equation (16) for actual film-metal laminate flexural rigidity by the application of the following factor

$$\frac{\hat{G}^{L}(t)}{\frac{1}{12} Et^3}$$

where $\hat{G}^{L}(t)$ is the measured flexural rigidity of the metal-plastic film laminates and $\frac{1}{12} Et^3$ is the flexural rigidity of the polyethylene alone. If the flexural rigidity correction factor is applied to equation (16) the following equation is obtained:

$$P_{cr} = \frac{\hat{G}^{L}(t)}{t} \frac{24}{\pi R^2 k^{\frac{1}{2}}} \left[\frac{10^{-2} k\rho}{4} + \frac{1}{\rho} \right] \qquad (18)$$

If equation (18) is rearranged as follows:

$$\frac{t}{\hat{G}^{L}(t)} = \frac{24}{\pi R^2 k^{\frac{1}{2}} P_{cr}} \left[\frac{10^{-2} k\rho}{4} + \frac{1}{\rho} \right]$$

with $$H(t) = \frac{t}{\hat{G}^{L}(t)}$$

and the following function defined

$$F^{c}(\rho) = \frac{24}{\pi R^2 k^{\frac{1}{2}} P_{cr}} \left[\frac{10^{-2} k\rho}{4} + \frac{1}{\rho} \right]$$

equation (18) may then be stated as

$$H(t) = F^{c}(\rho) \qquad (19)$$

with H(t) plotted in Figure 13 from the experimental values of $\hat{G}^{L}(t)$ given in Figure 5, curve C, and with the function $F^{c}(\rho)$ plotted in Figure 14, with the constants P_{cr}, R and k additionally listed, equation (19) has been solved graphically for film thickness for various values of ρ. The results are summarized in Table 16.

Table 16

Polyethylene Thicknesses of Composite Film - Solutions to Equation (19) (15×10^{-6} inches of Copper Plate on both sides)

ρ	$F^{c}(\rho) = H(t)$	$t \times 10^{3}$
5	53	0.17
10	29	0.18
22	18.6	0.29
30	18.1	0.30
100	36.0	0.18
199.5	62.5	0.15
199.5	62.5	$<$0.15

It is apparent from the above Table that the maximum thickness of polyethylene film corresponds to the minimum $F^{c}(\rho)$. At min $F^{c}(\rho) = 18.1$, $t = 0.30 \times 10^{-3}$ in.

3.3 Comparison of Derived Film Thicknesses

Table 17 summarizes the values of the film thickness for the various methods of calculation.

It is believed that the 0.30 film thickness is the most reliable of the five calculated thicknesses. Use has been made of the experimental flexural rigidity values of the actual material; and flexural rigidity is a key property in determining a material's resistance to buckling pressure. In addition, the use of a point load instead of a uniformly

Figure 14 THE FUNCTION $F^c(\rho)$

$$F^c(\rho) = \frac{24}{\pi R^2 k^{\frac{1}{2}} P_{cr}} \left(\frac{10^{-2} k\rho}{4} + \frac{1}{\rho} \right)$$

with R = 2550 Inches k = 0.50 $P_{cr} = 6.5 \times 10^{-4}$ psi

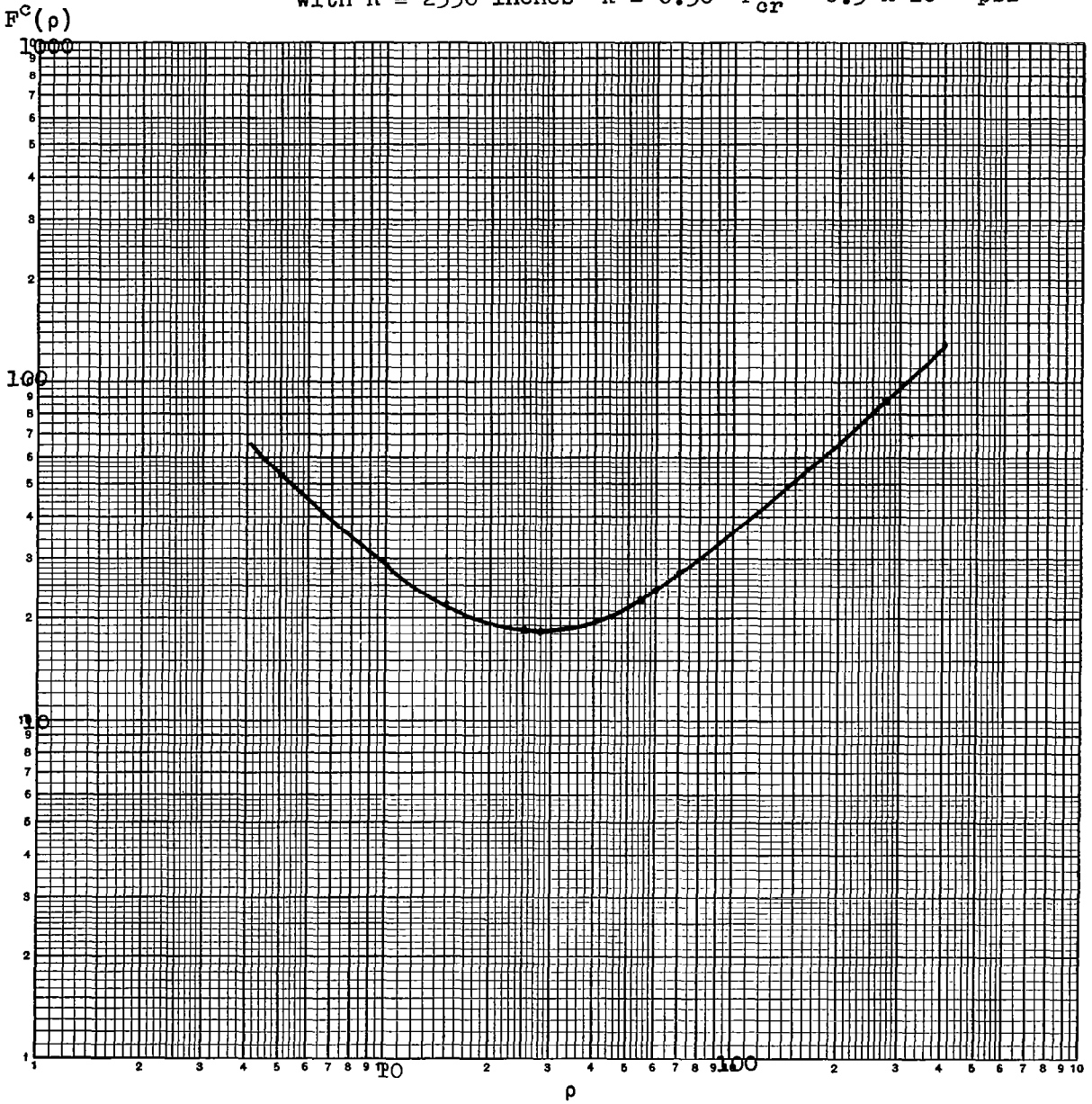

Table 17

Derived Thickness of Polyethylene Film

	Material	Model	Load	Composite Material Rigidity Correction Factor	Eq.	Thickness in. x 10^{-3}
1.	Polyethylene	Sphere	Uniform (P_{cr})	None	(8)	0.104
2.	Polyethylene	Spherical Cap Section	Uniform (P_{cr})	None	(10)	0.92-1.275
3.	Polyethylene	Spherical Cap Section	Point ($\pi r^2 P_{cr}$)	None	(16)	1.85
4.	Polyethylene ($+15 \times 10^{-6}$ in. Cu both sides)	Spherical Cap Section	Uniform (P_{cr})	$\frac{\text{flexural rigidity of composite film}}{\text{flexural rigidity of film}}$	(17)	0.15
5.	Polyethylene ($+15 \times 10^{-6}$ in. Cu both sides)	Spherical Cap Section	Point ($\pi r^2 P_{cr}$)	$\frac{\text{flexural rigidity of composite film}}{\text{flexural rigidity of film}}$	(19)	0.30

distributed load creates an additional safety factor, since a point load is a more severe condition.

3.4 Perforation Optimization - Satellite Weight

3.4.1 Satellite Weight vs. Void Fraction

With the point loaded spherical cap model established and an equation derived which accounts for the effect of the copper laminate, a polyethylene film thickness of 0.30×10^{-3} in. was calculated. The weight of the non-perforated satellite was then determined:

	Density (lb./ft.^{3})	Thickness (in.)	Area Weight (lb./ft.^{2})
Polyethylene	58.16	0.30×10^{-3}	1.454
Copper (electroless)	472.50	$2(15 \times 10^{-6})$	1.180
TOTAL.....			2.634

For a sphere with a diameter of 425 ft. the surface area is 567,344 ft.^{2} With a composite area weight of 2.634 lb./ft.^{2} the total weight of the non-perforated sphere is 1494.384 lbs.

The effect of perforation on the weight of the satellite can be seen from Table 18.

Table 18

Satellite Weights - Perforated
Film Thickness: 0.30 mil
Metal Thickness: 15×10^{-6} in. (both sides)

Percent Open Area	Total Weight (lbs.)
85	224.157
80	298.877
75	373.596
60	597.754
50	747.192
40	896.630
30	1046.069
20	1195.507
10	1344.946

Since flexural rigidity decreases with increasing percent open area and the effect of buckling pressure decreases with increasing percent open area, it is not possible to perforate to an arbitrary percent open area. It is necessary to find the maximum percent open area (which will give the lowest weight) that will still impart enough rigidity so that the film is capable of withstanding five times solar pressure. This problem is solved in the following section.

3.4.2 Perforation Optimization

With the point loaded spherical cap model established and an equation derived which accounts for the effect of the copper laminate, a polyethylene film thickness of 0.30×10^{-3} in. was calculated. From equation (18) and the thickness modification for the effects of perforation can be derived as follows:

$$(1-F_v)P_{cr} = \frac{\hat{G}^L_p(t,F_v)}{\hat{G}^L(t)} \frac{\hat{G}^L(t)}{t} \frac{24}{\pi R^2 k^{\frac{1}{2}}} \left[\frac{10^{-2} k\rho}{4} + \frac{1}{\rho} \right]$$

or
$$\frac{1-F_v}{Q(F_v)} \cdot H(t) = F^c(\rho) \qquad (20)$$

where F_v = void fraction

$$Q(F_v) = \frac{\hat{G}^L_p(t=0.30\times10^{-3})}{\hat{G}^L(t=0.30\times10^{-3})} = \frac{\text{Flexural rigidity after perforation of 0.30 mil laminated film}}{\text{Flexural rigidity before perforation of 0.30 mil laminated film}}$$

Equation (20) may be further modified in the following way

$$H(t) = \frac{F^c(\rho)}{A(F_v)} \qquad (21)$$

where $A(F_v) = \frac{1-F_v}{Q(F_v)}$

The most conservative film thickness of an unperforated laminate must satisfy the relation $H(t) = \min F^c(\rho)$. For a given void fraction F_v the conservative thickness of film required to withstand the specified buckling pressure must satisfy the following equation

$$H(t) \leq \frac{\min F^c(\rho)}{A(F_v)} \qquad (22)$$

or, conversely, for a given thickness a safe void fraction will satisfy equation (22). With H(t) established from min $F^c(\rho)$, [i.e., $H(t) = \min F^c(\rho)$], Figure 14, for unperforated laminate and the safe F_v requirement established by equation (22), it follows that $A(F_v) \leq 1$. With this condition established, the optimum void fraction, F_v, that allows $W_A = (1-F_v)(\rho t + \rho_{cu}\, t_{cu})$ to be a minimum can be determined. From the $A(F_v)$ curve (Figure 16) experimentally established (from flexural rigidity ratios $Q(F_v)$ see Fig. 15) and the condition $A(F_v)$ 1, F_v is found to be 0.40. Due to the fact that the data has been taken up to $F_v = 0.40$ and the fact that $A(F_v) = \frac{1-F_v}{Q(F_v)}$ will increase, above 0.40, since $Q(F_v)$ will decrease due to losses in rigidity from large fractions of open area, $F_v = 0.40$ was chosen to be the safe optimum point.

From the value of $F_v = 0.40$ and the unperforated satellite weight found to be 1494.384 lbs., the final perforated satellite weight is found to be:

$$W_T = (1-F_v)(1494.44 = 0.60(1494.44) = 896.6 \text{ lbs.}$$

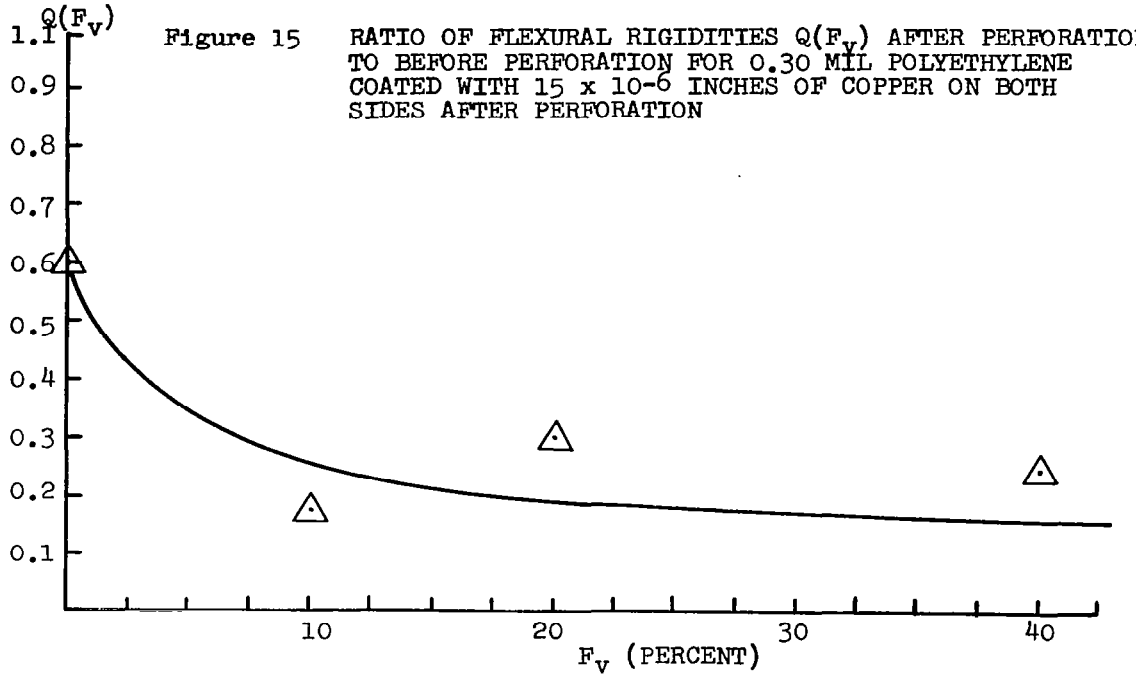

Figure 15 RATIO OF FLEXURAL RIGIDITIES $Q(F_V)$ AFTER PERFORATION TO BEFORE PERFORATION FOR 0.30 MIL POLYETHYLENE COATED WITH 15 x 10-6 INCHES OF COPPER ON BOTH SIDES AFTER PERFORATION

Figure 16 THE FUNCTION $A(F_V) = \frac{1 - F_V}{Q(F_V)}$ WHERE $Q(F_V)$ IS GIVEN IN FIGURE 15

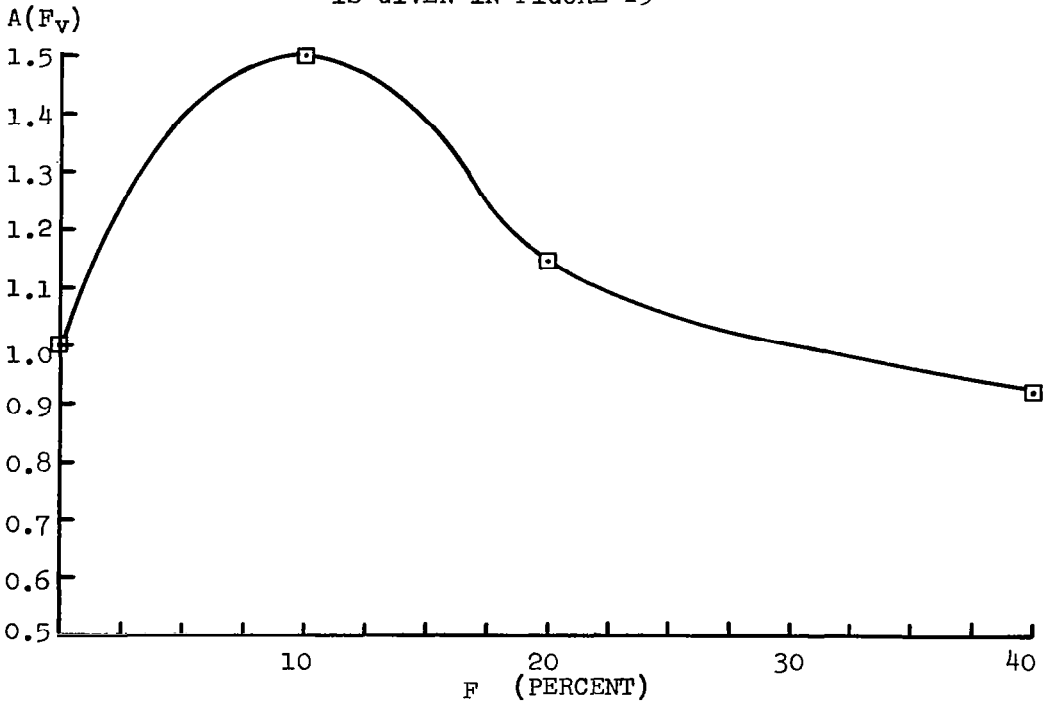

4.0 TEST MODELS AND PRODUCTION

The necessary procedures for the production of the large size satellites were also investigated during this program. In addition specific deliverable items (a spherical cap section, cylinders, and flat sections) were built. These models were constructed for two reasons:

(1) to investigate the problems involved in building fairly large size items from metallized plastics possessing the memory effect and

(2) to test the radio-frequency characteristics of the perforated metallized material. These studies resulted in the following:

a) Establishment of operating variables and procedures necessary for production of large test models.

b) The production of test items.

c) Design information necessary for scale-up.

The procedure for the production of a metallized expandable polyethylene item is briefly outlined below:

(1) Production of plastic film of known gauge and density; this is made by a film extruder.

(2) Irradiation of the extruded plastic - to impart "memory".

(3) Heat treatment - to impart dimensional stability.

(4) Perforation - if the material is a film it may be perforated to lower its weight and increase its resistance to solar pressure.

(5) Metallization - to impart radio-frequency reflectance characteristics and to increase the strength of the material.

(6) Cutting (Note 1) to cut the material into convenient gore sections for fabrication.

(7) Ultrasonic Bonding - to bond the gore sections into a single unit.

(8) Packaging - to reduce the volume of the structure and permit storage prior to deployment.

4.1 Operating Variables and Procedures in Construction of large deliverable items

The operating variables were established in experimenting first with the polyethylene mesh and then with the film. The procedures established are essentially the same, after the completion of step (2) above, for both the mesh and the film. Any differences will be mentioned as they occur. Emphasis will be given to the film since it will be used in the construction of the deliverable items and ultimately used in the construction of the sphere.

4.1.1 Base Material Manufacture

4.1.1.1 Film Extrusion

The biaxially oriented intermediate density polyethylene, film (PE12) is commercially available from Sea Space Systems Inc. Its manufacturing procedure is similar to that described in section 1.2.3 and reference 4.

NOTE 1

It should be noted that a thermal control coating must be applied at this stage, in a production schedule, for proper temperature control in space. The study of thermal control coatings was not included in the scope of this contract, although it will be investigated in a following study.

4.1.1.2 Mesh Production

Described in Section 1.2.3 above.

4.1.2 Irradiation

4.1.2.1 Dosage

Work under contract NASr-78 and the extraction study discussed in Section 1.2.1 indicate that a radiation dose of 15 Mrads is sufficient to induce a plastic memory into the polyethylene film. Higher doses may be required to increase the memory forces if needed.

4.1.2.2 Irradiation Source

Nearly all of the irradiation performed during this program was done using an electron accelerator. Some experimental sections of mesh were irradiated using a Co^{60} gamma source. The properties of the resultant mesh indicated that it was unsuitable for use in this program due to non-uniformity of absorbed dose.

4.1.2.3 Irradiation Atmosphere Tests

4.1.2.3.1 Initial Tests: Air, Nitrogen

A series of tests were performed to determine the effects of irradiation atmosphere and heat treatment on irradiated polyethylene film in preparation for the irradiation and heat treatment of the materials for the deliverable items. Various samples of film were irradiated to 15 Mrads. Some of the samples were irradiated in a nitrogen atmosphere, others in an air atmosphere. Half of the above irradiated samples were immediately heat treated to ca. $100^{o}C$. The irradiation, heat treatment atmosphere scheme is shown in Table 19.

Table 19

Irradiation Heat Treatment Atmosphere Experimental Scheme (Air, Nitrogen) Irradiation of 1 Mil Sea Space Polyethylene Film to 15 Mrads

Run. No.	Irradiation Atmosphere	Heat Treatment Atmosphere
1	Nitrogen	Nitrogen
2	Air	Nitrogen
3	Nitrogen	No Heat Treatment
4	Air	No Heat Treatment

Tensile tests were then performed about once every three days for almost a month. The tests which were repeated twice, A & B runs, (see Figures 17-20) in general show an increase in strength (reported as modulus of elasticity, E) with time which appears to persist. It is believed that some of the variations in the results are caused by the competing effects of oxygen degradation and post-irradiation crosslinking. Both effects are caused by residual post-irradiation trapped free radicals caused by the entering electrons. It therefore appears that the initial heat treatment given to some of the samples was not sufficient enough to decay the free radicals.

With the possibility in mind that the initial heat treatment was not sufficient to eliminate the free radicals, all four of the samples were carefully heat treated above their crystalline melting point on the 12th day (this means that two of the samples were heat treated twice.) Tensile tests were then performed on the samples to check for variations with time. The results, shown in Figures 21-24 still in general appear to rise somewhat, although the variation is less than before the second heat treatment.

4.1.2.3.2 Tests: Oxygen, Nitrogen, Air

To further evaluate the effects of atmosphere (especially the effect of oxygen) on polyethylene film during irradiation, samples of film were irradiated and heat treated in an oxygen atmosphere in combination with the other gases used in the first part of the experiment (nitrogen and air). The tests were conducted according to the scheme outlined in Table 20. Tensile tests were again conducted approximately every three days for three weeks.

Table 20

Irradiation Heat Treatment Atmosphere Experimental Scheme (Oxygen, Nitrogen, Air) Irradiation of 1 Mil Sea Space Polyethylene Film to 15 Mrads

Run No.	Irradiation Atmosphere	Heat Treatment
1	Oxygen	Oxygen
2	Oxygen	Nitrogen
3	Oxygen	None
4	Nitrogen	Oxygen
5	Air	Air

The results of this set of tests are summarized in Figures 25 - 29. In general, there is a fairly sharp increase in strength for all of the runs a few days after irradiation which then levels off approximately in 18 days. The samples show larger increases in strength in the 90° direction than in the 0° direction. In all cases there appears to be no degradation. In fact there is a net increase in strength for all tests. Also, the fact that there was a net increase (although small) in strength with samples irradiated in oxygen and heat treated in oxygen, indicates with some certainty that the effect of oxygen is not critical in the irradiation or

heat treatment of this polyethylene film under the conditions used in our evaluation. These results lead to the conclusion that irradiation and heat treatment in air will present no problem with regard to oxygen degradation. In fact, run No. 5, Figure 29 irradiation and heat treatment in air, shows approximately 10 psi increase at steady state over its initial unirradiated conditions. Additionally, samples originally irradiated for this program were tested after six months. These samples showed no degradation.

4.1.2.3.3 Effect of Dose

For informational purposes the initial tests listed in Table 19 were run at 30 Mrads to check the effect of increasing the dose on the strength time curves of the film. The results are given in Figures 30 - 33. The results in general increase sharply upon irradiation and gradually decrease. The decrease, although noticeable, does not indicate any serious degradation.

Figure 17 STRENGTH-TIME CURVES FOR IRRADIATED(15 MRADS) 1 MIL SEA SPACE STANDARD DENSITY POLYETHYLENE FILM

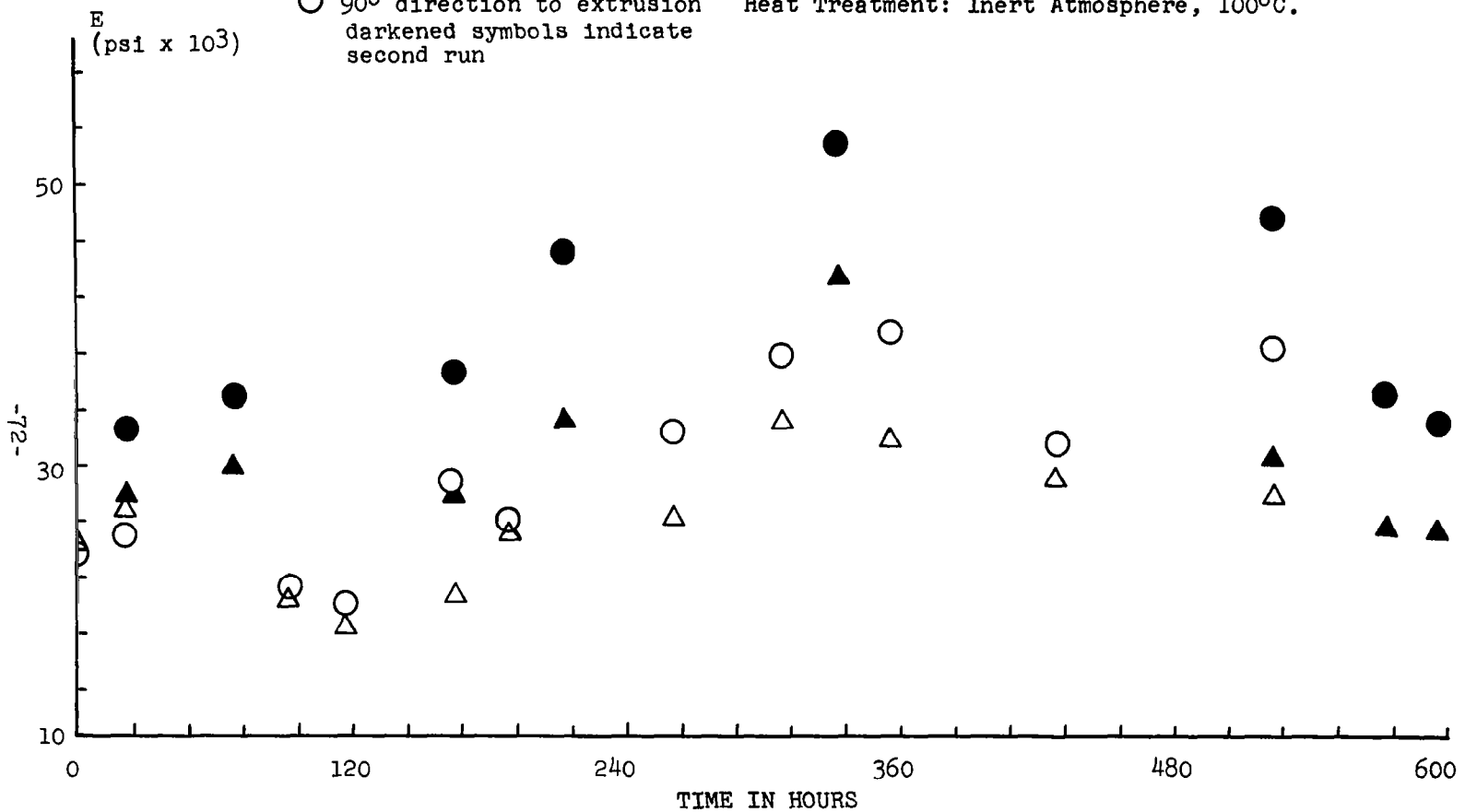

Figure 18 STRENGTH-TIME CURVES FOR IRRADIATED (15 MRADS) 1 MIL SEA SPACE STANDARD DENSITY POLYETHYLENE FILM

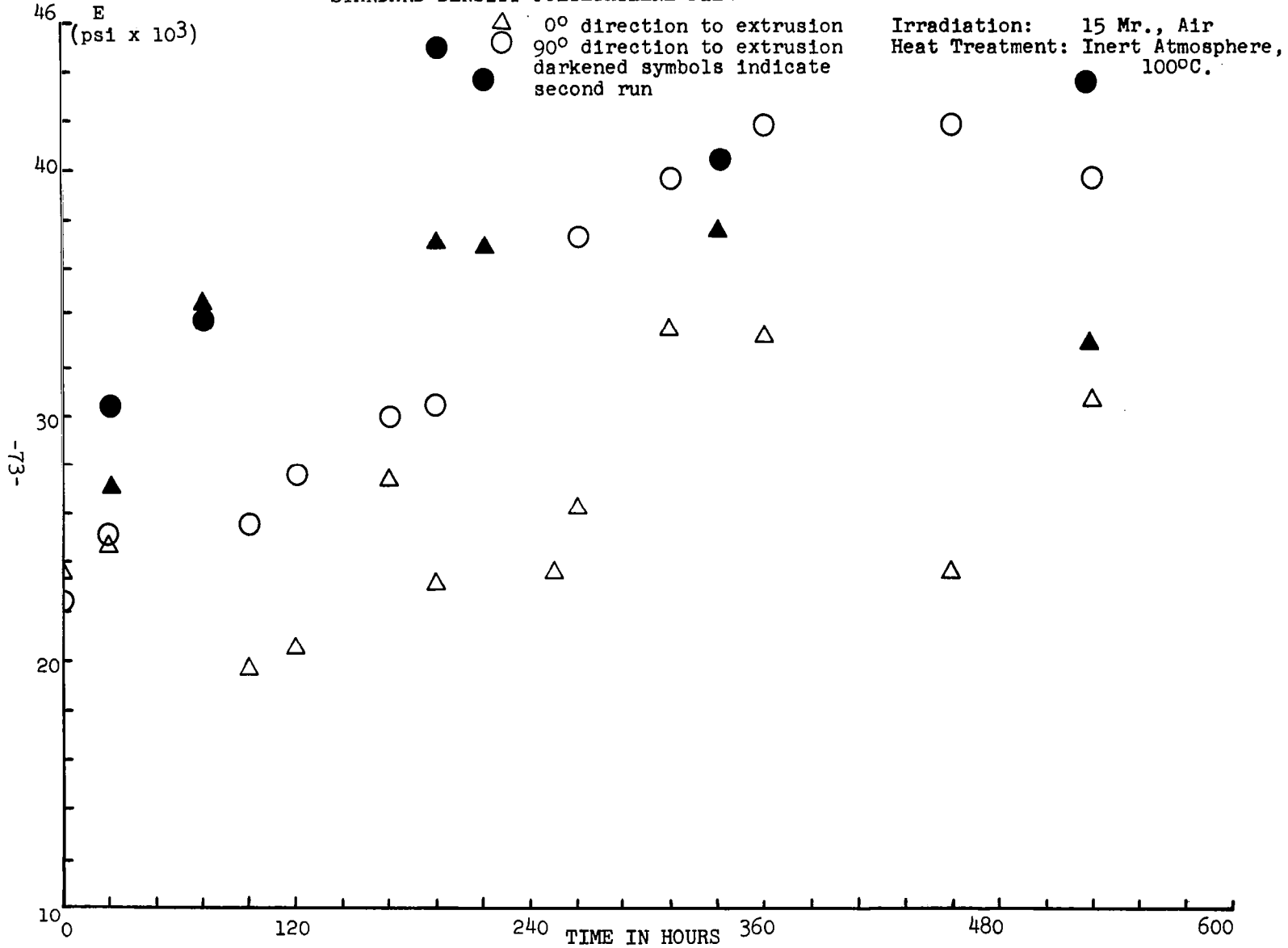

Figure 19 STRENGTH-TIME CURVES FOR IRRADIATED (15 MRADS) 1 MIL SEA SPACE STANDARD DENSITY POLYETHYLENE FILM

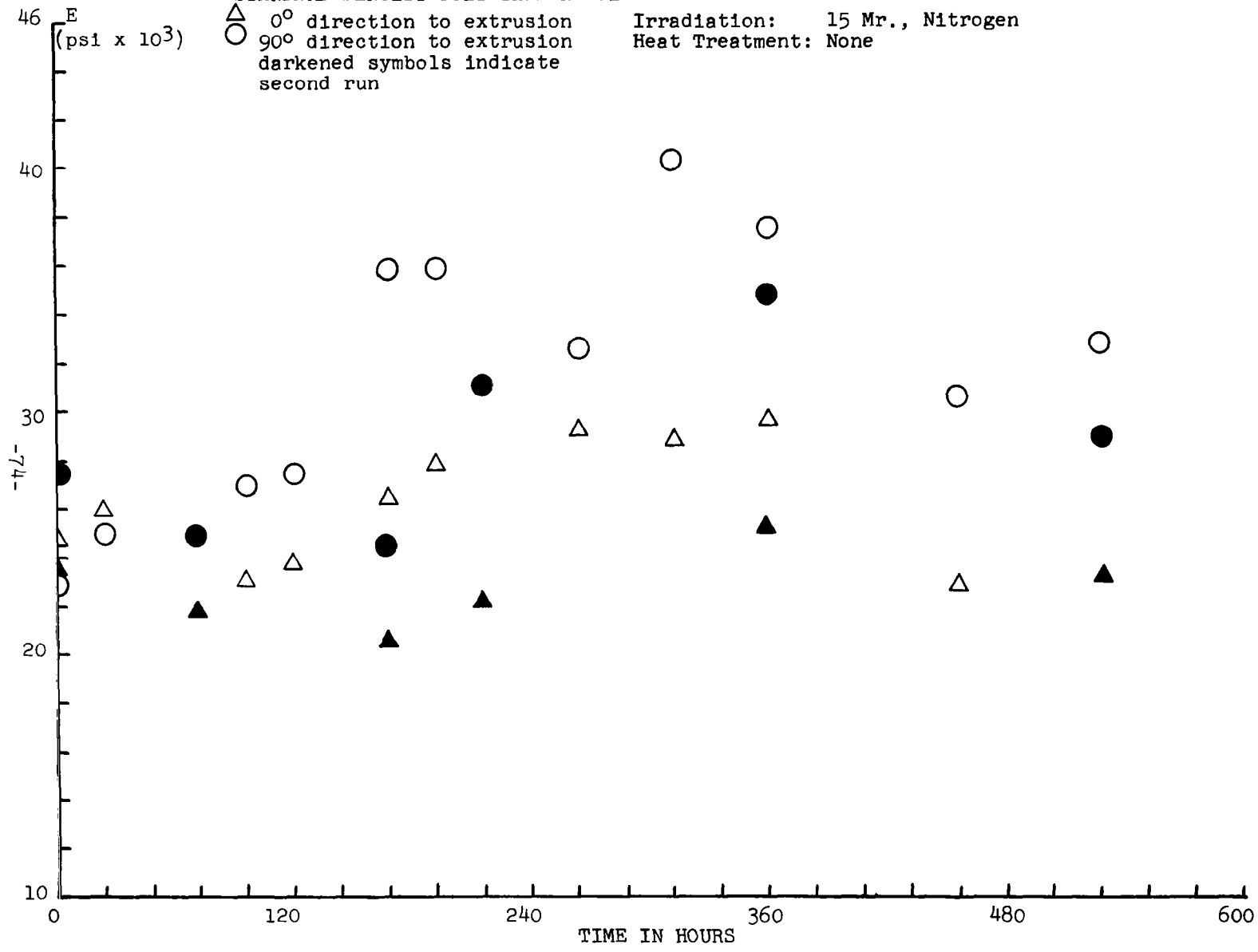

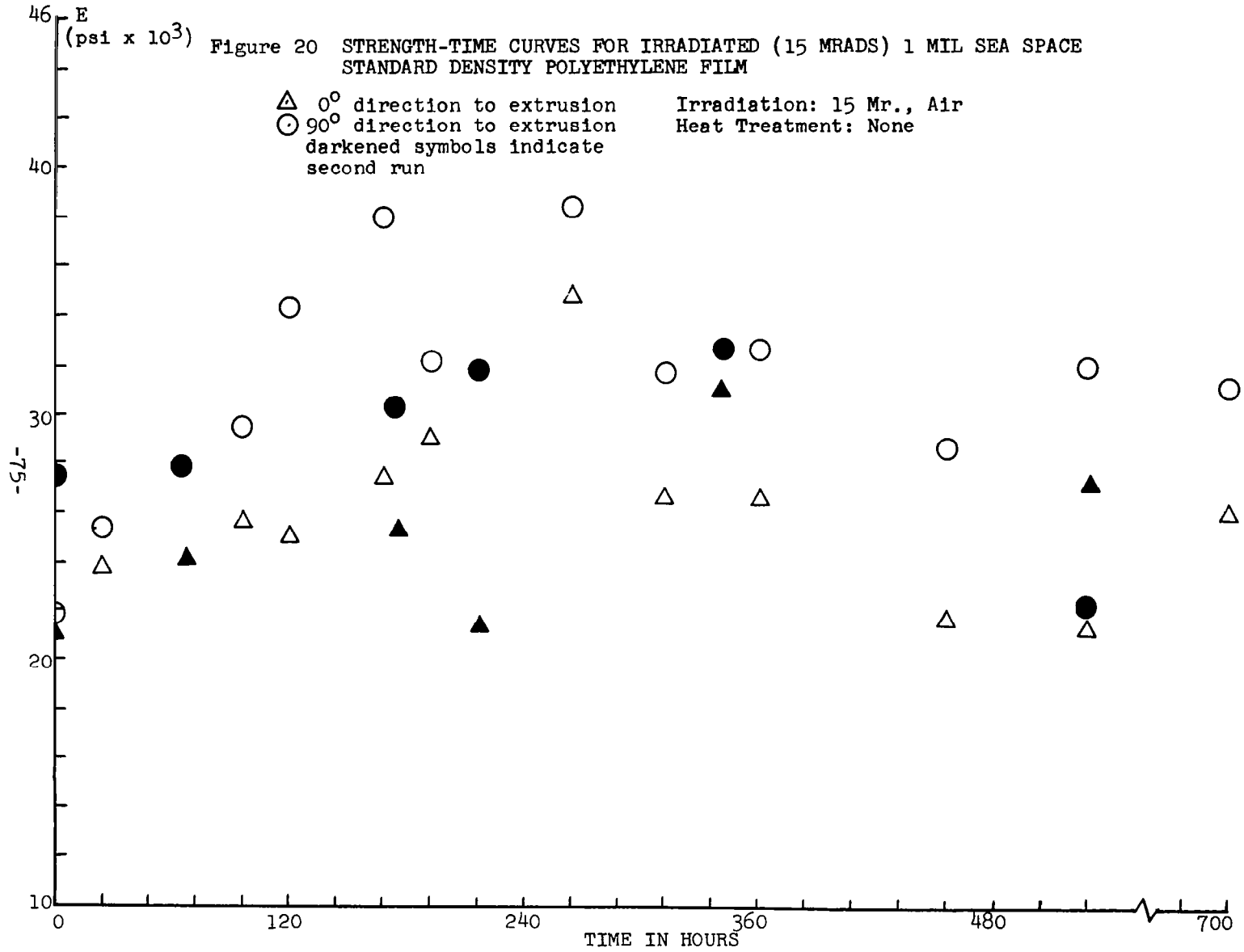
E
(psi x 10³)
46
40
30
20
10
0
120
240
360
480
700
TIME IN HOURS
Figure 20 STRENGTH-TIME CURVES FOR IRRADIATED (15 MRADS) 1 MIL SEA SPACE STANDARD DENSITY POLYETHYLENE FILM
△ 0° direction to extrusion
⊙ 90° direction to extrusion
darkened symbols indicate second run
Irradiation: 15 Mr., Air
Heat Treatment: None

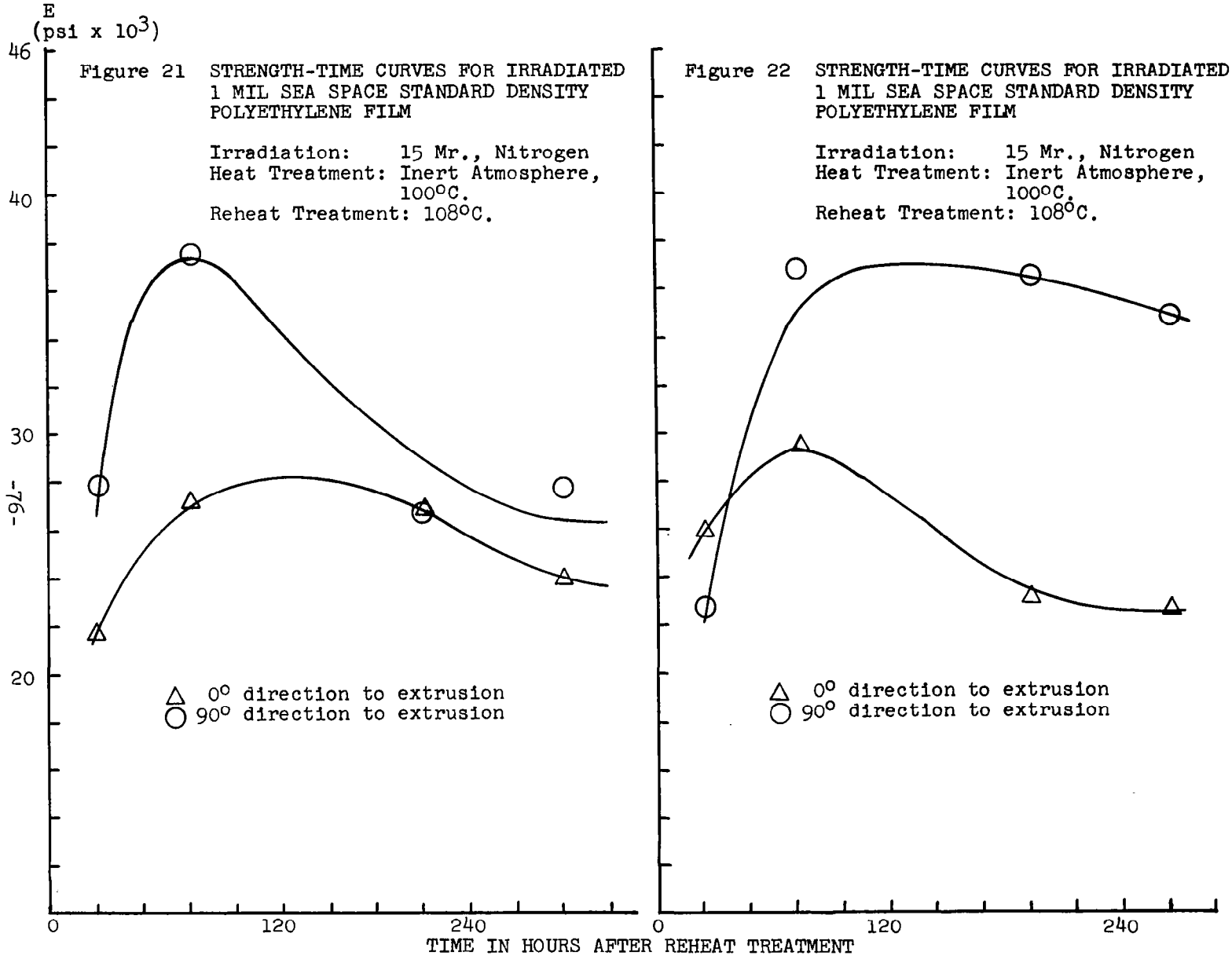
E
(psi x 10^3)
46
40
30
20
0
120
240
TIME IN HOURS AFTER REHEAT TREATMENT
Figure 21 STRENGTH-TIME CURVES FOR IRRADIATED 1 MIL SEA SPACE STANDARD DENSITY POLYETHYLENE FILM
Irradiation: 15 Mr., Nitrogen
Heat Treatment: Inert Atmosphere, 100°C.
Reheat Treatment: 108°C.
△ 0° direction to extrusion
○ 90° direction to extrusion
Figure 22 STRENGTH-TIME CURVES FOR IRRADIATED 1 MIL SEA SPACE STANDARD DENSITY POLYETHYLENE FILM
Irradiation: 15 Mr., Nitrogen
Heat Treatment: Inert Atmosphere, 100°C.
Reheat Treatment: 108°C.
△ 0° direction to extrusion
○ 90° direction to extrusion

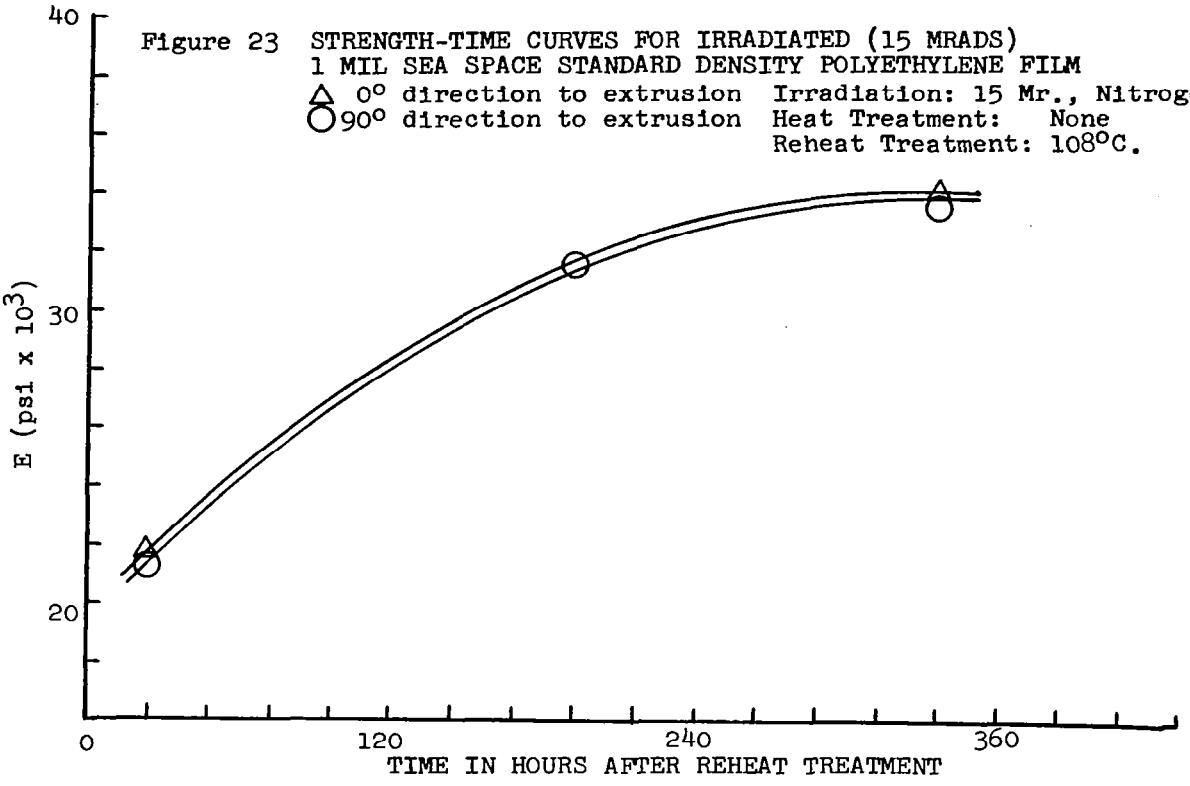

Figure 23 STRENGTH-TIME CURVES FOR IRRADIATED (15 MRADS)
1 MIL SEA SPACE STANDARD DENSITY POLYETHYLENE FILM
△ 0° direction to extrusion Irradiation: 15 Mr., Nitrogen
○ 90° direction to extrusion Heat Treatment: None
Reheat Treatment: 108°C.

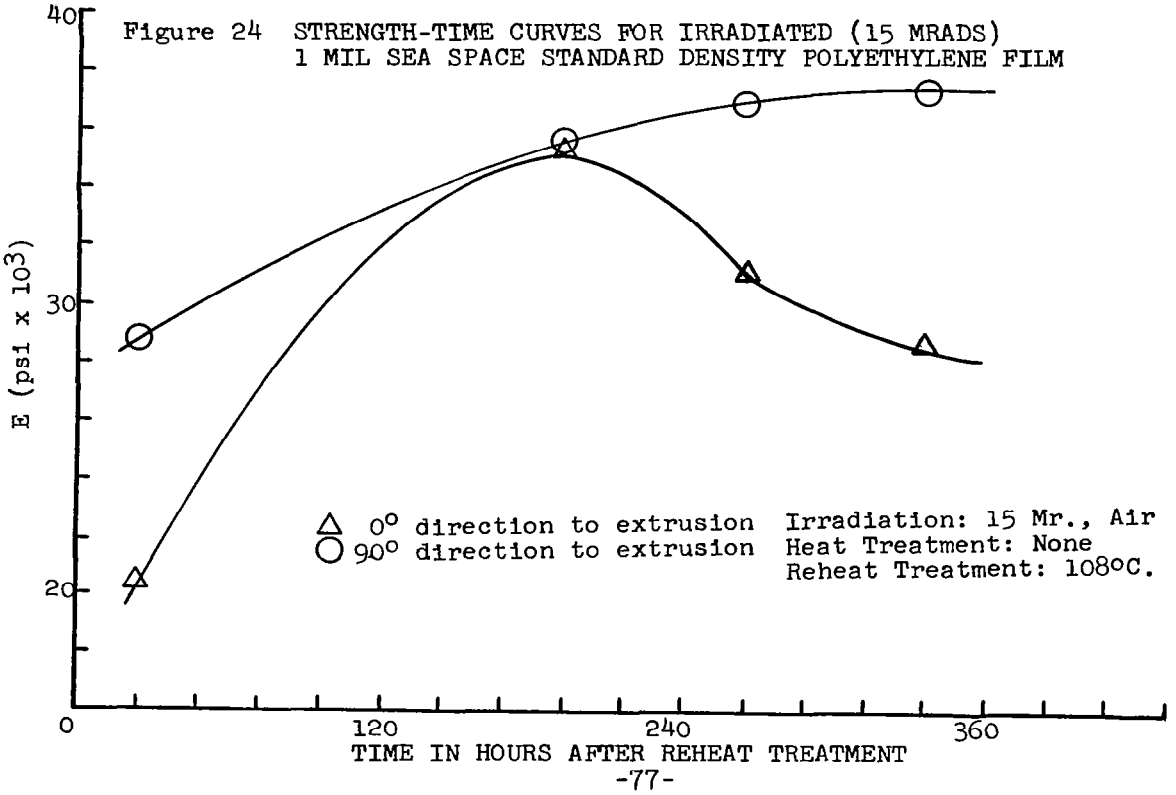

Figure 24 STRENGTH-TIME CURVES FOR IRRADIATED (15 MRADS)
1 MIL SEA SPACE STANDARD DENSITY POLYETHYLENE FILM
△ 0° direction to extrusion Irradiation: 15 Mr., Air
○ 90° direction to extrusion Heat Treatment: None
Reheat Treatment: 108°C.

Figure 25 STRENGTH-TIME CURVES FOR IRRADIATED (15 MRADS) 1 MIL SEA SPACE STANDARD DENSITY POLYETHYLENE FILM

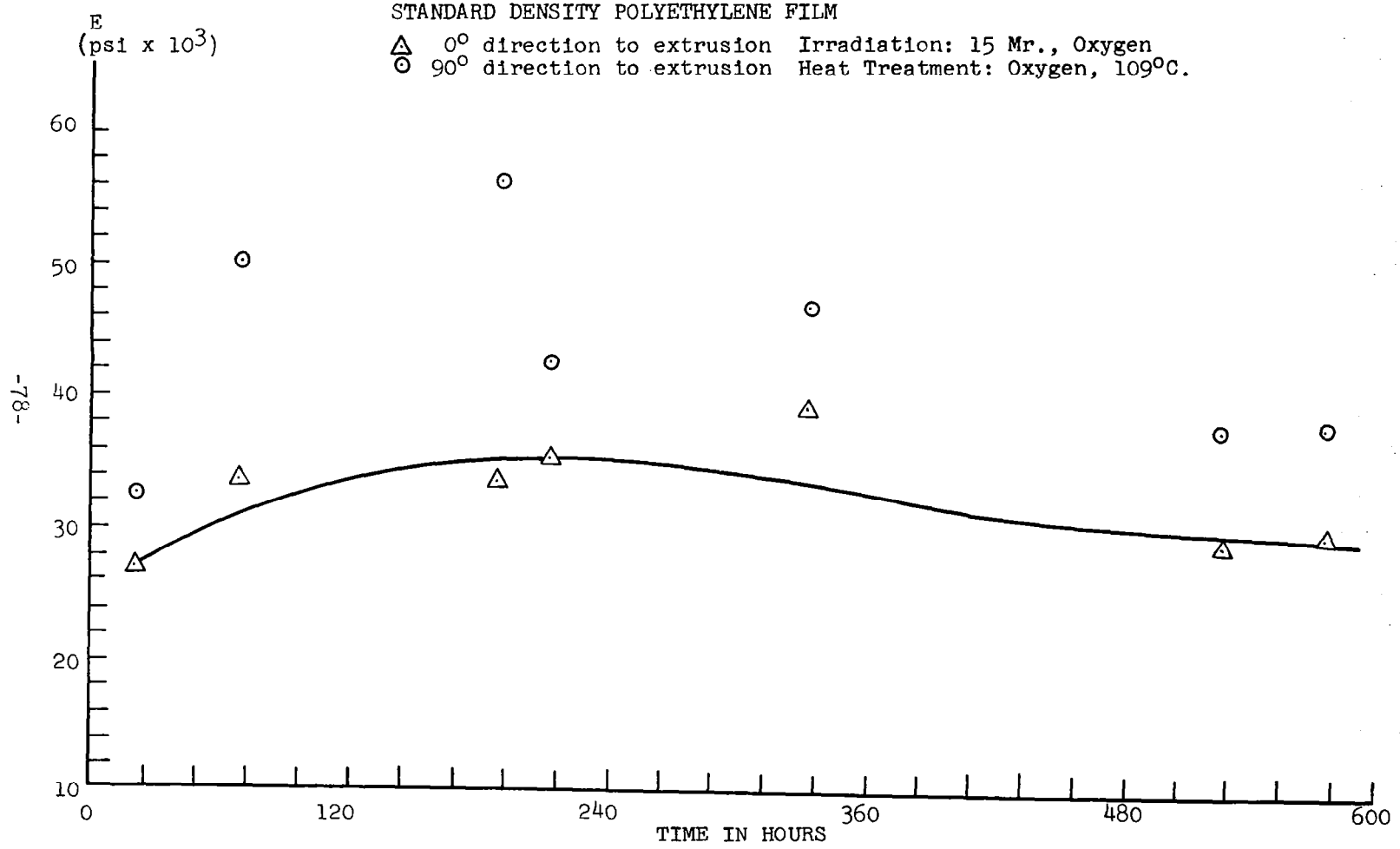

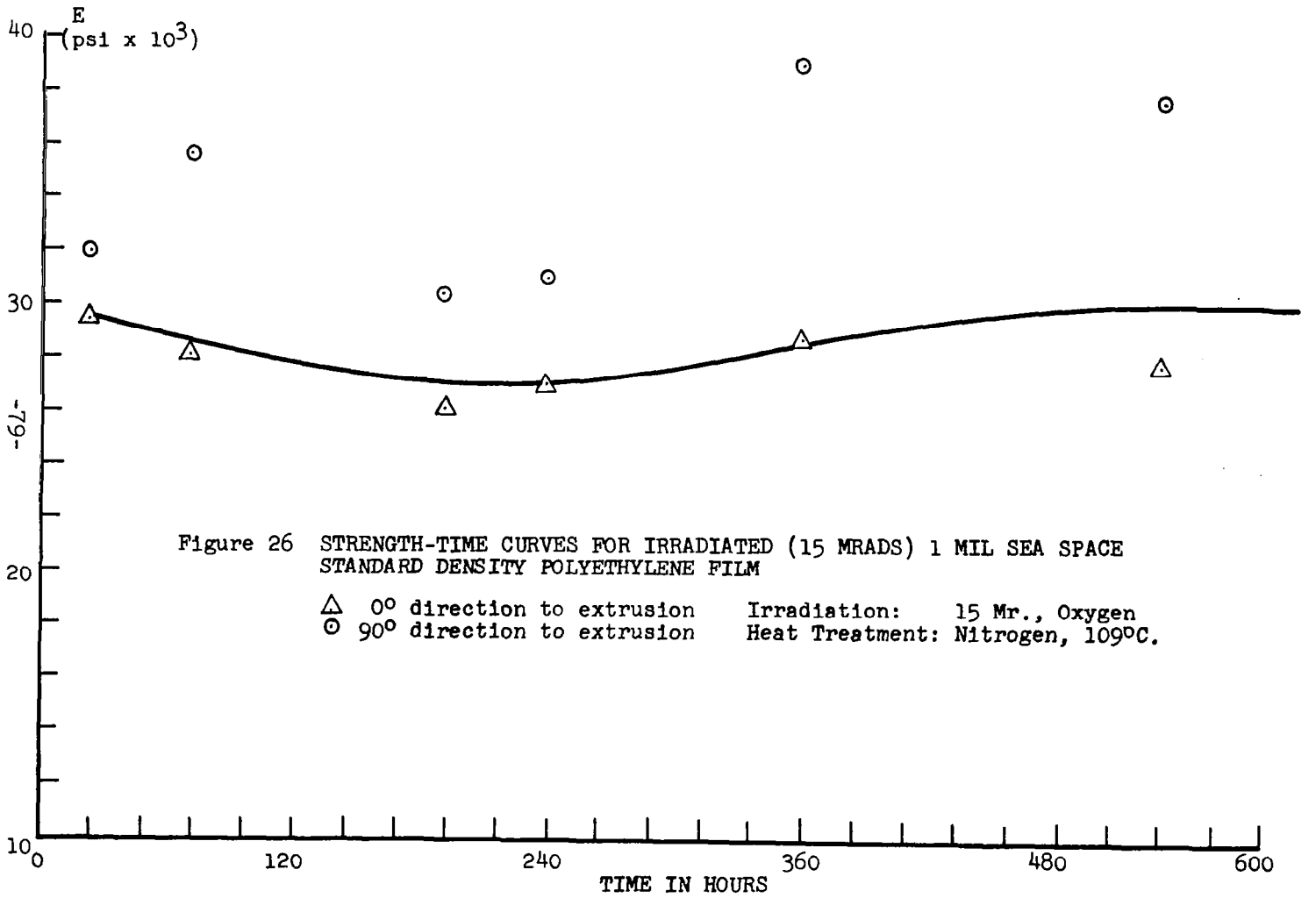

Figure 26 STRENGTH-TIME CURVES FOR IRRADIATED (15 MRADS) 1 MIL SEA SPACE STANDARD DENSITY POLYETHYLENE FILM

△ 0° direction to extrusion
⊙ 90° direction to extrusion

Irradiation: 15 Mr., Oxygen
Heat Treatment: Nitrogen, 109°C.

Figure 27 STRENGTH-TIME CURVES FOR IRRADIATED (15 MRADS) 1 MIL SEA SPACE STANDARD DENSITY POLYETHYLENE FILM

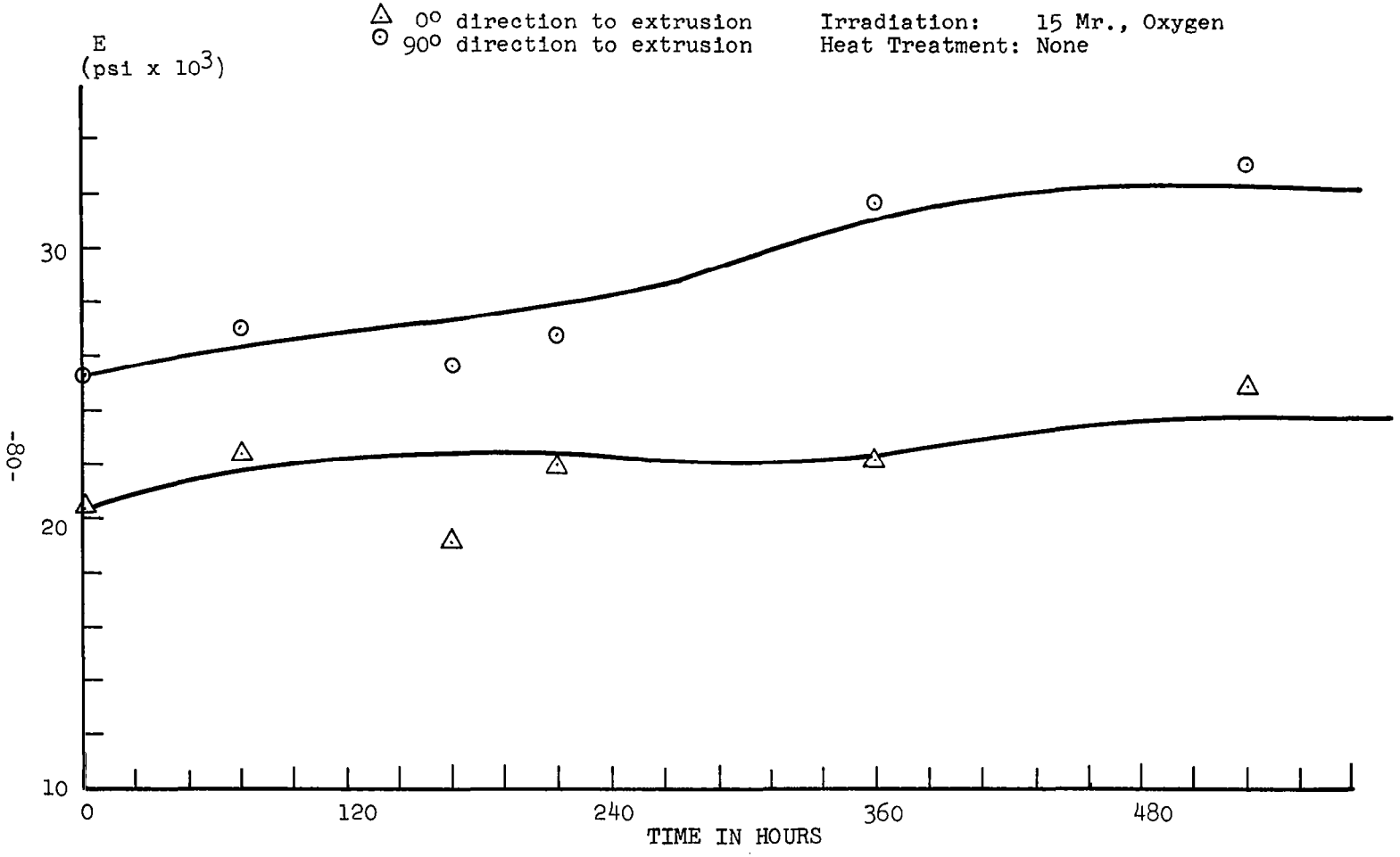

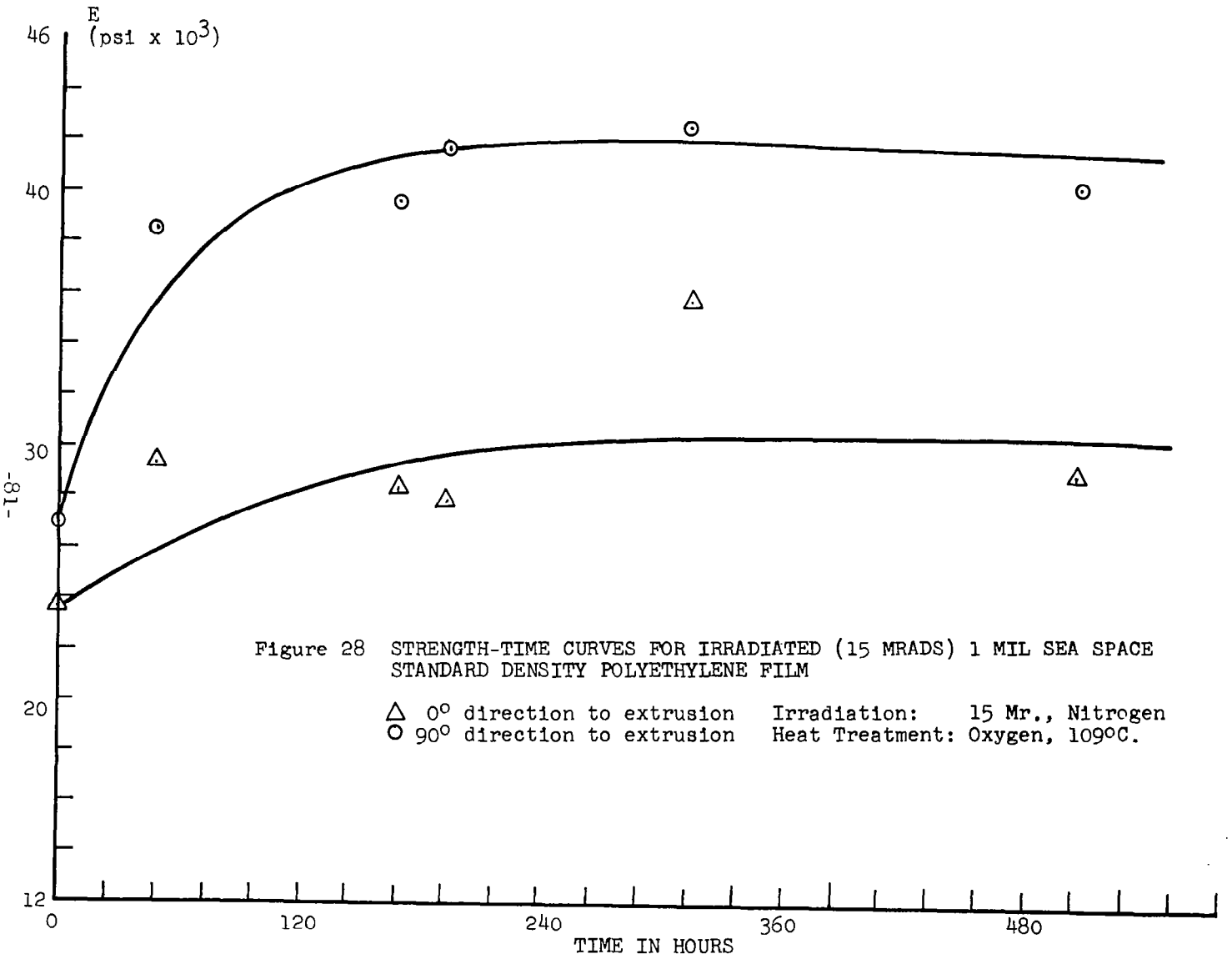

Figure 28 STRENGTH-TIME CURVES FOR IRRADIATED (15 MRADS) 1 MIL SEA SPACE STANDARD DENSITY POLYETHYLENE FILM

△ 0° direction to extrusion Irradiation: 15 Mr., Nitrogen
○ 90° direction to extrusion Heat Treatment: Oxygen, 109°C.

Figure 29 STRENGTH-TIME CURVES FOR IRRADIATED (15 MRADS)
1 MIL SEA SPACE STANDARD DENSITY POLYETHYLENE FILM

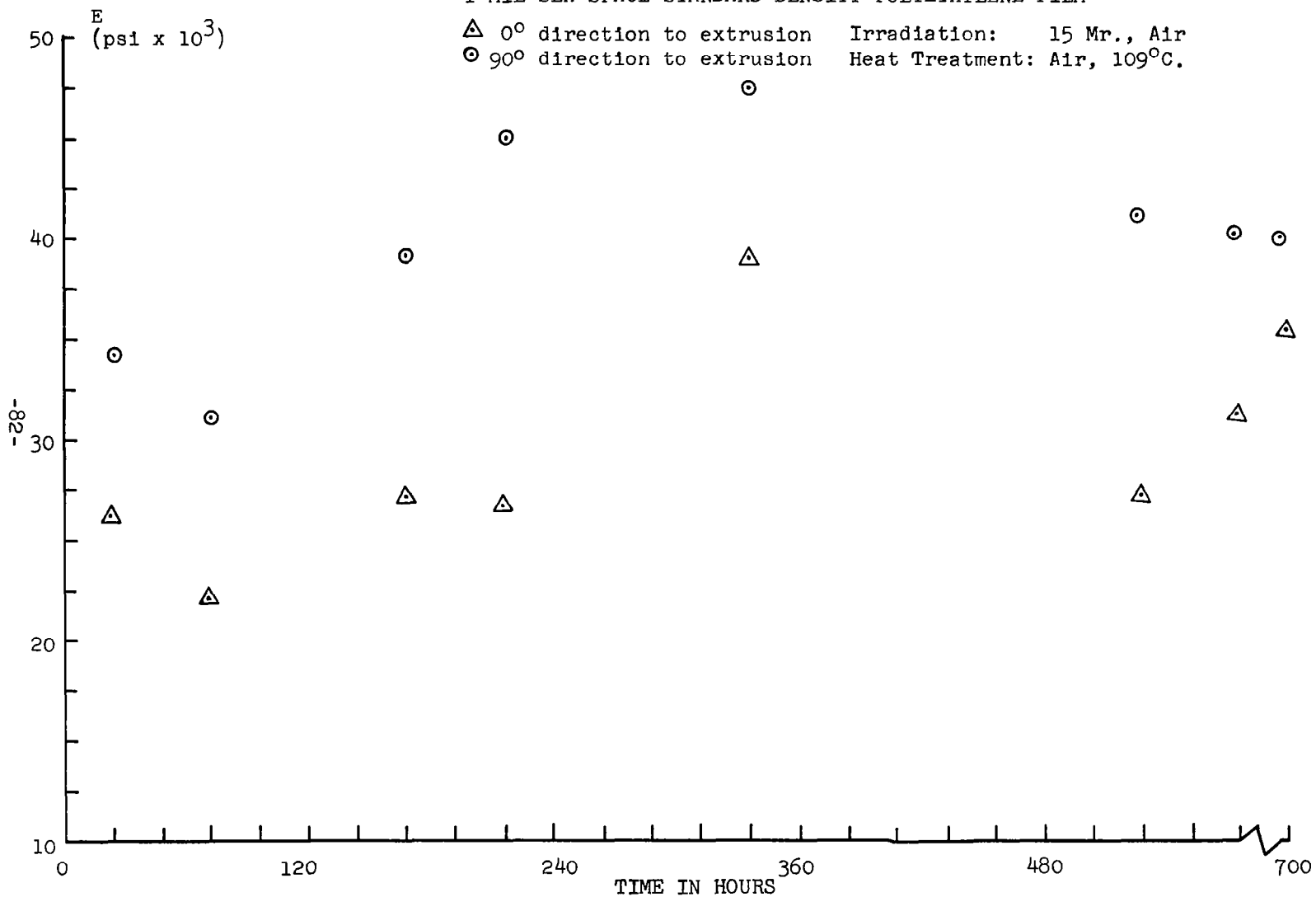

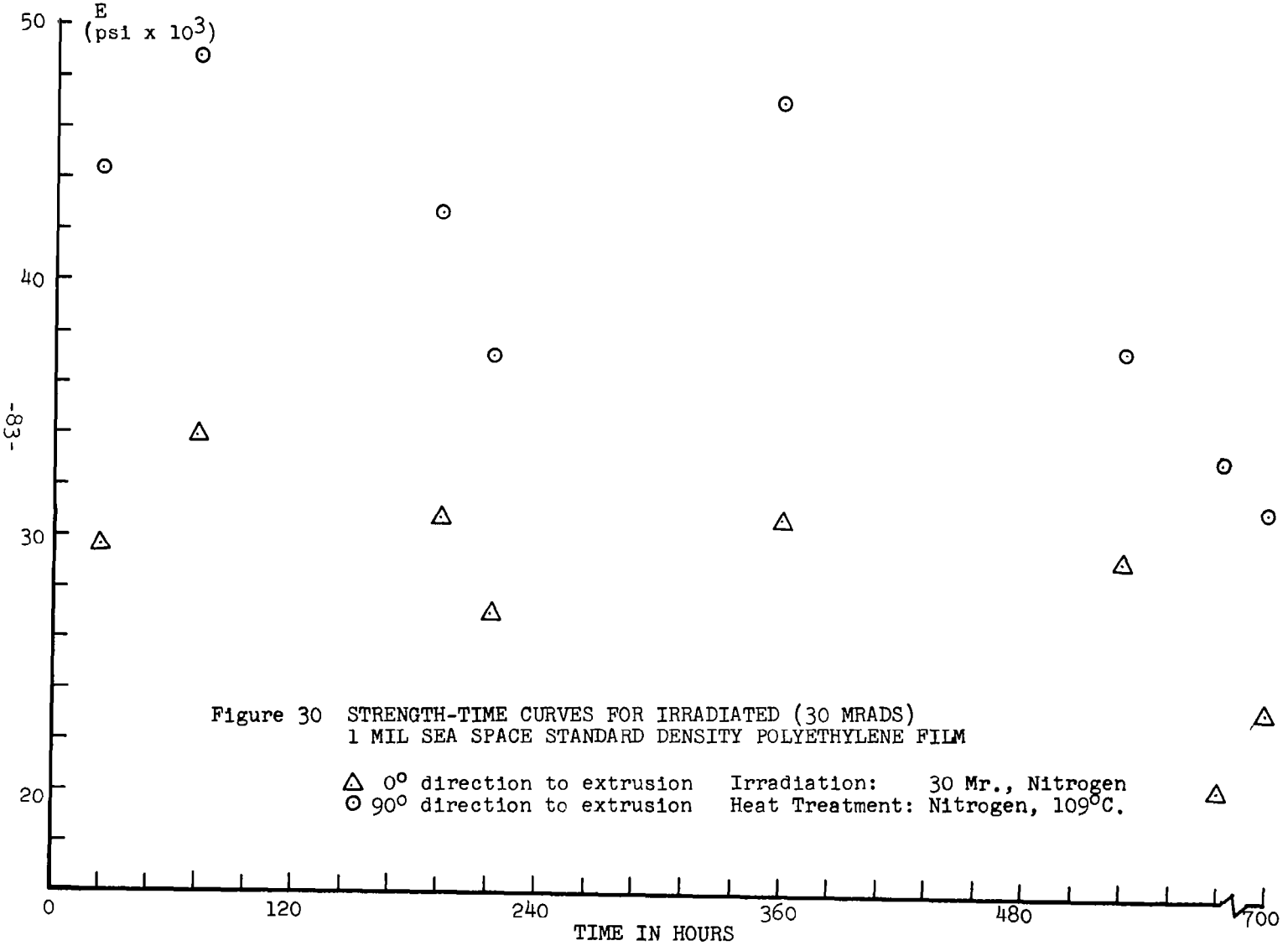

Figure 30 STRENGTH-TIME CURVES FOR IRRADIATED (30 MRADS)
1 MIL SEA SPACE STANDARD DENSITY POLYETHYLENE FILM

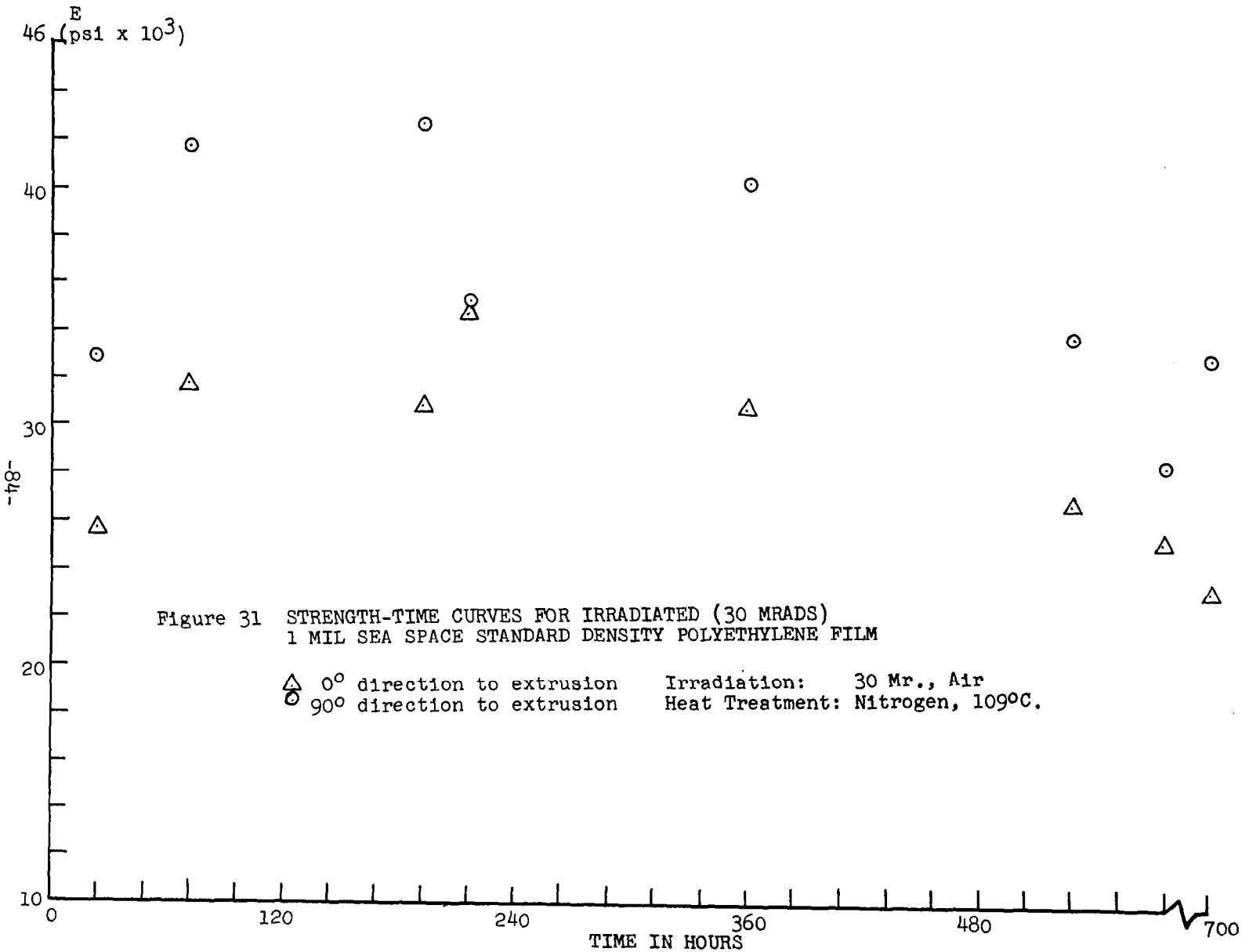

Figure 31 STRENGTH-TIME CURVES FOR IRRADIATED (30 MRADS)
1 MIL SEA SPACE STANDARD DENSITY POLYETHYLENE FILM

Figure 32 STRENGTH-TIME CURVES FOR IRRADIATED (30 MRADS)
1 MIL SEA SPACE STANDARD DENSITY POLYETHYLENE FILM

△ 0° direction to extrusion Irradiation: 30 Mr., Nitrogen
○ 90° direction to extrusion Heat Treatment: None

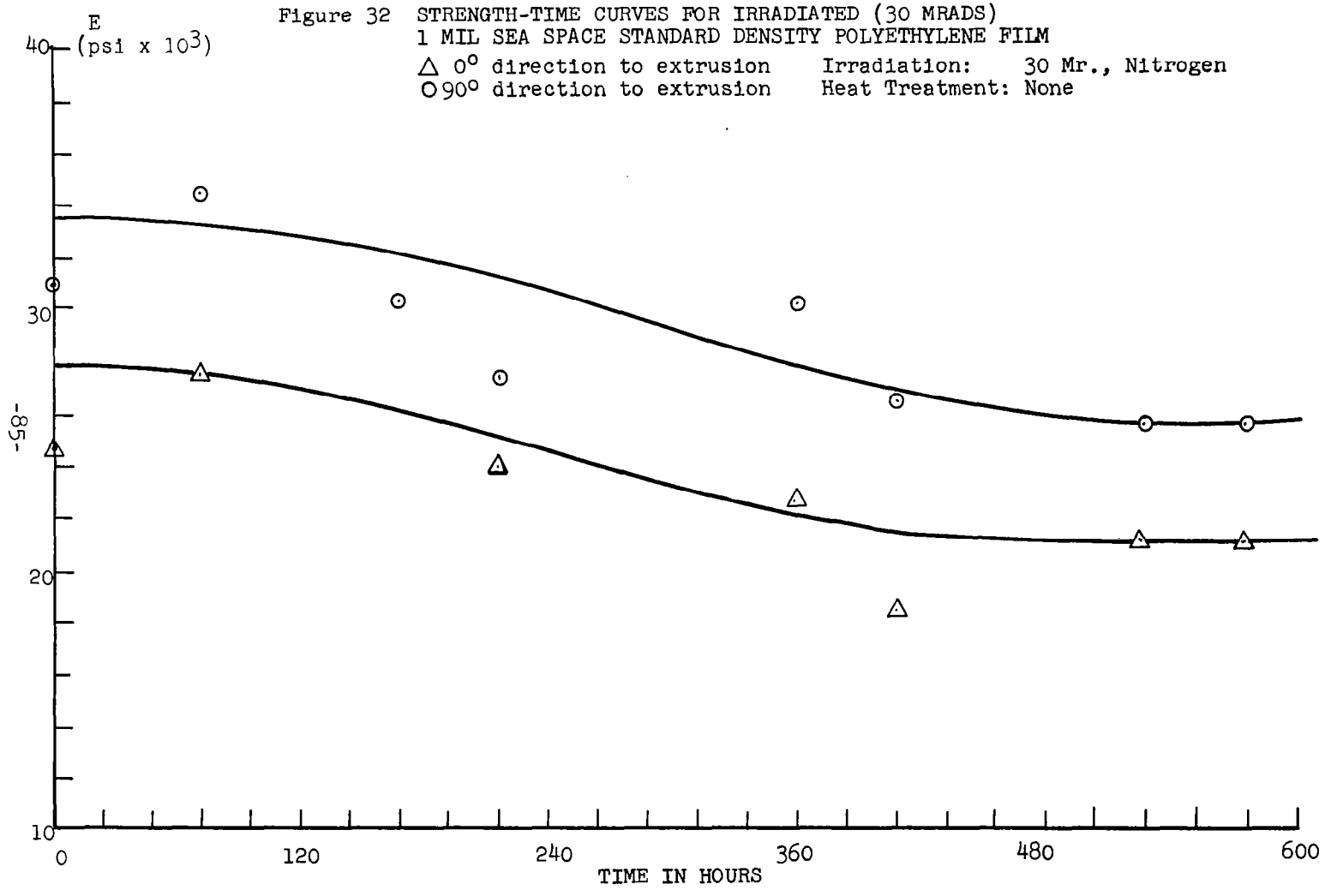

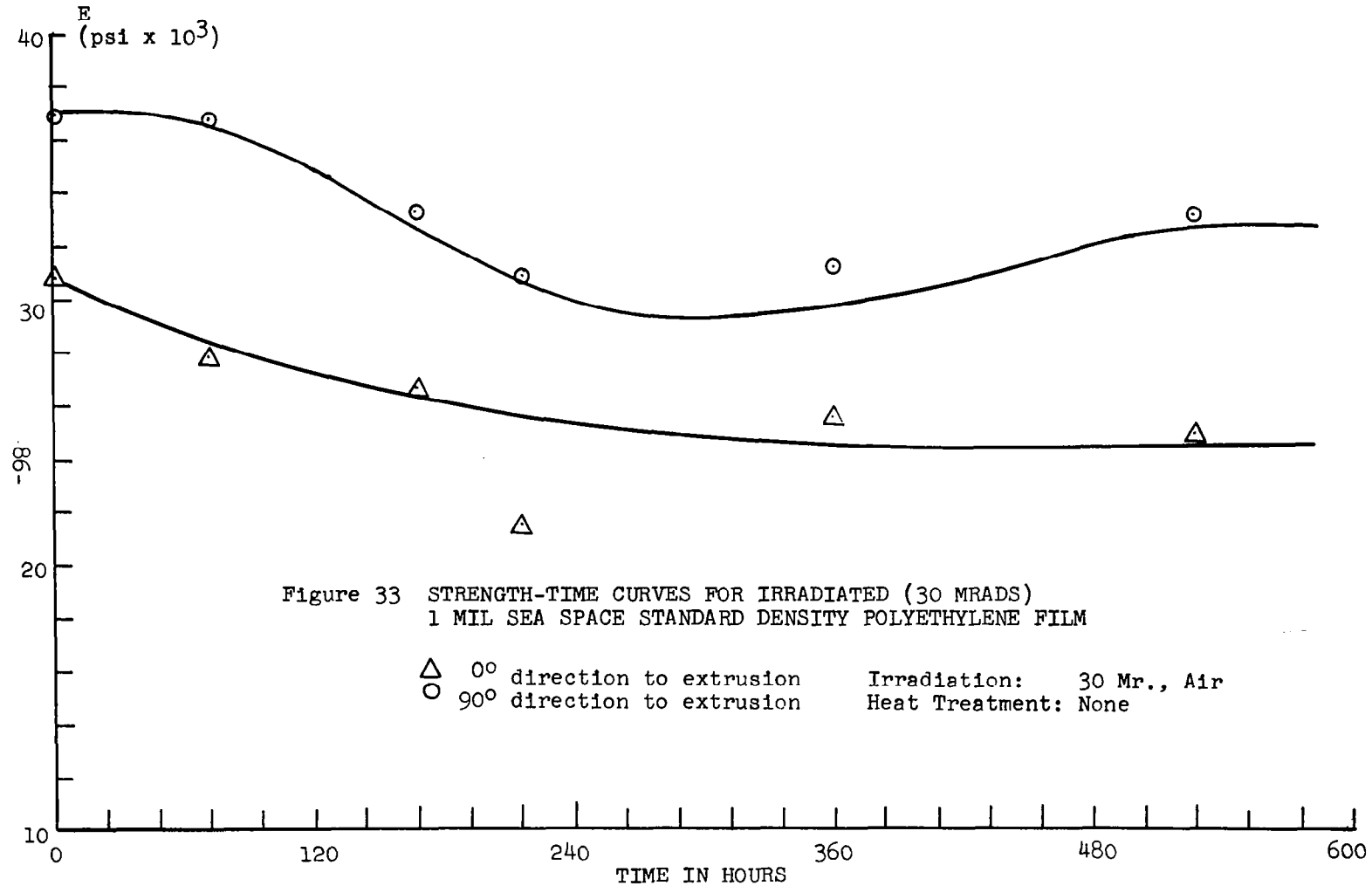

Figure 33 STRENGTH-TIME CURVES FOR IRRADIATED (30 MRADS)
1 MIL SEA SPACE STANDARD DENSITY POLYETHYLENE FILM

△ 0° direction to extrusion
○ 90° direction to extrusion

Irradiation: 30 Mr., Air
Heat Treatment: None

4.1.2.3.4 Scatter in the Irradiation Atmosphere Tests

The scatter observed in many of the irradiation strength-time tests is in all probability due to the effects of the effectiveness of dose variation with sample thickness. For a given sample (or bundle of samples) of a material the dose at the surface of the sample and to about 2mm. inward is not 100% effective since the high speed of the electrons do not have sufficient time to interact with the molecules. Data showing how interaction efficiency varies with depth from the surface is given in Figure 34, which was taken from "Radiation Chemistry of Polymeric Systems." [19]

Figure 34: PERCENTAGE DEPTH DOSE IN WATER FOR HIGH ENERGY ELECTRONS

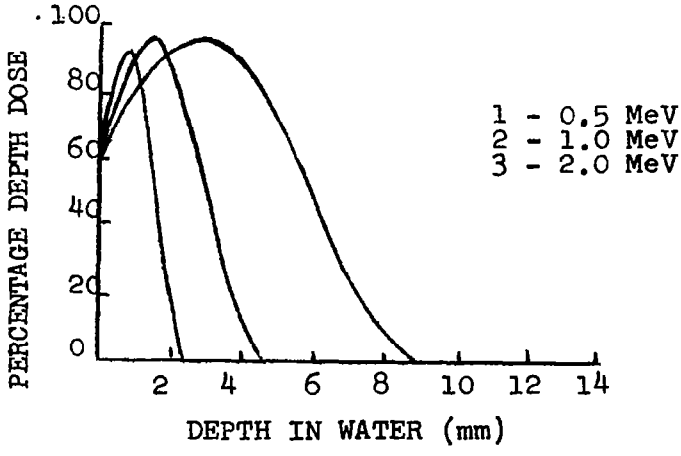

It can be seen that for a 1.0 Mev accelerator the effective dose may vary between 60 and 100% for samples 2 mm. thick or less. It is believed that since many of our samples were within this depth range, they received non-uniform doses as given by the above curve. This situation has been corrected for the irradiation of the deliverable items and samples for the testing program. The applied dose was increased to account for the lower efficiency at and near the surface. The total dose the film received on its surface and throughout will be a constant 15 Mrads, since there will be very little variation in dose with depth and only one thickness was used.

4.1.3 Heat Treatment

It has been found that irradiated polyethylene exhibits a small amount (less than 5%) of shrinkage when heated near its crystalline melting temperature. If the material is heated to just above its crystalline melting temperature after it is cross-linked the residual shrinkage would be removed for all future steps. A temperature above the crystalline melt temperature (T_m) has been chosen for the following reasons. The shrinkage at elevated temperatures is due to the recovery of residual strains induced in the material during and after extrusion. The recovery (analogous to creep recovery) proceeds much faster at elevated temperatures. Above the crystalline melt temperature the molecules are in nearly their most mobile state so they can recover more rapidly into a new less aligned equilibrium state.

It should be pointed out that upon cooling the heat treated material the main precaution that must be observed is that the material should not be quenched. Quenching may cause

the polyethylene, which is in an amorphous state above its T_m, to remain amorphous. This is undesirable since the properties (in strength) of a quenched amorphous polymer are usually much poorer than the crystalline polymer.

In light of this the rate of cooling of the cross-linked polyethylene has always been slower than the usual rates of film cooling as it emerges from an extruding process.

4.1.4 Perforations

The only specifications necessary for the perforation of the film is the perforation pattern. The perforation pattern is determined from rigidity and resistance considerations which have been described (Section 2.3) as well as the restriction that the largest hole dimension can be no greater than 0.10 in. due to radio-frequency reflectance considerations. This is so providing the film is perforated before it is metallized; since the perforating operation causes cracks to propagate in the metallic coating from the perforation, weakening the material as can be seen in Figures 8 and 9.

4.1.5 Metallization

The metallization which is necessary for strength, and radio-frequency reflectance should yield a metal coating with a thickness of ca. 2200 Å (and have a surface resistance of less than 2 ohms/sq.). In the metallization of the test models these specifications were set. Two metal coating processes were tried during the course of this program. The processes tried were electroless copper plating and vacuum deposition with aluminum. It was found that the electroless copper process was successful for the program while vacuum deposition processes are not perfected sufficiently to be used to produce a workable metallized

material suitable for passive communications satellites using polyethylene as a base material.

4.1.5.1 Electroless Copper Plating

An electroless copper plating process whose solutions* are manufactured by Enthone Inc. a division of ARSCO, in West Haven, Conn. was applied to both mesh and film to determine the operating variables and procedures necessary to plate copper on polyethylene with good adhesion.

4.1.5.1.1 Recommended Plating Cycle

The following plating cycle was recommended by Enthone after experimentation with the Rexwell polyethylene mesh.

Suggested Plating Cycle

Samples of the Rexwell mesh (7.5 in. x 1.0 in.) were treated in accordance with the plating cycle suggested by Enthone which is presented below.

1. Cleaning in Enplate PC-452, 8 oz./gal., 150°F., 2 mins.
2. Cold Water Rinse.
3. Neutralize in Enplate AD-480, 8 oz./gal., at room temperature, 10-20 seconds.
4. Cold Water Rinse.
5. Condition in Enplate Conditioner 472, full strength, at room temperature, 10 minutes.
6. Thorough Cold Water Rinse.
7. Sensitize in Enplate Sensitizer 432, diluted 1 part Concentration to 15 parts deionized water, at room temperature, 1 minute.
8. Cold Water Rinse. (NOTE: This rinse must be very thorough in order to avoid contamination of subsequent solutions.)

* Enthones Electroless plating solutions are commercially available ready formulated propriety solutions.

9. Activate in Activator 440, diluted 1 part Concentration to 15 parts deionized water, at room temperature, 1 minute.

10. Thorough Cold Water Rinse. See note above.

11. Plating: Electroless Copper Plate in Enplate CU-400 made up 2 parts CU-400A, 5 parts CU-400B, and 9 parts deionized water, at room temperature, Time: variable.

12. Thorough Cold Water Rinse.

13. Dry.

Before proceeding further a brief discussion of the purpose of each of the above plating steps will be listed. Since each of the solutions are proprietary and the development of the mechanism and theory of electroless plating is beyond the scope of this contract, only a very approximate outline will be given.

(1) Cleaning (Enplate PC 452) - Removed of greases and dirt from polyethylene with a detergent cleanser.

(2) Cold Water Rinse.

(3) Neutralize (Enplate AD-480) - To remove any residual alkaline detergent of step (1) to protect the highly acidic bath (5).

(4) Cold Water Rinse.

(5) Condition (Enplate 472) - The conditioner contains chromate salts and sulfuric acid. It oxidizes and unsaturates the surface of the film rendering it more receptive to the tin salt adhesion in step (7).

(6) Thorough Cold Water Rinse. This rinse must be very thorough in order to avoid drag-in of conditioner to bath (7) which will contaminate it. The remaining cold water rinses should be additionally thorough so the baths following others will not be contaminated.

(7) Sensitize (Sensitizer 432) - This step deposits or complexes Sn^{++} on the surface of the polyethylene.

(8) Thorough cold water rinse.

(9) Activate (activator 440) - The deposition or complexing of Pladium is accomplished in this step.

(10) Thorough Cold Water Rinse.

(11) Plate (Cu 400 A and B) - In this step the actual electroless deposition of copper is accomplished At first copper oxide deposits upon the surface of the film which then rapidly changes to copper with increasing deposition.

(12) Cold water rinse and drying.

4.1.5.1.2 Plating Cycle for Mesh

The basic plating cycle and operating conditions given above had to be modified in order to achieve a satisfactory plate. The modifications are as follows:

1. In the conditioning step (5) in order to achieve thorough oxidation, it was necessary to increase the operating temperature to 30° - 40°C. range and increase the immersion time to 25 minutes. The heating was accomplished by use of a chemically-pure lead sheathed immersion heater.

2. In the plating step (11), moderate air dispersion and operating temperatures in the range of 65° - 75°F. were necessary so as to deactivate the bath. This was required for two reasons: to preserve the bath and to prevent the excess formation of poorly conductive copper oxide in the plated copper. It must also be pointed out that an excess of dissolved air deactivates the solution so as no plating occurs.

The immersion time in the plating step was held to 10 minutes, so as to give a nominal plating thickness of 10×10^{-6} inch. This is in accordance with information received from Enthone stating that the plating rate in a bath at the

stated concentrations is 1 x 10^{-6} in./min.

3. Agitation of the mesh in the following baths was necessary to insure proper liquid contact (and removal of adhering gases) in the following steps:

Conditioner (5)

Sensitizer (7)

Activator (9)

Plating (11)

4. After each step very thorough (but gentle) spray rinsing was applied to the treated mesh to prevent "drag in" from one processing solution to the next. This was necessary to preserve each bath as well as to insure proper contact of solution with the mesh.

5. In order to protect the copper surface an anti-oxidant treatment step (13) has been added to the plating cycle. Treatment consisted of immersing the plated mesh in a solution of 1 part Entek Cu55 and 99 parts deionized water for a minimum time of 15 minutes. The mesh was then rinsed and dried rapidly.

4.1.5.1.3 Plating Cycle Film

The plating cycle for the film incorporates the recommended plating cycle 4.1.5.1.1 and the modifications for the mesh with one exception. In the conditioning step (5) the temperature was raised to 40° - 50°C range and the immersion time was increased to 1 hour.

4.1.5.2. Aluminum Deposition

The vapor deposition of aluminum was investigated as a second means of metallizing the polyethylene film. The vapor deposition processes was investigated as an alternative to

electroless plating mainly because of its lower cost. It was found that the vapor deposition of aluminum process could not adequately be applied to polyethylene film.

The main problem in the deposition of aluminum on polyethylene is the fact that polyethylene has poor heat stability resulting in a loss of dimensional stability during the aluminum deposition application. The loss in dimensional stability becomes greater as the thickness of the aluminum coat applied gets greater (see Table 21 and Figure 35). Although it is possible to deposit the required thickness of aluminum to give a satisfactory surface conductivity the resultant laminate material becomes badly distorted (wrinkled, warped and curled). Even with a deposition thickness of only 500 Å the loss in dimensional stability is still observed. The above results indicate that the state of the art of aluminum deposition on polyethylene is not sufficiently advanced to warrant the application of aluminum in sufficient thickness on polyethylene to obtain a laminate material that has dimensional stability.

Table 21

Properties of Aluminized Polyethylene Film, Aluminized by National Metallizing Div. of Standard Packaging Co., Trenton, N. J.

Film Type	Aluminum Thickness (angstroms)	Sample Size (in. x in.)	Resistance (ohms/sq.)	Description
Run # 1 PE 12				
Unirradiated	1500	2 x 3.5	0.85	badly wrinkled
Irradiated	1500	2 x 3	0.30	badly wrinkled and black
Irradiated, Heat Treated	1500	2 x 3.5	0.57	badly wrinkled
Unirradiated	2800	2 x 3.5	1.14	wrinkled, black
Irradiated	2800	1.5 x 3	0.75	wrinkled
Irradiated, Heat Treated	2800	2 x 3.5	0.85	wrinkled, slightly black
Run # II				
Unirradiated (PE 12)	500	3 x 5	2.00	wrinkled
Irradiated (PE 11)	500	11.5 x 11.5	4.50	wrinkled
Irradiated (PE 11)	500	11 x 9	5.00	wrinkled

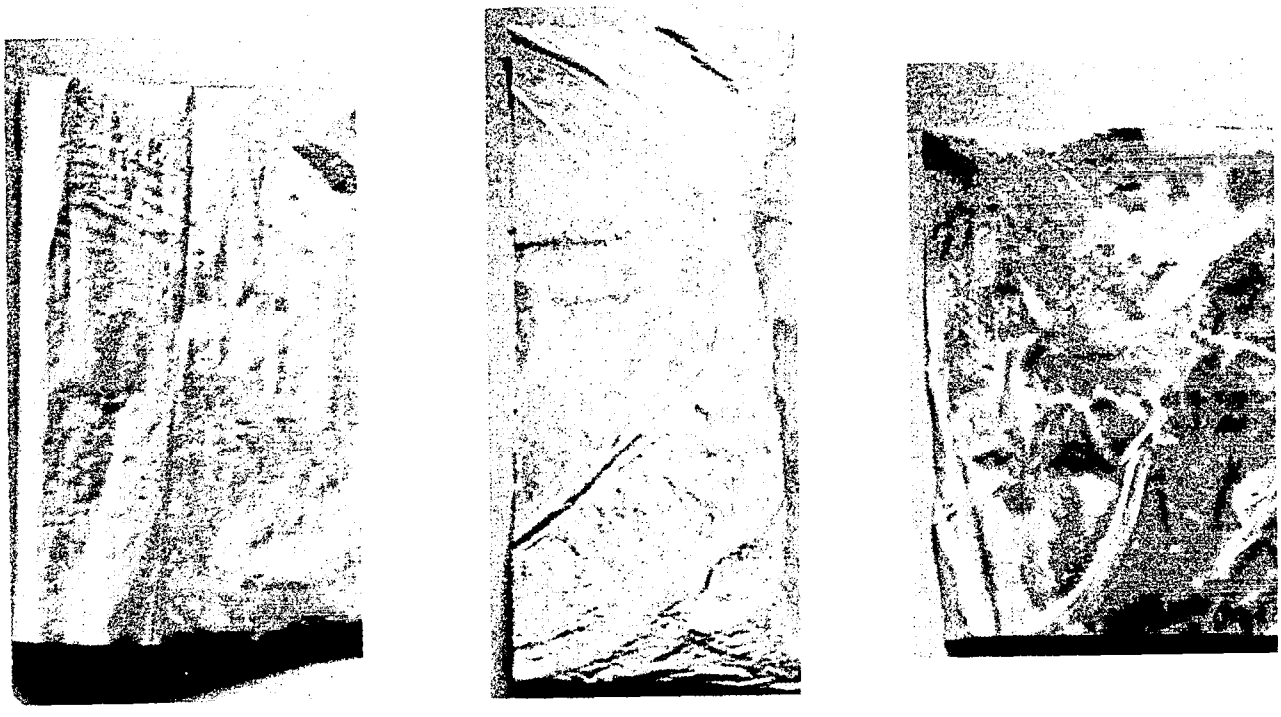

A B C

Figure 35 ALUMINIZED IRRADIATED FILM

A - 500 Å

B - 1500 Å

C - 2800 Å

4.1.6 Cutting

The cutting of the polyethylene copper laminate presents no problems. The material was continuously slit using ordinary film handling equipment for large size pieces. For small patterns the film has been cut using a template. Tolerances of $\pm$0.05" can be realized.

4.1.7 Ultrasonic Bonding

The bonding of all sections of laminated material was accomplished by ultrasonic bonding (ultrasonic welding) techniques. In general, ultrasonic bonding is accomplished by placing two samples of material, usually a plastic, to be bonded under a bar and oscillating the bar at ultrasonic frequency. The high frequency of oscillation induces motion only at the surfaces of the material thereby inducing heat at the surface permitting the two surfaces to mesh together. Since very little motion is induced in the interior of the samples there is no heat build-up there. In this way there is no distortion or damage produced in the bonded film.

The ultrasonic bonder used in all experimental runs as well as in producing the test models was an ultrasonic seal "402" model bonder manufactured by Ultrasonic Seal; Division of Kleer-Vu Industries, Inc., New York, N.Y. A schematic diagram of the bonder is given in Figure 36.

Figure 36: SCHEMATIC DIAGRAM OF ULTRASONIC BONDER

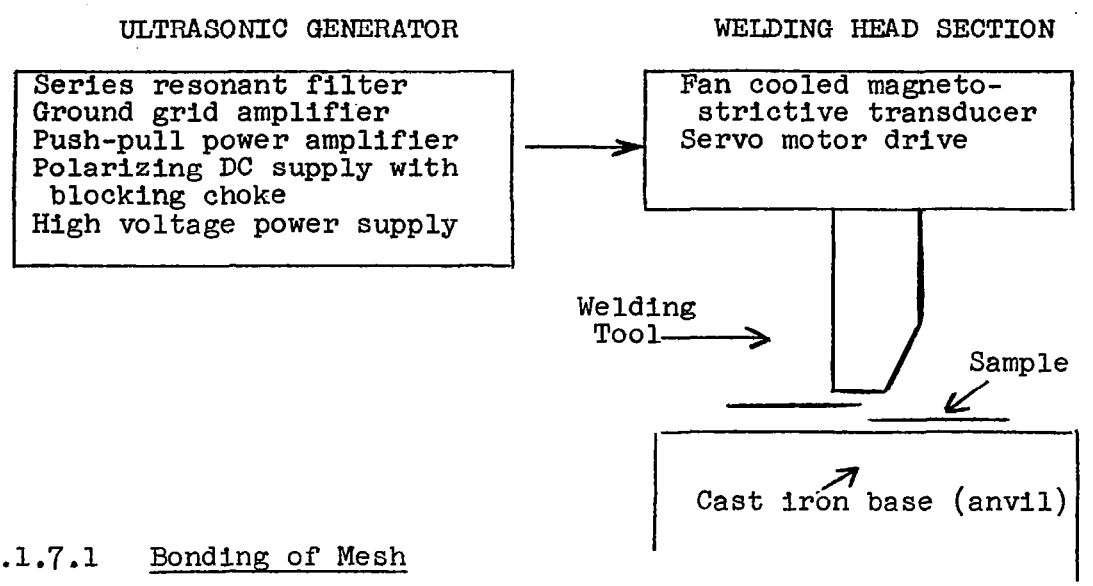

4.1.7.1 Bonding of Mesh

At first, continuous ultrasonic bonding methods were attempted. The specimens to be bonded were passed between a bar continuously operating at an ultrasonic frequency and an anvil. The operation caused tearing and buckling of the mesh at the bond and had to be discontinued.

It was then necessary to use an intermittent bar welding operation. This operation consists of placing the sample area to be bonded between the bar and the anvil, applying pressure then oscillating the bar at ultrasonic frequency, and then moving another area for the same treatment. This operation resulted in a smooth and pressed bond.

Upon close examination of the bonded material, it was observed that the bonded mesh easily peeled. This failure to achieve a satisfactory bond was due to the interference of the thin copper coating on the mesh surface. At first it was believed that cleaning action caused by ultrasonic frequency would sufficiently remove enough copper to permit a

polyethylene bond. This was not the case. (This indicates that the copper polyethylene bond is more than a mechanical bond.) It was then necessary to remove selected areas of copper with nitric acid so samples could be bonded. With the removal of copper from selected areas of the mesh, it was found that a strong and true bond was achieved at those areas. See Table 3.

With the establishment of the proper mesh surface conditions and operating tool, the following operating conditions were used to bond the mesh.

Operating Conditions:

1. Bar used: 1/2 inch wide, 2-$\frac{1}{2}$ inches long, Monel metal, flat face.
2. Frequency: 20,000 cycles/second
3. Pressure: 70-80 psi
4. Clearance: 0.030-0.040 inch
5. Power: 400 Watts
6. Contact time: 1.5 second (ultrasonic frequency applied)
7. Hold time: 0.5 second (for cooling)

4.1.7.2 Bonding of Film

The conditions for the bonding of the crosslinked film are essentially the same as for the mesh. The copper must be removed from the areas to be bonded and the ultrasonic welding bar is applied intermittently. Additionally, 30 mil Teflon coated fiberglas is needed below the sample while 5 mil polyvinyl chloride film was needed above for proper heat dissipation and to achieve the best motion at the sample surfaces to insure an adequate bond. The photograph in Figure 37 shows the complete setup.

Operating Conditions:

Bar used: 1/4 inch x 2-$\frac{1}{2}$ inch (inverse knurled Monel metal)
Frequency: 20,000 cycles/second
Pressure: 35 lbs.

clearance: 5 mils
Power: 400 watts
Contact Time: 1.5 seconds
Hold Time: 1 second (for cooling)

The above conditions achieved a most satisfactory bond between sheets of irradiated polyethylene. The strength of the bond is nearly as strong as the polyethylene itself as can be seen in the results of the testing program, Section 6.2.5.

4.1.8 Packaging

As part of the testing program, experiments were run to determine the ability of the copper laminated polyethylene film to be packaged. The main factor examined in the tests related to packaging is the ability of the laminate to be folded. It was found that the laminate has excellent folding properties. Samples were force folded under a variety of conditions (mainly high and low temperatures - see Fold Resistance Tests, Section 6.2.4, and electrical continuity was measured across the fold. It was found (see Testing Program) that there was only a negligible increase in resistance (4 ohms/sq.) across the fold and that only a negligible amount of damage to the copper coating occurred see the (left) photomicrographs of Figs. 68 and 69. In general a copper laminated polyethylene film could be folded with a sharp crease with only negligible damage occurring to the material. A complete folding and packaging scheme will be given in Section 4.3.1.3 of the scale-up.

4.2 Test Model Fabrication Procedures

With the establishment of the operating variables and procedures, test models were built.

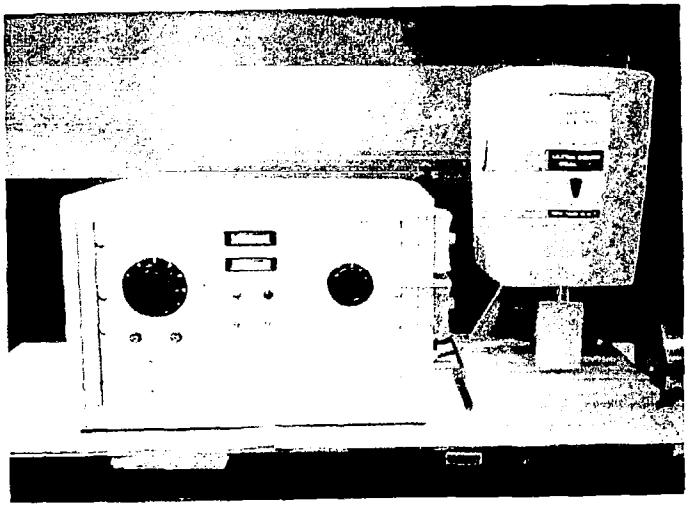

Ultra-Sonic Welding Assembly

Left: Generator
Right: Heat Mechanism

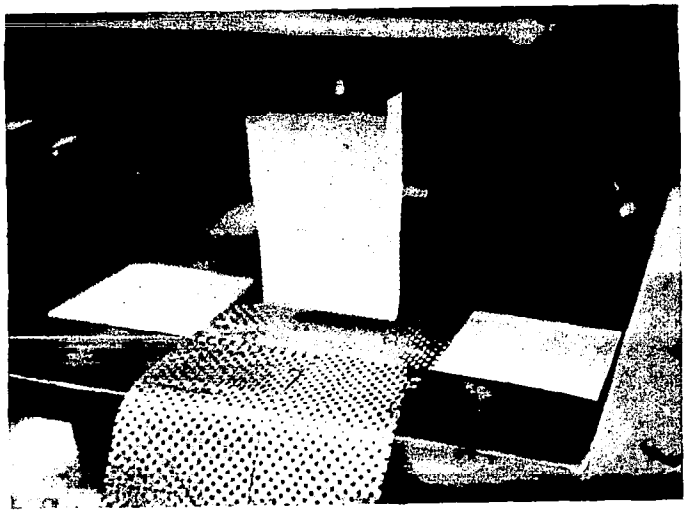

Detail of Head Assembly

Top to Bottom: welding head, polyvinylchloride film, perforated sample to be bonded, Teflon coated fiberglas and base.

Figure 37 ULTRA-SONIC WELDER

4.2.1 Mesh

The steps in the mesh fabrication program will only be given for the spherical cap section. The other steps for the fabrication of the cylinders are essentially the same. The only exception is that the mesh used for the construction of the cylinders was irradiated on a cylindrical form so as to impart a memory into the material that will always give a cylindrical shape upon restoration.

4.2.1.1 Cap Section Design

The design for the spherical cap section consists of a number of gore segments cut so as to give a circular boundary when bonded together and finally trimmed. A sketch of the construction design can be seen in Figure 38.

The length and width of all gore subsegments (except those on the circular boundary) are 49.00 and 14.50 inches, respectively.

It has been shown in Appendix VI that the difference between the maximum arc length contained in the cap section surface and the corresponding diameter lying in the cap section base is only 0.01 feet (Figure 39).

This result implies that any arc contained in the cap section surface is approximately (i.e., within 0.08 inch) equal in length to its projection in the circular base of the cap section.

It has also been shown in Appendix VI that the width of the center gore segment remains essentially constant. It varies 0.023 in. from a maximum of 14.500 in. at the equator to a minimum of 14.477 in. where the sides of the segment intersect the circular boundary of the cap section.

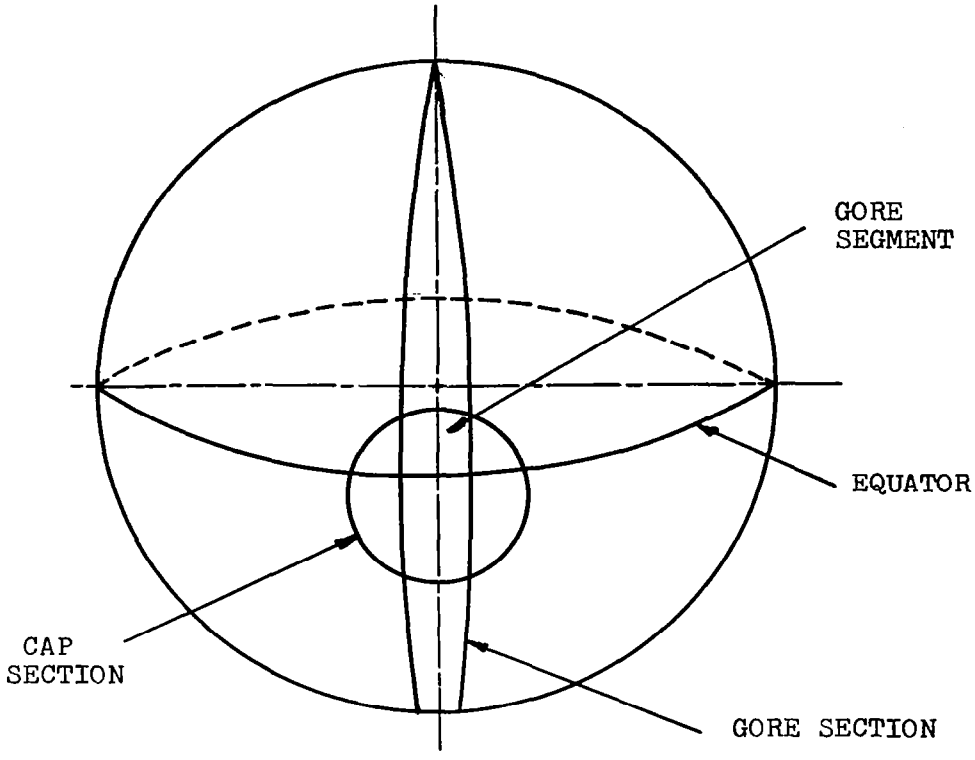

Figure 38 LOCATION OF CAP SECTION WITHIN GORE SECTION OF CONSTRUCTED SPHERE

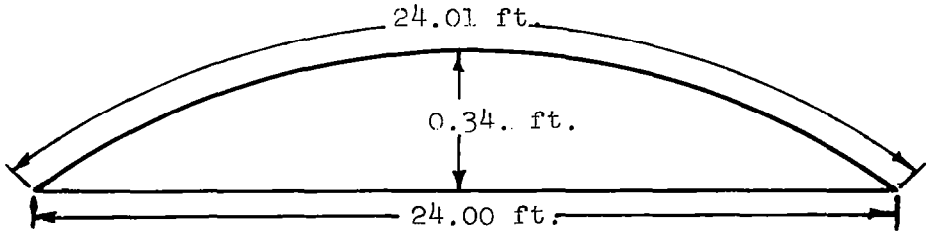

Figure 39 CAP SECTION CROSS-SECTION

In view of the small curvature exhibited by the cap section, the individual gore segments were cut in the form of flat rectangles using a metal template as a guide. Subsequently, one end of each gore segment was trimmed to provide the required curved boundary.

In actuality, each segment was composed of a number of 49-inch long subsegments. This was necessary since 4-foot lengths of 14.5-inch wide mesh constituted the most convenient sizes for plating and irradiation.

4.2.1.2 Cap Section Fabrication

4.2.1.2.1 Irradiation - Mesh

The polyethylene mesh was machine irradiated to 15 Mrads with an electron accelerator at High Voltage Engineering, Burlington, Mass. The mesh was irradiated continuously as a flat section by passing it by the electron beam through use of rollers.

4.2.1.2.2 Heat Treatment - Mesh

According to Section 4.1.3 the following operating conditions were chosen:

Operating Temperature: 140-145°C.
Atmosphere: Nitrogen
Heating Time: 2 hrs.

In addition, at least one-half hour was allowed for bringing the mesh up to 140°C. from room temperature.

The same minimum time interval was employed for returning the mesh to room temperature after the 2-hour heat treatment period has elapsed. This procedure insured against thermal shock (quenching).

During the heat treating process, the mesh subsegments lay on flat, horizontal aluminum trays to insure flatness.

4.2.1.2.3 Electroless Plating - Mesh

Successful electroless copper plating of the deliverable items was accomplished. There was approximately a 20% rejection during the plating of the mesh due to incomplete wetting of the mesh in the plating baths and improper rinsing, which tended to prevent good treating liquid films from being formed on the mesh surface. The rejection decreased as techniques improved and strict adherence to the operating procedures were observed.

4.2.1.2.4 Ultrasonic Bonding - Mesh

After cutting of the subsegments, fabrication was completed by bonding them together ultrasonically using the techniques and operating conditions given in section 4.1.7.1. The "spot weld" bonding scheme is outlined in Figure 40.

4.2.2 Film

Flat sections and cylinders were constructed out of metallized polyethylene film.

4.2.2.1 Irradiation - Film

4.2.2.1.1 Irradiation of Flat Film

In the irradiation of the flat material the film was placed in a flat position on a steel conveyor passing the electron beam. Two methods were tried before achieving successful irradiation. At first the film was irradiated in 8 layer thicknesses in an attempt to pass more material per given irradiation time. Since electron irradiation causes a heat build-up in any substance it strikes and the 8 thicknesses of film were rolled on a film winder after passing the beam, the film had little chance to cool and some sticking occurred rendering the film unacceptable for use. The next attempt,

equally unsuccessful, consisted of placing a single layer of film on the conveyor and placing it across the beam, and allowing it sufficient time to cool before rolling. In this case the heat build-up in the steel conveyor was great enough to make the film stick and fuse to it in spots. The third approach which was successful consisted of lining the conveyor with paper and passing the film on top of the paper across the beam and then allowing the film and paper sufficient time to cool before winding. Figure 41, a schematic diagram demonstrates this method.

4.2.2.1.2 Irradiation of Cylinders

The film cylinders were irradiated in cylindrical form, to obtain a permanent cylindrical shape, on a steel core of 7.5 in. diameter. The core was lined with paper to prevent the film from sticking on the metal. Additionally, the core was rotated to give a uniform dose throughout the surface of the cylinder. After each pass, sufficient time (an hour or greater) was given for the cylinder to cool. With the above precautions, no sticking or fusing occurred.

4.2.2.2 Heat Treatment - Film

The heat treatment of the crosslinked polyethylene film on a continuous basis presented a number of problems some of which have not been resolved as yet. It has been shown (Section 4.1.3) that an effective heat treatment should be done at a temperature above the T_m. In the actual continuous

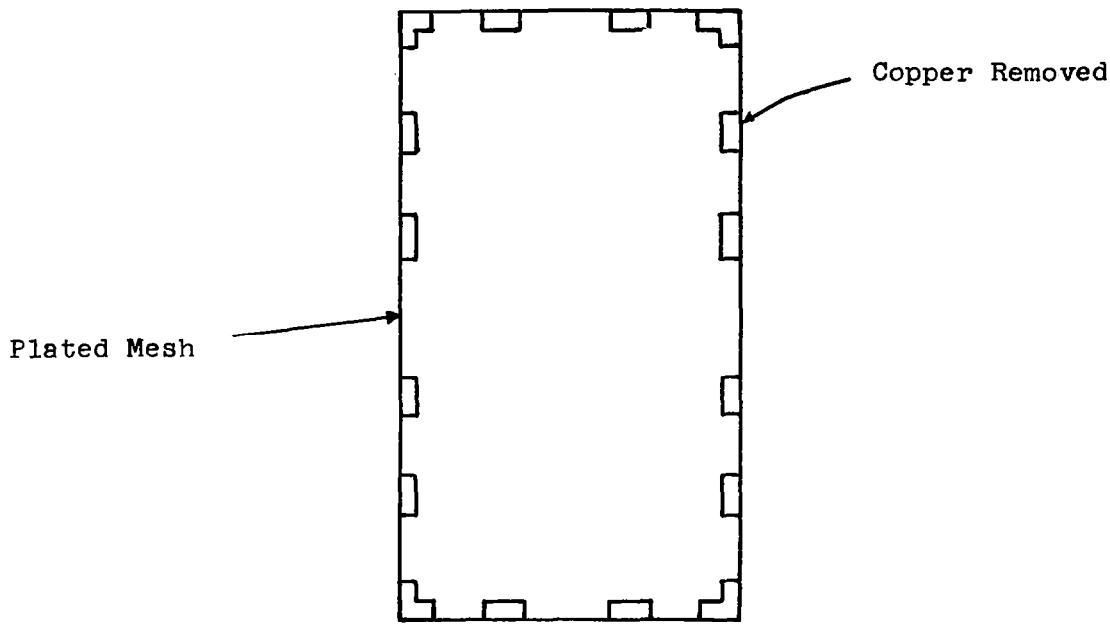

Figure 40 SELECTED AREAS OF REMOVED COPPER

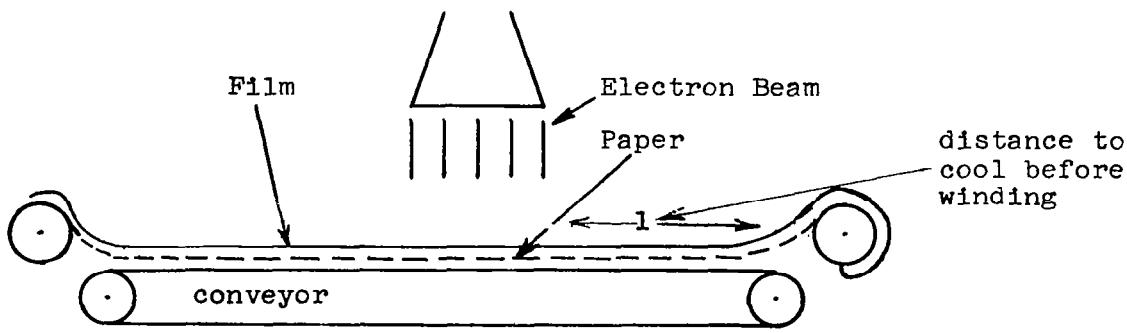

Figure 41 SCHEMATIC DIAGRAM OF CONTINUOUS FILM IRRADIATION

heat treatment where the film is passed horizontally through an annealing oven using film handling equipment (take up rolls with rate and tensioning controls) it was very difficult to control the tension of the film at its T_m. This control problem would result in a distorted unusable film. It was then necessary to go to a lower temperature (93°C.) to accomplish the annealing operation. This was necessary since it was beyond the scope of work to run an experimental commercial scale continuous heat treatment study. Recommendations are made on the solution to this problem in Section 4.3.

4.2.2.3 Electroless Plating - of Film

Successful electroless copper plating of the deliverable items constructed out of film was accomplished using the operating variables already described. The film was plated on 39 in. x 20 in. polyethylene frames to facilitate handling. During the course of the plating operation quality control tests enumerated in Appendix V were executed to insure proper bath composition. Additionally, electrical resistance measurements were run on the plated sheets of film to insure that the surface conductivity of each piece was less than 2 ohms/square. The surface conductivity in ohms/sq. of the plated film is reported in Tables 4 and 5 of Appendix VII.

4.2.2.4 Ultrasonic Bonding - of Film

With the adherence of the operating variables set forth in Section 4.1.5.1.3 successful ultrasonic bonding of the irradiated polyethylene film material was accomplished. Due to the nearly complete lack of electrical continuity across

even a spot welded bond it was decided to remove all of the copper at the bond. To determine if completely discontinuous subsegments of the test models give different radio-frequency reflectance characteristics than models whose subsegments have electrical continuity, half of the test models were made to have electrical continuity across subsegments by applying a small conductive film across the bonds every 10 inches with a conductive lacquer, whose properties are given in Table 22.

Table 22

Properties of Conductive Lacquer*

Continuous Phase (Solvent): Butyl Acetate
Disperse Phase: Powdered Silver
Conductive Film Thickness: Less than 1 mil
Surface Resistance: Less than 0.01 ohms/sq.

*Manufactured by E.I. DuPont de Nemours & Co., Electrochemicals Department, Wilmington, Delaware.

4.3 Scale Up

The fabrication of a full size 425 foot diameter satellite would require the following steps in the production scheme to be scaled up.

a) Heat Treatment

b) Electroless Plating

c) Packaging

Other phases of the construction have been done with equipment which has the capacity for fabrication of the large sphere.

4.3.1 Stages Requiring Scale Up

4.3.1.1 Heat Treatment

As previously discussed the heat treatment of the irradiated polyethylene film above its T_m on a continuous basis resulted in distortion of the film due to difficulty in the control of the tension on the film. An experimental run would have to be undertaken before large quantities of the film could be heat treated to determine the minimum tension which would eliminate orientation of the film during heat treatment.

A method of successfully controlling the tension would be to pass the film through the annealing oven vertically, letting the tension be that of the weight of the film. In this set-up distortions due to over-tensioning or film sagging could be eliminated. Alternately, the film could be laid on a travelling bed so that no tension would be on the film during the heating and cooling cycle.

4.3.1.2 Electroless Plating

The Enthone electroless plating process requires a full scale up to continuous operation of all the treating steps. To construct a 425 foot diameter satellite, approximately 700,000 ft. of 20 in. wide film is needed. This includes scrap, excess, material for testing, etc. The approximate rate of plating has then been set at 150 ft. per hour of film plated with 15 x 10^{-6} in. of copper on both sides. The operating variables in this scale up will be those given in Section 4.1.5.1.3 above; only the residence time in the actual plating bath will be changed to 15 minutes. In addition, the quality control tests as given in Appendix V will still apply to the large baths described below.

It is obvious that the continuous operation proposed here would require design of special tanks for steps 5, 11, and 13 which would permit the film to be festooned, thus, decreasing the length of the tank while still maintaining the required residence time.

4.3.1.2.1 Plating Baths

The size of the plating baths is based on the length of the film required to be immersed in the bath in order to obtain the correct residence time for a particular processing speed. This would vary for each step and for a continuous process be governed by the slow step in the overall process. The length of travel is given by

$$L = VT \qquad (23)$$

where V = the rate of film production (150 ft./hr.)

T = the residence time

L = the length of travel

Table 23 below gives a summary of the length of travel for each bath.

Table 23

Summary of Immersed Lengths of Travel in all Plating Baths to obtain a Copper Thickness of 15×10^{-6} in. on Polyethylene Film

Bath	T (Residence Time) (min.)	L (Length of Travel) (ft.)
1 Cleaner	2	5.0
3 Neutralizer	1/3	0.833
5 Conditioner	60	150
7 Sensitizer	1	2.5
9 Activator	1	2.5
11 Plating bath	15	37.5
13 Antioxidant	15	37.5

With the length of travel for each bath established the tanks for each step may be designed. In general, each bath will be equipped with a recirculating pump, solution reservoirs, film rolls and control equipment.

4.3.1.2.1.1 Cleaning Bath

The cleaning bath would be 5 feet long and 5 inches in depth. It would be constructed out of 316 stainless steel. A 55-gallon recirculating reservoir would be connected to the tank. The cleaner detergent solution would flow countercurrent to the direction of film motion. The following diagram shows schematically the general set up for single pass immersion.

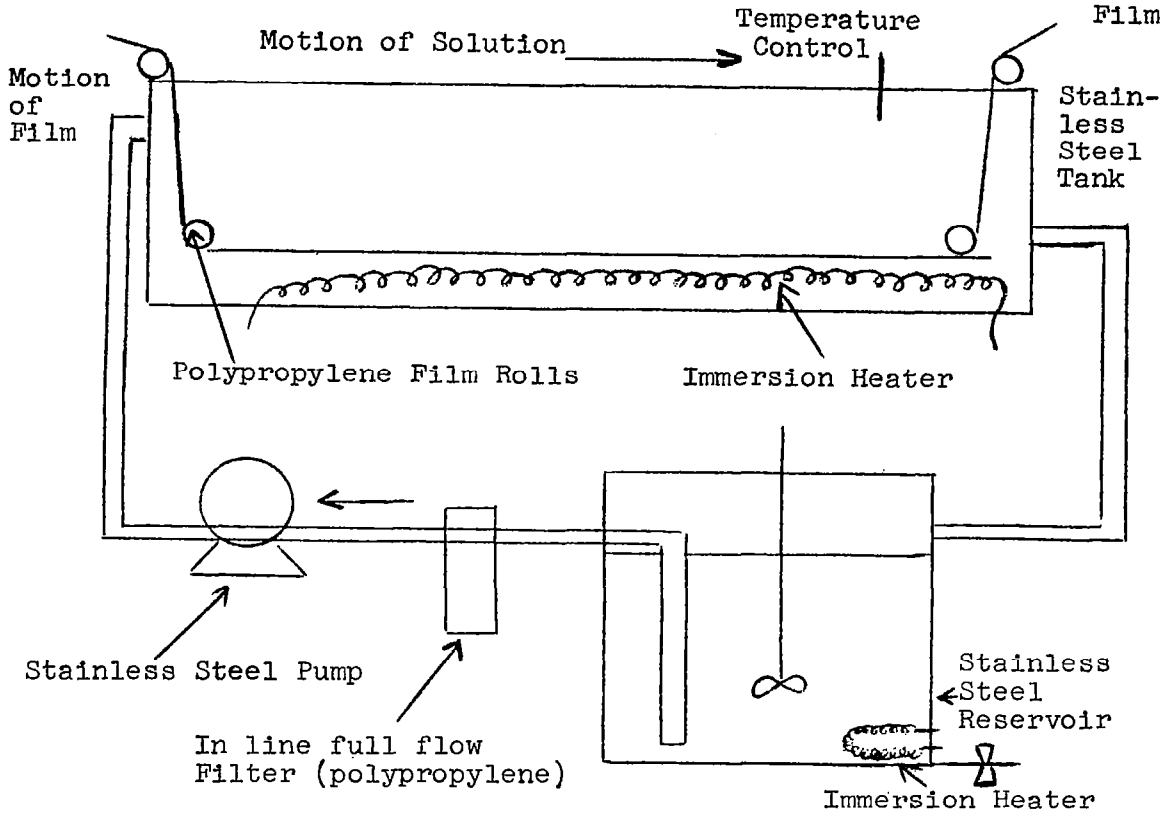

Figure 42 SCHEMATIC OF SENSITIZER OR ACTIVATOR SYSTEMS

4.3.1.2.1.2 Neutralizing Bath

The neutralizing bath would have the same set up as the cleaning step; only there would be no need for heating or temperature control.

4.3.1.2.1.3 Conditioning Bath

The conditioning bath requires 150 feet of travel to obtain a residence time of 1 hour. In this case it would be necessary to have the film travel more than one pass in the bath in order to decrease the length of the tank. The set up for this step would appear as follows:

Figure 43 CONDITIONER BATH

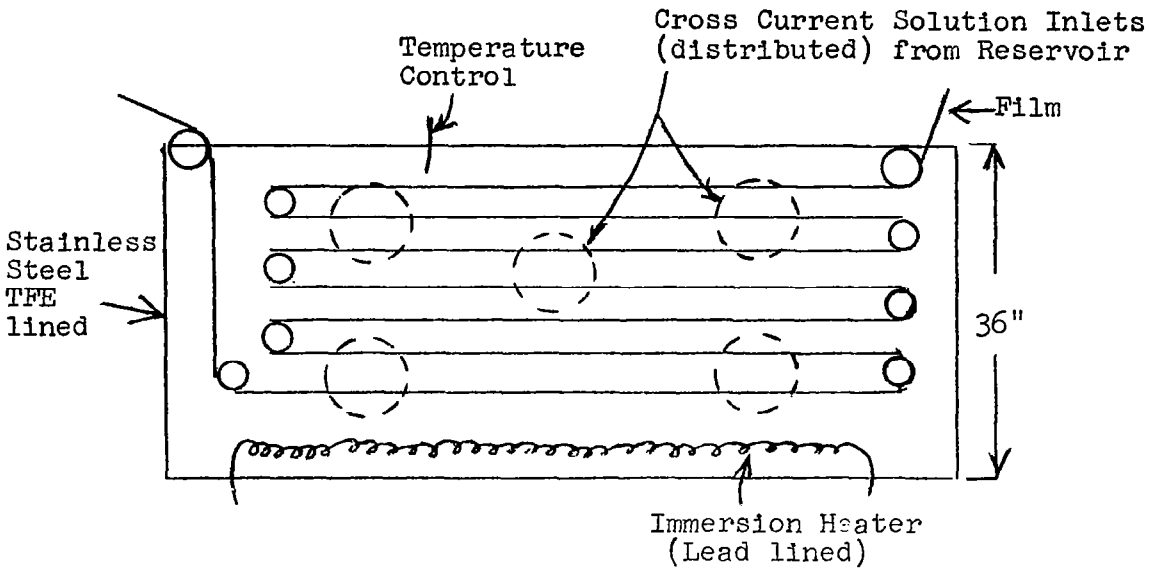

The tank and reservoir for this step would be 316 stainless steel lined with tetrafluoroethylene (TFE) film. The tank would be greater than 36" high and 15 feet long to accommodate 10 film passes. All auxiliary fixtures in the tank and reservoir would be lined except the immersion heater which would be lined with chemically pure lead. The reservoir would be 100 cubic feet in volume.

4.3.1.2.1.4 Sensitizer and Activator Stages

The sensitizer and activator stages would be very similar to the cleaning operation stage. The bath length for these stages would be 2.5 ft. and no heating or temperature controls would be needed.

4.3.1.2.1.5 Electroless Plating Bath

The plating bath needs 37.5 feet of travel at 150 ft. per hour to obtain a residence time of 15 minutes. It would therefore be necessary to have a multiple pass bath to lower its length. A bath length of 5 feet would be satisfactory with

a height of about 3 feet to accommodate between 7 and 8 passes. As in the conditioner bath the solution flow would be cross-current with a number of inlet entrances to insure satisfactory liquid mixing. Since the plating bath life is dependent upon temperature and air distribution, the plating bath would be water jacketed for cooling and would have air dispersion. The bath reservoir, piping and pump would be made out of 316 stainless steel. The bath and reservoir would be polyethylene lined so it may be cleaned with nitric acid to remove any copper that may plate out. It would additionally be necessary to have a replaceable full flow polypropylene filter (3-5 micron porosity) in line to remove free particles of copper from the solution. A schematic diagram of the plating system is shown in the following Figures 44 and 45.

Figure 44 ELECTROLESS PLATING BATH

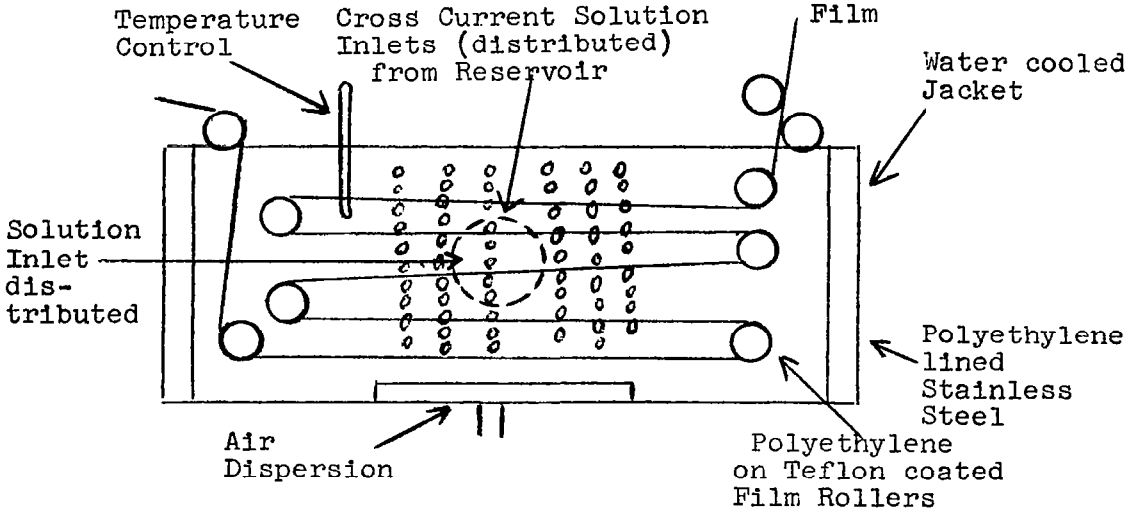

Figure 45 - SCHEMATIC DIAGRAM OF PLATING BATH SYSTEM

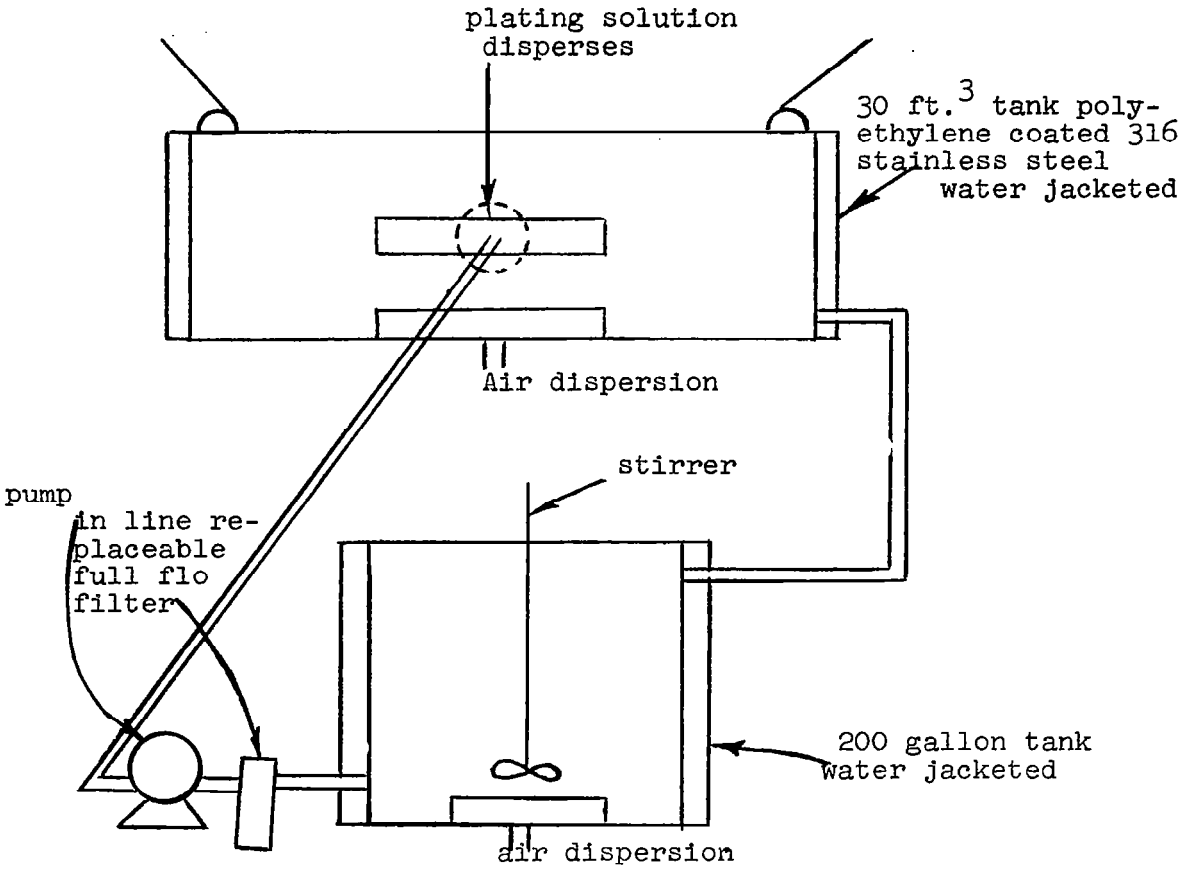

4.3.1.2.1.6 Antioxidant Step

This bath will have the same dimensions as the plating bath but with the same auxiliary equipment as the cleaning step.

4.3.1.2.1.7 Rinsing Steps

The rinsing of the film as it goes from bath to bath would be accomplished by spraying with deionized water. After the final rinsing step, the plated film would be air dried.

4.3.1.3 Packaging

The ultrasonic bonding, folding and packaging

will be done in essentially one step. The design requires the ultrasonic bonding of 801 20 in. wide gore segments with two 15.94 foot chord diameter polar caps. To reduce excessive handling, the gore segments will be folded immediately after they are ultrasonically bonded. The initial longitudinal fold (pleat) will be in an "S" shaped configuration as shown in the following diagram:

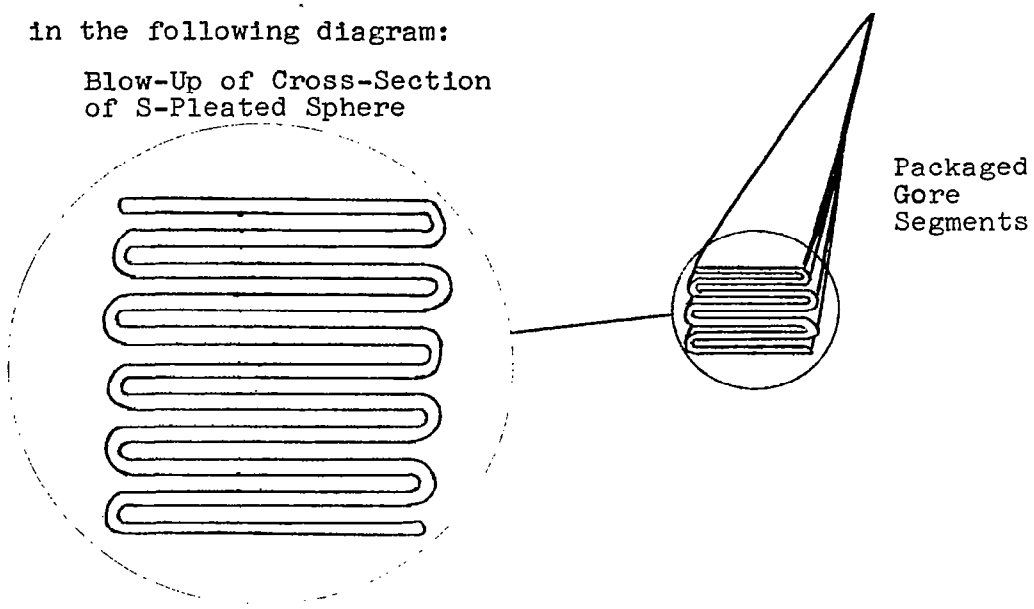

The 800 thicknesses of film will give a total thickness of ca 0.80 in. The long pleated package of folded gore segments will then be transversely folded ca. 134 times to obtain a package approximately 20 in. wide, 60 in. long and 107.2 in. high.

5.0 MEMORY EFFECT

5.1 Experimental Tests

Three (3) sets of tests were conducted to characterize and demonstrate the plastic memory effect. The first test was a tensile test used to characterize the basic memory forces. The second and third tests were used to demonstrate the memory effect and to determine possible resistances to it. These tests were deployment tests of cylinders and flat sections in a 1-g environment.

5.1.1 Memory Effect and Characterization of Memory Forces - Tensile Tests

It has been found from an investigation of the literature concerning the theory of rubber elasticity that memory forces (of a crosslinked material) can be characterized above the T_m by measurement of the modulus of elasticity (E) of the film. It has been determined theoretically that the modulus of elasticity can be given by the following equations:

$$E = 3\ vkT \quad \text{(ref. 2)} \qquad (1)$$

where T = absolute temperature (above T_m)
K = Boltzmann constant

$$v = \frac{N\rho}{M_c}\left(1 - \frac{M_c}{M_n}\right)$$

where N = Avagadro's Number
ρ = density
M = molecular weight between crosslinks
M_n^c = number average molecular weight

With the above equations as a guide it is now possible to conclusively prove that very thin, crosslinked polyethylene film exhibits a plastic memory even if it is not possible to demonstrate this with a model test in a 1-g field. In unirradiated thermoplastics, i.e., linear polymers, once the T_m

is exceeded the plastic exhibits permanent flow properties and the memory phenomenon is not observed as ($M_c \rightarrow M_n$ and $v \rightarrow 0$). Irradiation of the thermoplastic, however, causes the development of crosslinks in the thermoplastic, thereby, changing the linear structure to the three-dimensional network. Radiation, in effect, vulcanizes the plastic and makes it an elastomer. The elastomeric properties, however, are not observed at temperatures below the T_m because the crystalline forces are much greater than the memory force. When the crystalline forces are eliminated by exceeding the melting point, the memory force is observed. In this way, the memory forces of the crosslinked polyethylene film can be characterized by measuring E above T_m. A tensile test performed above the T_m is conducted and the modulus of elasticity is measured. This modulus is then a direct indication of the memory force exhibited in the crosslinked polyethylene film. Additionally, after the film is deformed, the tension is released and the film springs back to its original dimensions thereby completing a memory cycle. If the film were not crosslinked the modulus of elasticity above the T_m would be essentially zero, and the film would exhibit permanent set characteristics after any deformation, i.e., it would not spring back. These experimental results based on the above theory have been demonstrated (see Table 24 and Figure 46 below). It can be seen from these results that the crosslinked film does possess a modulus of elasticity above the T_m and that additionally, the film can be deformed and restored (cycled with minimal hysteresis loss) to its original dimensions when it is above its T_m. Furthermore,

the results qualitatively conform to the above equation. As irradiation dose is increased the molecular weight between crosslinks decreases thereby resulting in a stronger film. Additionally, equation (1) predicts that the modulus should increase with temperature. Although this is not observed, the decrease with increasing temperature is small and can well be due to thermal degradation.

Table 24

Characterization of Memory Forces - Modulus of Elasticity, E
PE 12 Irradiated to 15 and 70 Mrads*

Dose Mrads	120°C. E (psi x 10^3)	140°C. E (psi x 10^3)	150°C. E (psi x 10^3)
15	0.044	0.035	0.030
70	0.343	0.230	0.210

*Strain rate 2 in./min.

Figure 46: TYPICAL STRESS CURVE OF ELASTOMERIC POLYETHYLENE

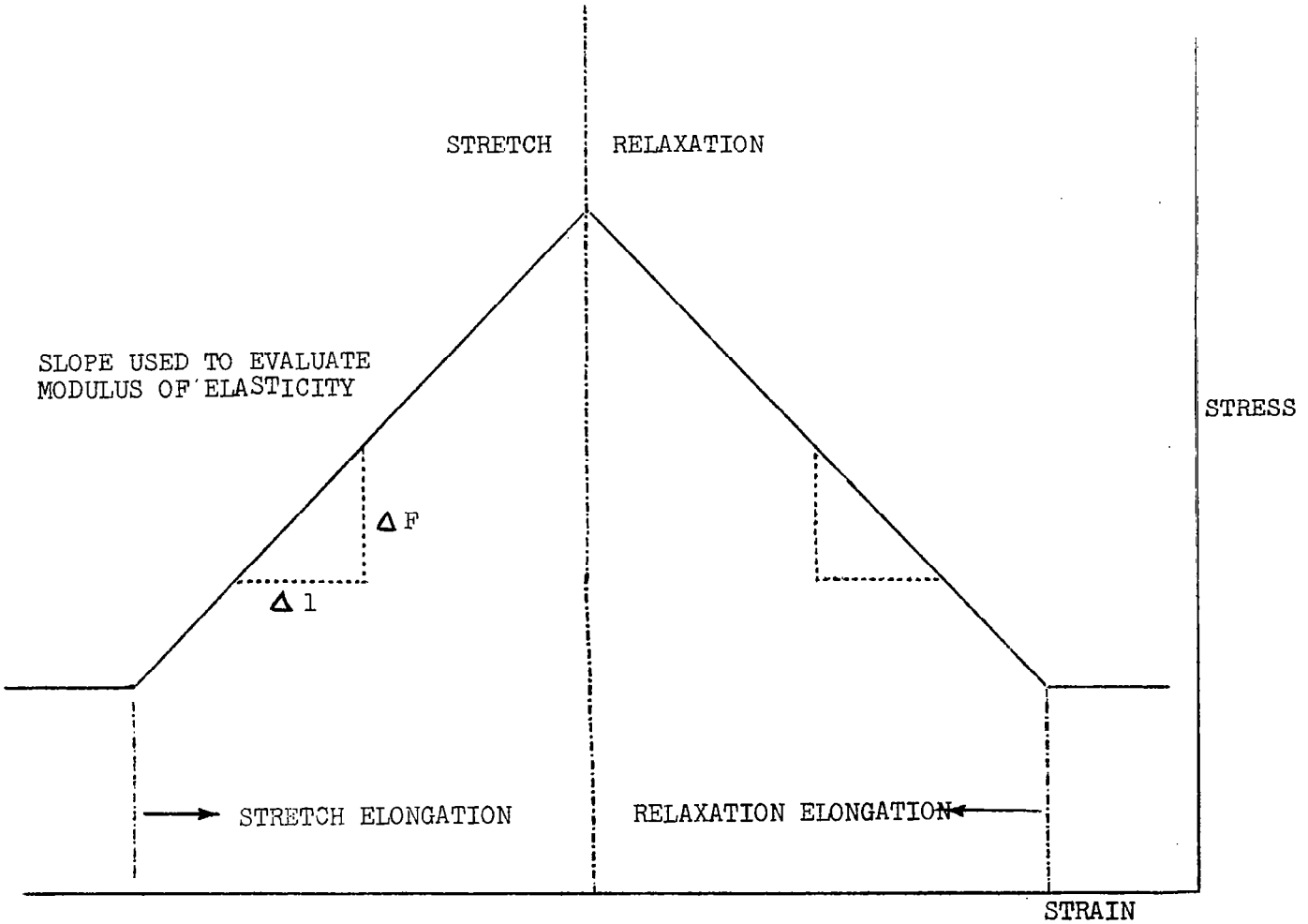

5.1.2 Fold Resistance Tests

Samples of completely processed film were force folded under a variety of conditions (see testing program Section 6.2.4), and subsequently placed in an oven at 120°C. (above the crystalline melting point). The samples were then allowed to unfold. The degree of restoration of each sample was then measured. It was found that the degree of restoration ranged from 0°(none) to 90° (50%).

5.1.3 Cylinder Deployment Tests

Cylinders constructed from material irradiated on a cylindrical form(7.5 in. diameter),to induce a cylindrical memory, were folded along their longitudinal axis as shown in Figure 47 to give a flat configuration. The folded cylinders were then placed upright in an oven at 120°C as shown in the following diagram.

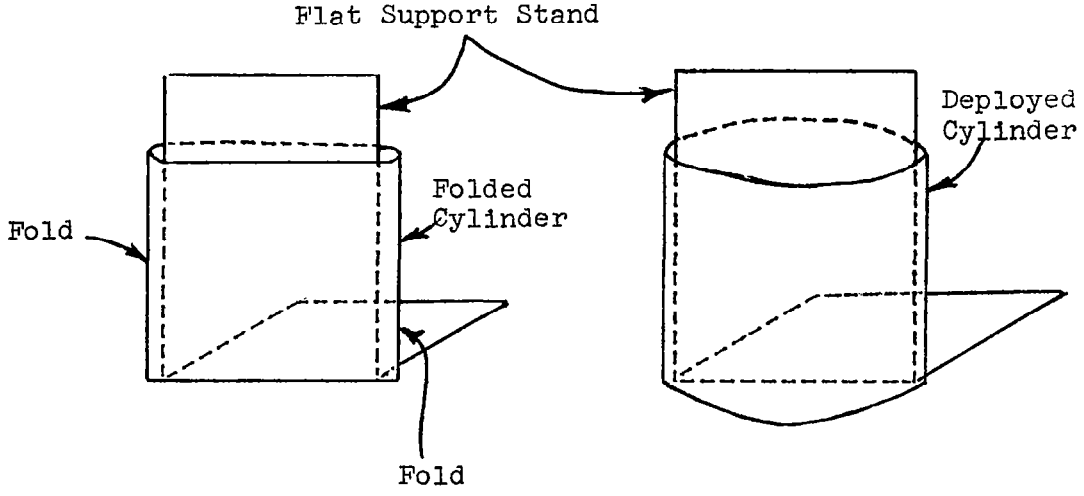

(Cylinder is Original Configuration before Folding)

Figure 47: SCHEMATIC OF CYLINDER DEPLOYMENT TESTS

The cylinders were then allowed to unfold and restore. At first, unplated cylinders of 1 foot length were tested. It was found that considerable warping (due to gravity) and sticking (blocking) occurred. See Figure 48. Therefore it was decided to use 6 inch cylinders. A variety of cylinders were used to determine different effects. Plated and unplated cylinders were used to determine the effects of surface blocking on restoration. Plated cylinders with and without copper at the fold were used to determine the effect of the metal coating on restoration. The results of the cylinder tests are summarized in Table 25 and Figures 48-50.

Table 25

Summary of Cylinder Restoration Tests
(Base Material PE 12 irradiated on a cylinder)

Description of Cylinder	Dimensions Diameter (in.)	Dimensions Length (in.)	Dimensions after Restoration* Major Axis (in.)	Dimensions after Restoration* Minor Axis (in.)	Comments
1 unplated	7.5	12	10.5	0.25	Considerable warping and blocking, little restoration
2 plated	7.5	6	7.75	5.00	Warping, no blocking, partial restoration
3 plated (copper removed from fold)	7.5	6	8.25	2.75	Warping, no blocking, partial restoration
4 unplated	7.5	6	8.75	0.38	Considerable warping and blocking, little restoration
5 unplated	7.5	6	8	5.25	Warping, no blocking, partial restoration

*An approximate elliptical configuration was obtained after restoration.

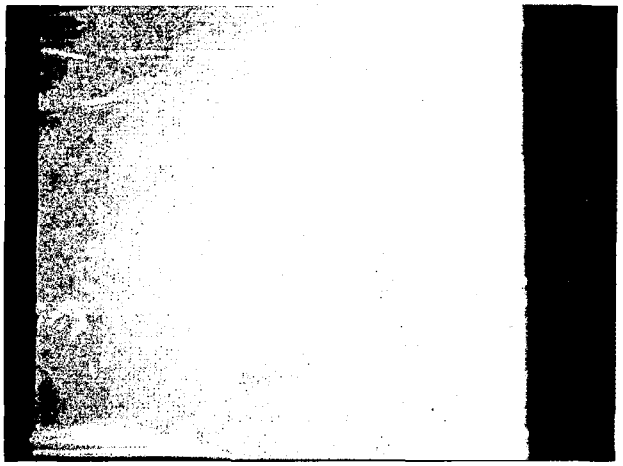

Before Test
Cylinder # 1

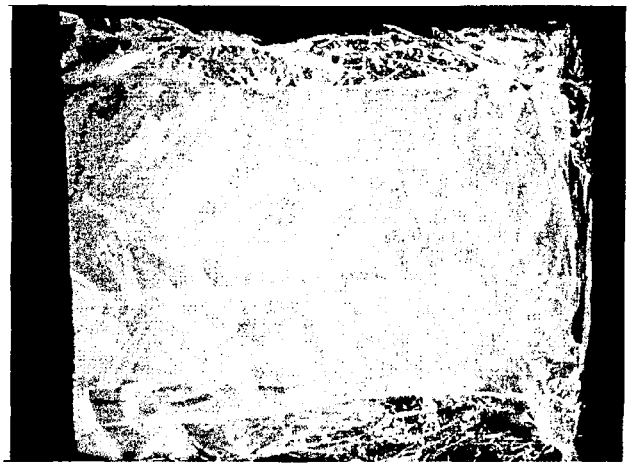

After Test

Height 12"
Diameter 7.5"

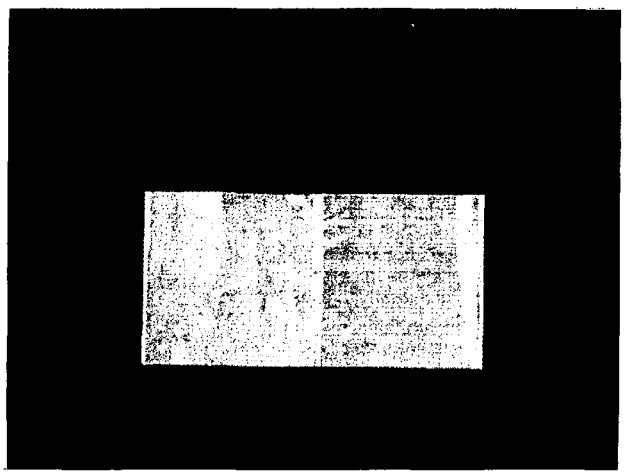

Before Test
Cylinder # 4

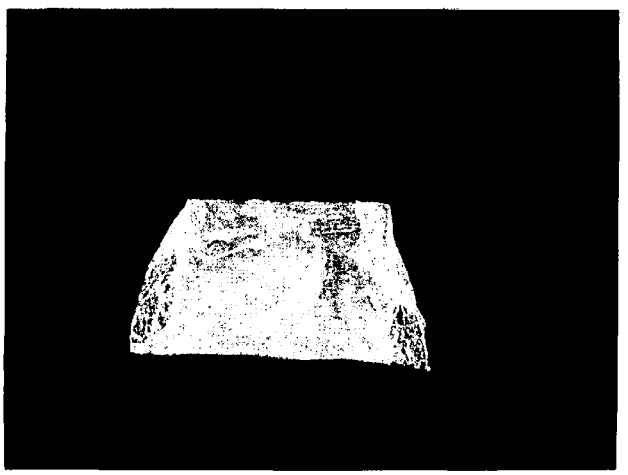

After Test

Height 6"
Diameter 7.5"

Figure 48 PHOTOGRAPHIC RESULTS OF CYLINDRICAL MEMORY TESTS ON UNPLATED MATERIAL

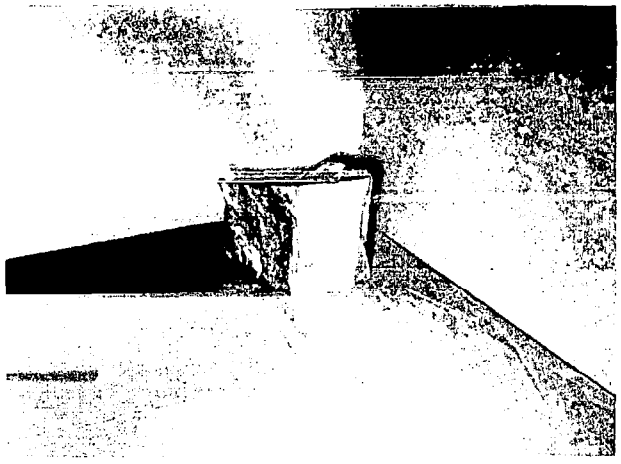

After Test

Cylinder # 2

Height 6"
Diameter 7.5"

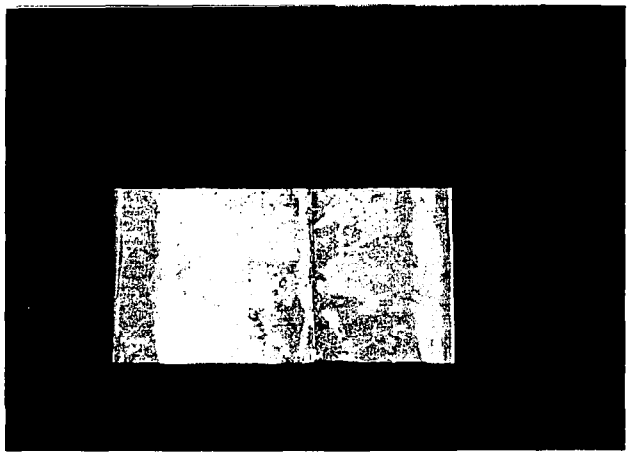

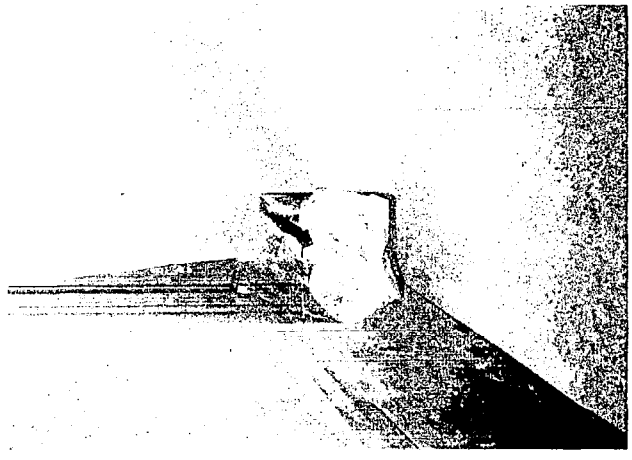

Before Test
Cylinder # 5

Height 6"
Diameter 7.5"

After Test

Figure 49 PHOTOGRAPHIC RESULTS OF CYLINDRICAL MEMORY TESTS ON PLATED MATERIAL

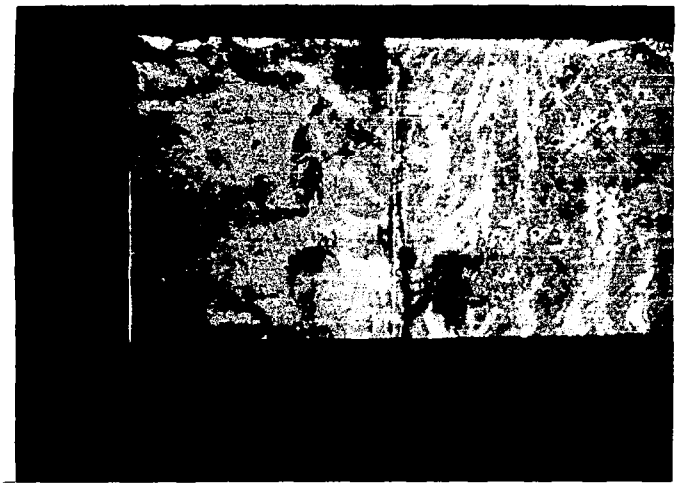

Before Test

After Test

Cylinder # 3 Height 6" 1" Width of Copper removed
Diameter 7.5" along folds

Figure 50 PHOTOGRAPHIC RESULTS OF CYLINDRICAL MEMORY TEST ON PLATED MATERIAL WITH COPPER REMOVED FROM FOLDS.

5.1.4 Conclusions on Memory Tests

Of the three (3) memory tests performed only the tensile test method conclusively proved the existence of the memory and characterized and measured the fundamental memory forces. The other two (2) tests, deployment tests, did not show complete restoration. In the deployment tests it has been observed that the following forces resist restoration: blocking, gravity, and air currents. The blocking effect only predominates when the film is not metallized. The effects of gravity and air currents were observed on all of the tests and limited the effective demonstration of the memory of thin film materials. Although the effect of air currents can be eliminated by running the deployment tests in a vacuum chamber, the effect of gravity on the thin film material cannot be eliminated in a 1-g field. A number of follow on tests are then suggested to conclusively demonstrate deployment using the memory effect. With the development of a non-blocking thermal coating, deployment tests should be run in a vacuum to eliminate the effects of air currents. The next test should be a 0-g deployment test (in space) on a small 3 dimensional model. The 0-g test would substantiate the feasibility of the plastic memory effect in the deployment of thin film items. In fact, it is strongly believed by the authors, a test in a 0-g environment presents the only means of demonstrating deployment of thin film materials exhibiting the memory effect.

5.2 Deployment

A complete and definitive deployment study cannot be made at this stage since a thermal control heat transfer study

and 0-g deployment tests on small test models is first needed. With the assumption of the operability of the memory effect a means of heating the surface of the sphere to above its T_m must be achieved. Two methods of deployment are possible. In the first method deployment would be initiated by preheating the folded structure in its canister prior to erection. In the second method expandable struts would rapidly expose most of the sphere's surface to the sun. Heat would then conduct through the rest of the unexposed area expanding the complete structures.

Another area needing study closely connected with deployment is vacuum frictional effects (cold welding). Again, a study of vacuum frictional effects should properly follow the thermal control study, since the vacuum frictional effects of the thermal control coating would be the surface requiring investigation.

6.0 TESTING PROGRAM

The testing program on the perforated, plated PE 12 film is essentially divided into two parts: (1) an initial qualifications program checking the film with processing and (2) a final qualifications program examining the finished film under various environmental conditions. In the final qualifications program both bonded and unbonded material were tested. The complete testing program is outlined in the following table.

Table 26

Testing Program Scheme

Material	T	FR	CFE	FdR	B	R	PM
Unprocessed	Yes	Yes					
Irradiated	Yes	Yes					
Irradiated-Heat treated	Yes	Yes					
Irradiated-Heat treated-Plated	Yes	Yes			Yes	Yes	Yes
Irradiated-Heat treated-Plated-Perforated*	Yes	Yes	Yes	Yes	Yes	Yes	Yes
Irradiated-Heat treated-Plated-Perforated-Bonded*	Yes	Yes	Yes	Yes	Yes		Yes

*Final qualifications tests run at a variety of test conditions: vacuum, pressure, high temperature, low temperature, irradiation.

T = Tensile test

FR = Flexural rigidity test

CFE = Cyclic flexure endurance test

FdR = Fold resistance test

B = Blocking test

R = Electrical resistance measurement

PM = Photomicrograph

In general, it has been found that the film was able to withstand nearly all of the above tests. The results of the testing program are presented in the following sections.

6.1 Initial Qualifications Testing Program

The initial qualifications testing program was conducted to test the material after each processing step. Flexural rigidity (described in Appendix IV) and tensile tests (described in Appendix I) were performed to follow the effects of processing. Photomicrographs (250x) were taken of the surface of the plated material, and, additionally resistance measurements were made on all continuous plated material. The results of the initial qualifications tests are given in Table 27 and Figs. 51 through 56. The results show that the final material is ca. five times stiffer than the original film. Figures 51 through 56 show that the material must be stretched ca. 30% in order for it to begin to lose electrical continuity. The photomicrographs in Fig. 56 show the surface condition of the metallized film (both perforated and non-perforated) before and after a tensile test. It can be seen that the copper coating is continuous and relatively smooth before the tensile test. What appear to be scratches in the photomicrographs are actually extrusion lines. The photomicrograph of the perforated sample before tensile testing also shows that the ragged edges on the perforated boundary are coated copper. After the tensile test the samples are shown to be cracked at the metallic surface as would be expected.

6.2 Final Qualifications Testing Program

The final qualifications testing program was aimed at investigating the effects of different environmental conditions that would be encountered in space on the completely processed PE 12, a minimum of 2 runs were used for all determined values.

Table 27

Properties of Processed Sea Space Film
(Thickness = 1 mil, Density = 0.931 gm./cc., T_m = 117°C)

Direction (Degrees)	Area Weight ($lb/ft^2 \times 10^{-3}$)	F_y* (lbs)	ε_y* (%)	E* (psix10^3)	G** ($lb\ in^2/in \times 10^{-6}$)
Unprocessed Film					
0	4.65	0.699±0.005	2.28±0.15	31±4	4.28±0.50
45	4.65	0.578±0.010	2.06±0.15	29±3	5.77±2.55
90	4.65	0.643±0.009	1.76±0.34	37±4	5.54±1.71
Irradiated Film					
0	4.65	0.69±0.01	2.44±0.41	29.1±1.7	4.92±1.44
45	4.65	0.57±0.005	1.94±0.18	29.5±1.6	5.52±1.35
90	4.65	0.63±0.12	1.74±0.24	37.4±3.8	7.60±2.83
Heat Treated Film					
0	4.65	0.74±0.06	2.8 ±0.4	26.9±2.1	6.02±2.37
45	4.65	0.72±0.08	2.9 ±0.5	25.0±2.3	5.10±1.68
90	4.65	0.81±0.05	2.6 ±0.1	30.9±1.7	5.62±1.84
Irradiated, Heat Treated, Plated					
0	5.31	0.73±0.06	0.58±0.07	126 ±6	30.6 ±6.67
45	5.31	0.68±0.03	0.53±0.05	129 ±6	28.4 ±4.82
90	5.31	0.72±0.07	0.51±0.07	141 ±7	29.2 ±4.77

Table 27 (Continued)

Direction (Degrees)	Area Weight ($lb/ft^2 \times 10^{-3}$)	F_y* (lbs)	ϵ_y* (%)	E* ($psi \times 10^3$)	G** ($lb\ in^2/in \times 10^{-6}$)
Irradiated, Heat Treated, Plated, Perforated					
0	4.14	0.42±0.03	0.67±0.12	-	27.0±5.83
45	4.14	0.52±0.05	0.66±0.09	-	25.8±4.27
90	4.14	0.44±0.04	0.65±0.08	-	25.1±3.64

* Determined by Tensile Tests described in Appendix I, test run ten times.

** Determined by Flexural Rigidity Tests described in Appendix IV, test run ten times.

Figure 51 SURFACE RESISTANCE VS. STRAIN FOR COMPLETED MATERIAL, NON-PERFORATED (in 0° and 45° Directions)

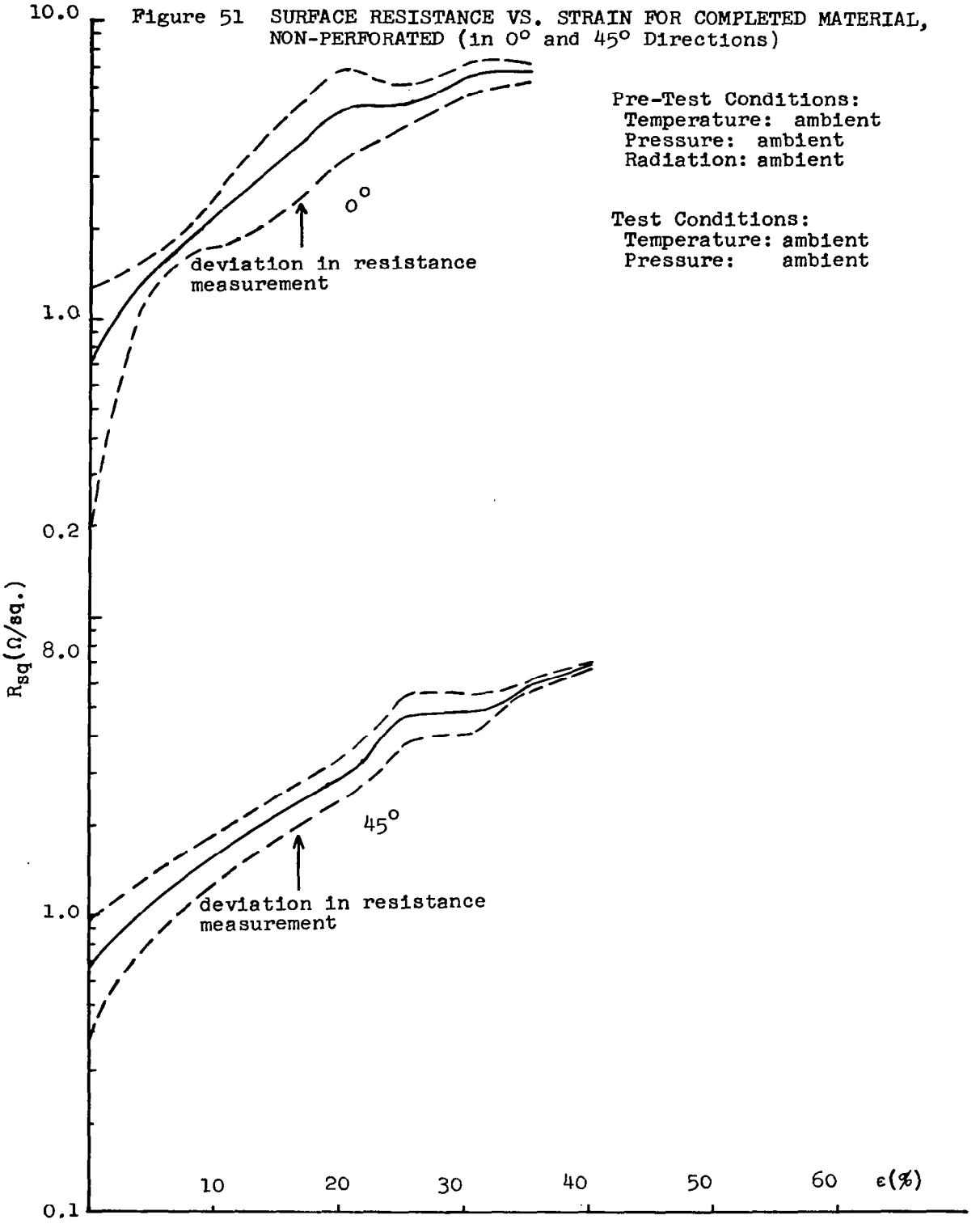

Figure 52 SURFACE RESISTANCE VS. STRAIN FOR COMPLETED MATERIAL, NON-PERFORATED (in 90° Direction)

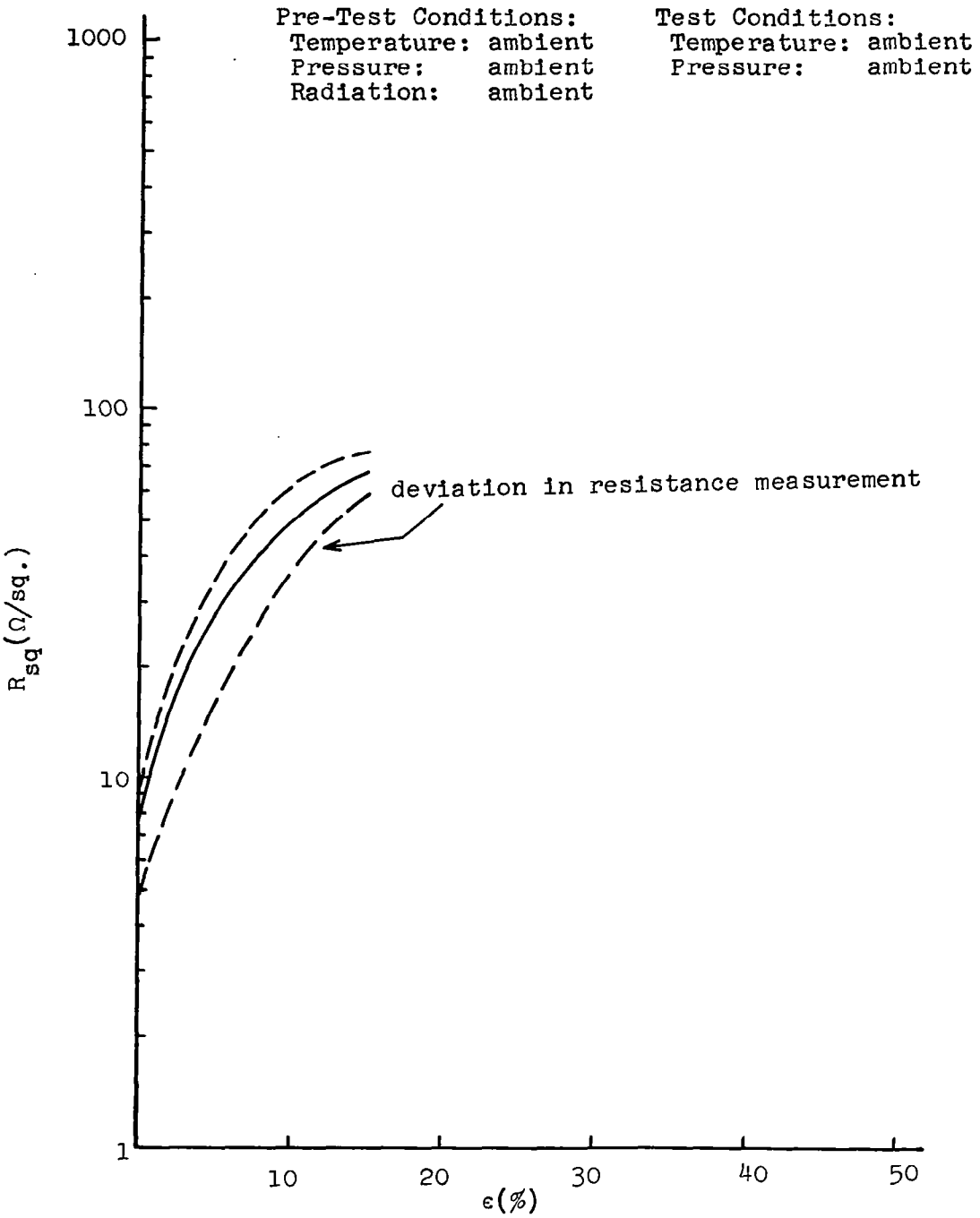

Figure 53 SURFACE RESISTANCE VS. STRAIN FOR COMPLETED MATERIAL (in 0°Direction)

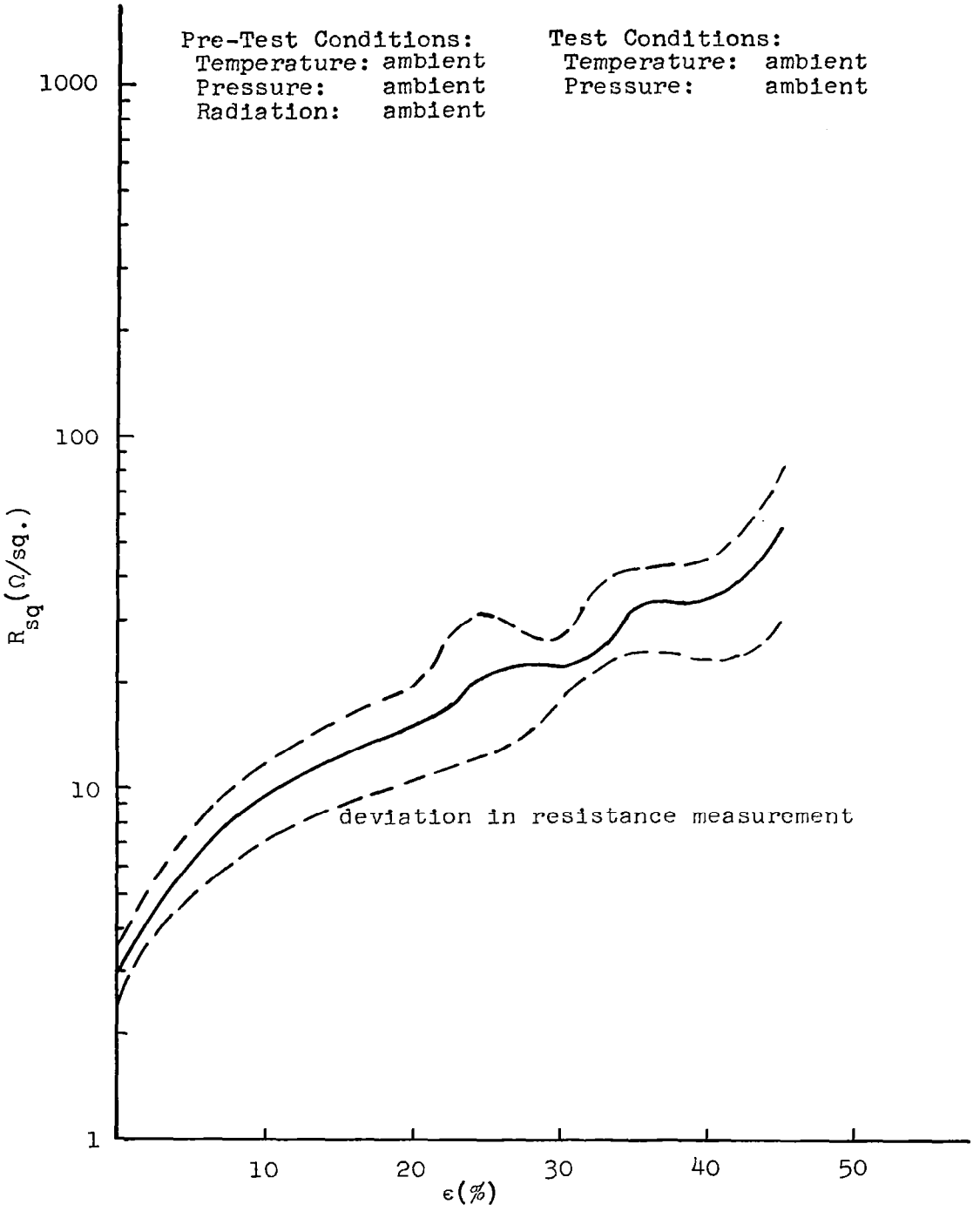

Figure 54 SURFACE RESISTANCE VS. STRAIN FOR COMPLETED MATERIAL (in 45° Direction)

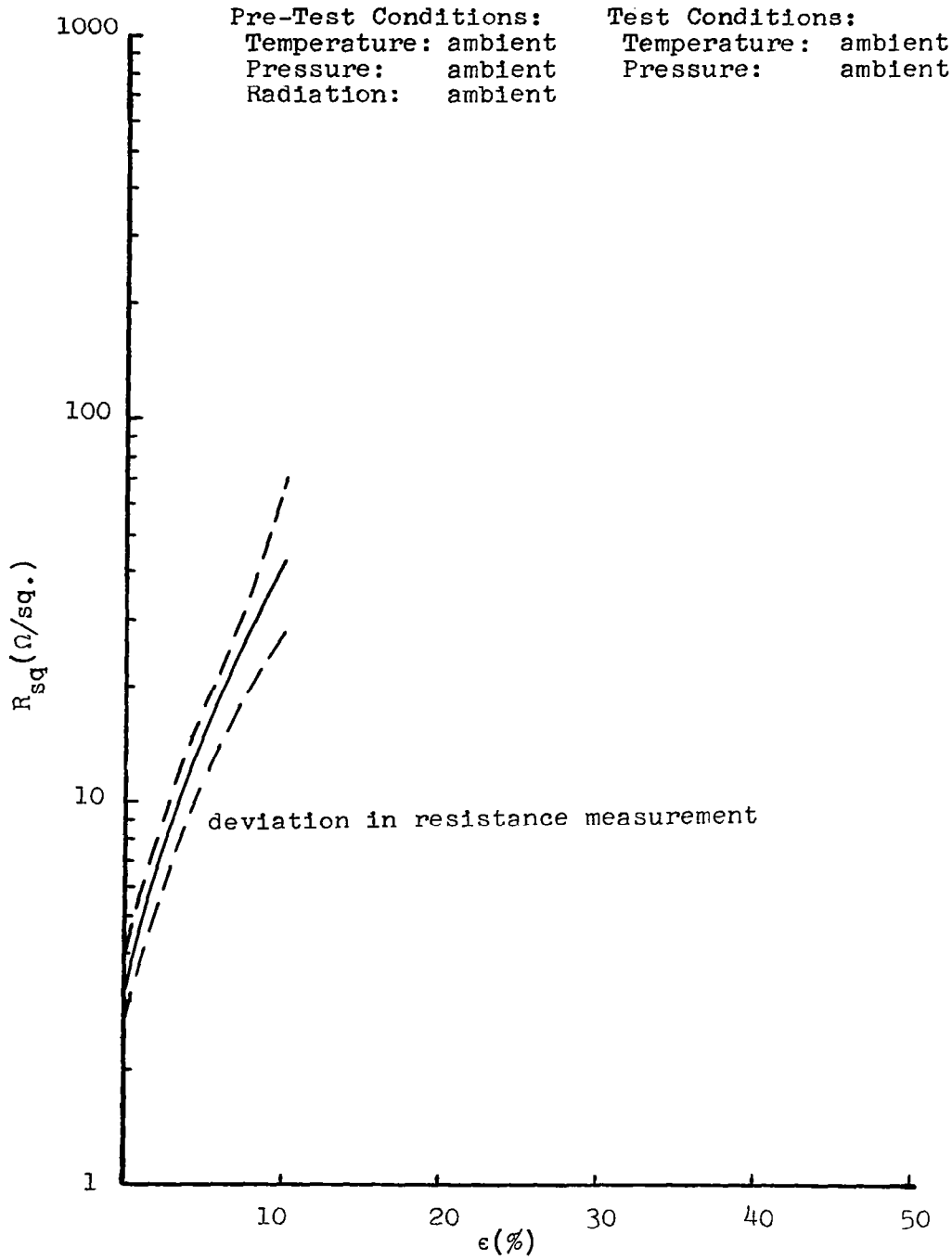

Figure 55 SURFACE RESISTANCE VS. STRAIN FOR COMPLETED MATERIAL (in 90° Direction)

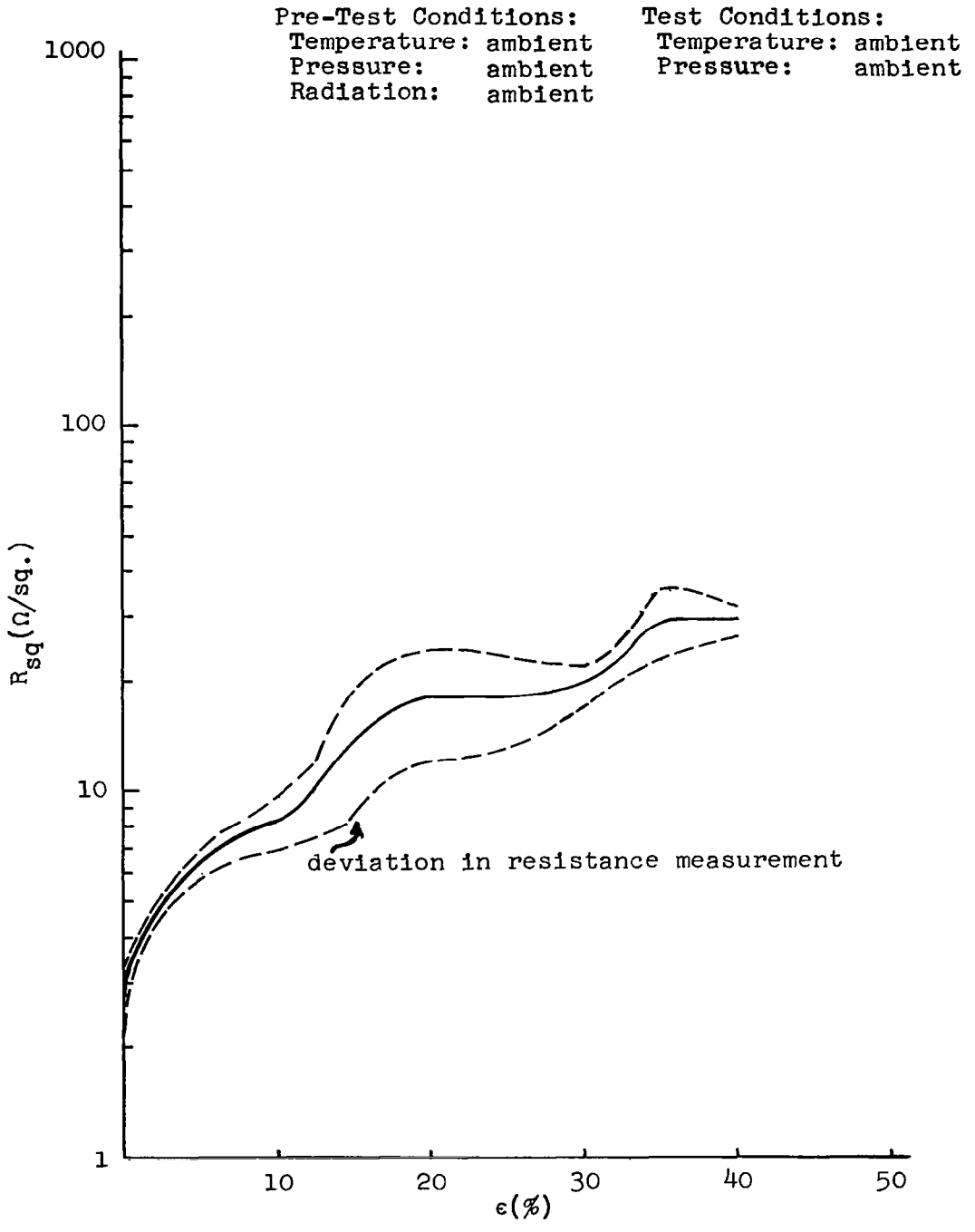

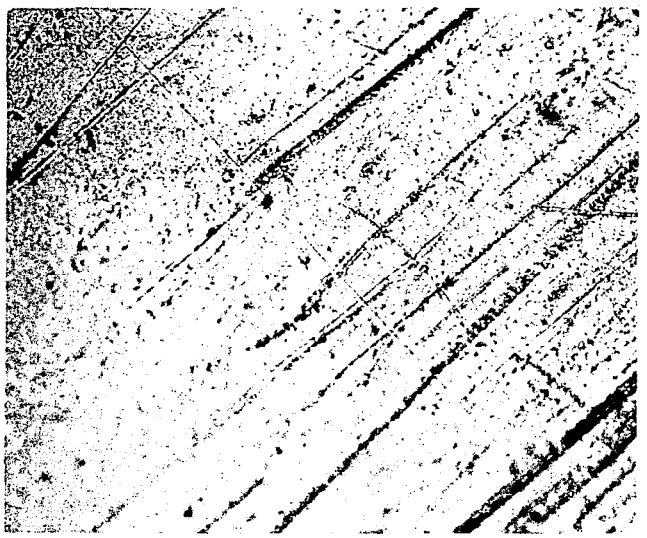

Before Tensile Test
Pre-Test Conditions: Ambient

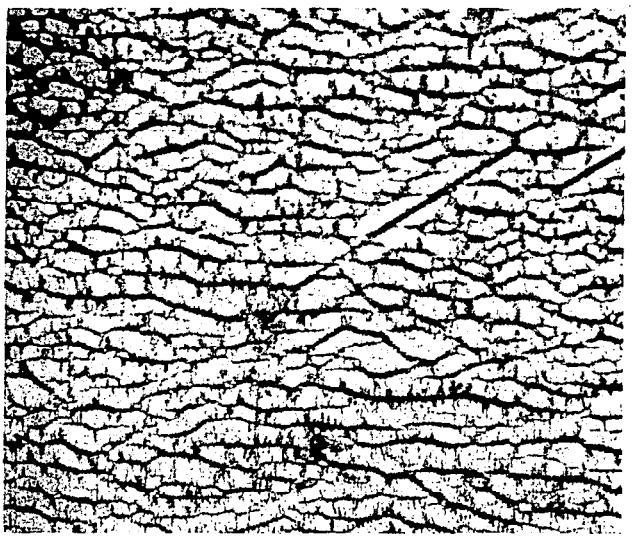

After Tensile Test
Test Conditions: Ambient

TENSILE TEST ON UNPERFORATED, PLATED MATERIAL

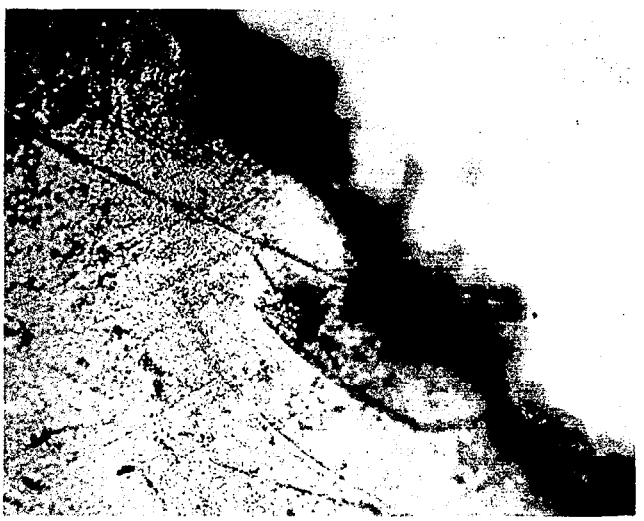

Before Tensile Test
Pre-Test Conditions: Ambient

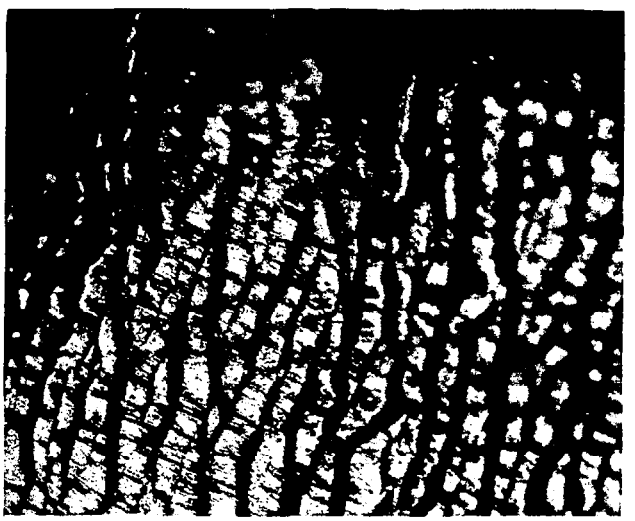

After Tensile Test
Test Conditions: Ambient

TENSILE TEST ON PERFORATED, PLATED MATERIAL

Figure 56 PHOTOMICROGRAPHS OF PLATED MATERIAL, PERFORATED AND UNPERFORATED (250x)

The conditions applied are as follows: high (117°C.) and low temperature (-70°C.), cycling between -196°C. and 100°C., vacuum (1 microtorr) and radiation (85 Mrads).

6.2.1 Tensile Tests

The results of the tensile tests are presented in Table 28. It can be seen that none of the conditions resulted in any degradation of the material. Only the high temperature condition resulted in a loss of strength. This loss is reversible and expected since there is a loss in modulus above the T_m. Additionally, resistance measurements were taken during the tensile test; it is seen from Figures 56 through 66 that the plated film must be strained to ca. 20% before a loss in continuity results.

6.2.2 Flexural Rigidity Tests

The flexural rigidity tests were additionally performed under a variety of pre-test and test conditions listed in Table 29. The flexural rigidity tests were performed according to the ASTM Standard D1388-55T summarized in Appendix IV. The results of the flexural rigidity test on the completely processed PE 12 are listed in Table 29. It is seen that only at the elevated temperature is the rigidity significantly decreased.

6.2.3 Cyclic Flexure Endurance Test

In the cyclic flexure endurance test 1 in. x 5 in. samples of completely processed PE 12 under various pre-test conditions listed in Table 30 were flexed about a curved bar, according to Figure 67 for 200 cycles. The surface resistance of the copper coating was continuously monitored. It was found that all 24 of the samples were able to be flexed for 50 cycles with minimal increase in surface resistance; on the other hand, 22 out of the 24 samples tested maintained a surface resistance

Table 28

Final Qualifications Test: Tensiles[a]

Pre-Test Condition			Test Condition		F_y (lbs. x 10^{-2})			ϵ_y (%)		
Temp.	Press.	Rad.	Temp.	Press.	0°	45°	90°	0°	45°	90°
amb.[b]	micro-torr[d]	amb.	amb.	amb.	45±5	57±3	55±1	0.74±0.07	0.64±0.13	0.62±0.02
amb.	amb.	85 Mr.	amb.	amb.	71±1	108±8	80±4	1.88±0.03	1.83±0.68	2.15±0.20
amb.	amb.	85 Mr.	-70°C.	amb.	88±6	102±2	83±13	1.60±0.05	1.14±0.26	1.33±0.13
amb.	amb.	85 Mr.	117°C.	amb.	6.1±1.7	3.8±0.6	4.0±0.4	2.59±1.21	1.35±0.15	3.20±0.80
amb.	micro-torr[d]	amb.	-70°C.	amb.	225±15	253±8	215±5	1.94±0.02	1.70±0.10	1.68±0.23
amb.	micro-torr[d]	amb.	117°C.	amb.	3.2±0.6	4.9±0.4	1.6±0.6	12.4 ±8.7	1.83±0.58	2.03±0.58
LN_2 BW 50X[c]	amb.	amb.	amb.	amb.	55±4	54±4	47±1	0.76±0.11	0.67±0.04	0.60±0.01

[a] All tensile tests in testing program performed at 0.2 in./min., as described in Appendix I

[b] amb. = ambient

[c] LN_2 BW 50X = cycled in liquid nitrogen and boiling water 50 times

[d] = 48 hours

Figure 57 SURFACE RESISTANCE VS. STRAIN FOR COMPLETED MATERIAL (in 0°, 45° and 90° Directions)

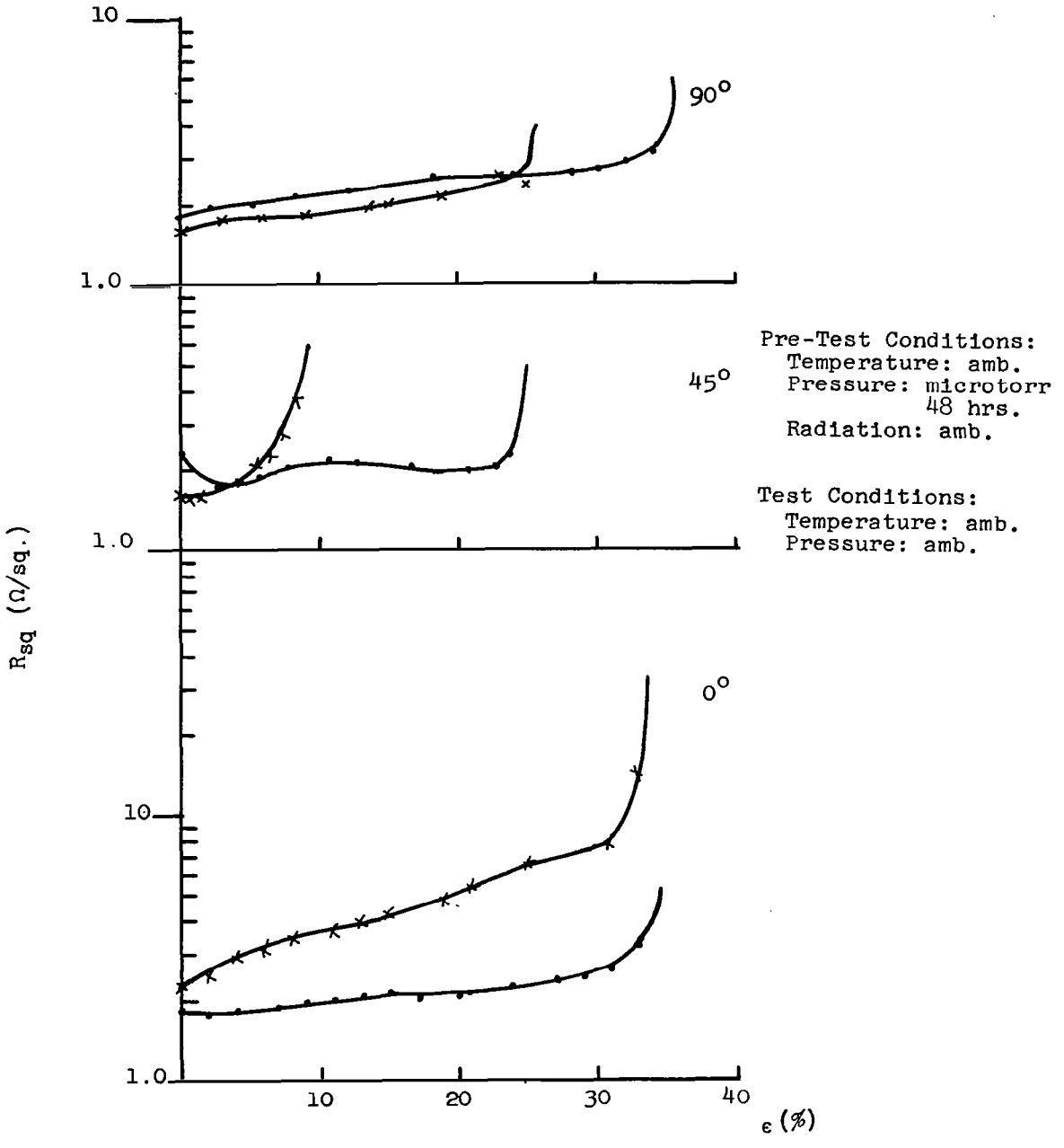

Figure 58 SURFACE RESISTANCE VS. STRAIN FOR COMPLETED MATERIAL (in 0° and 45° Directions)

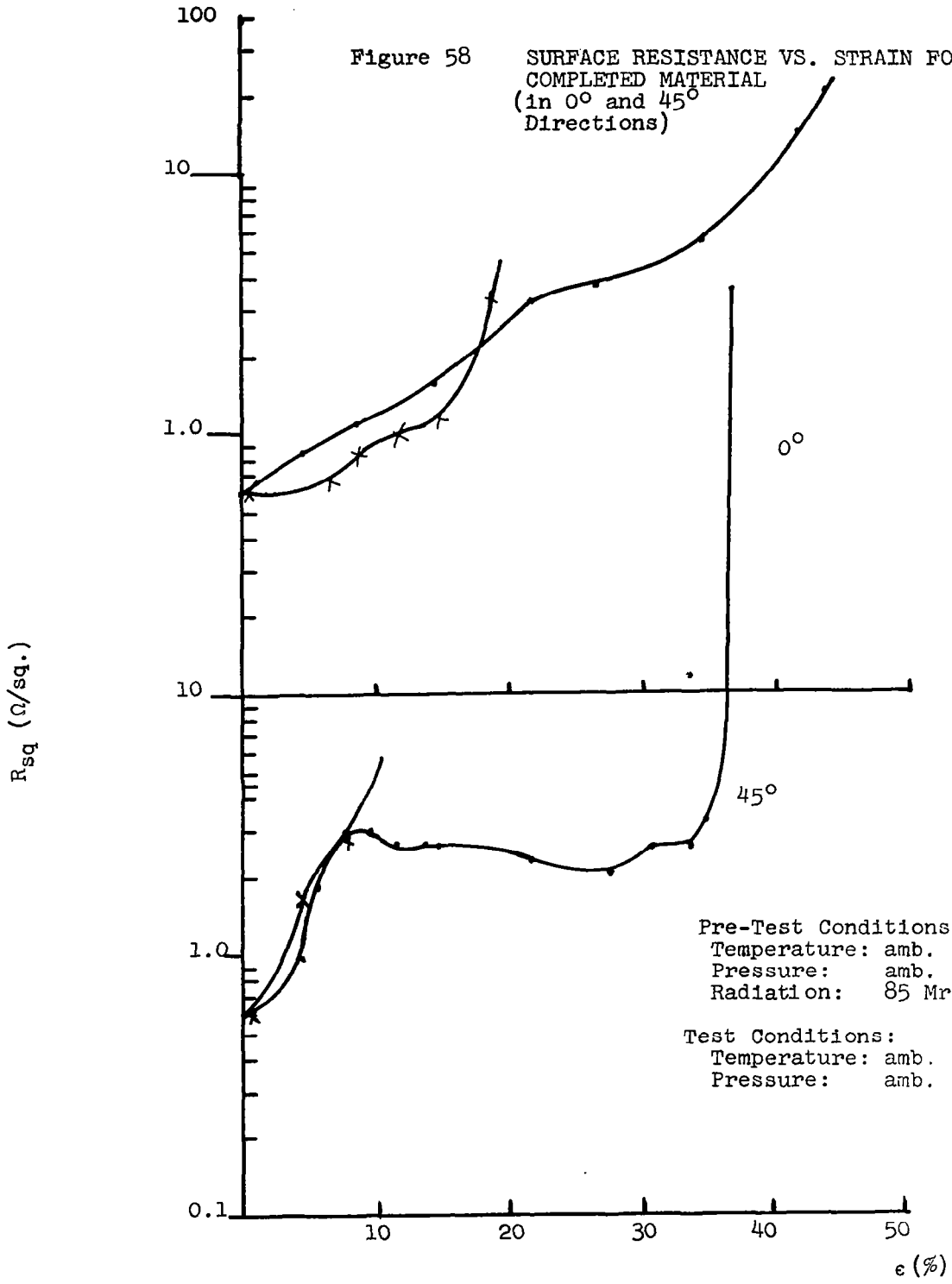

Figure 59 SURFACE RESISTANCE VS. STRAIN FOR COMPLETED MATERIAL
(in 90° Direction)

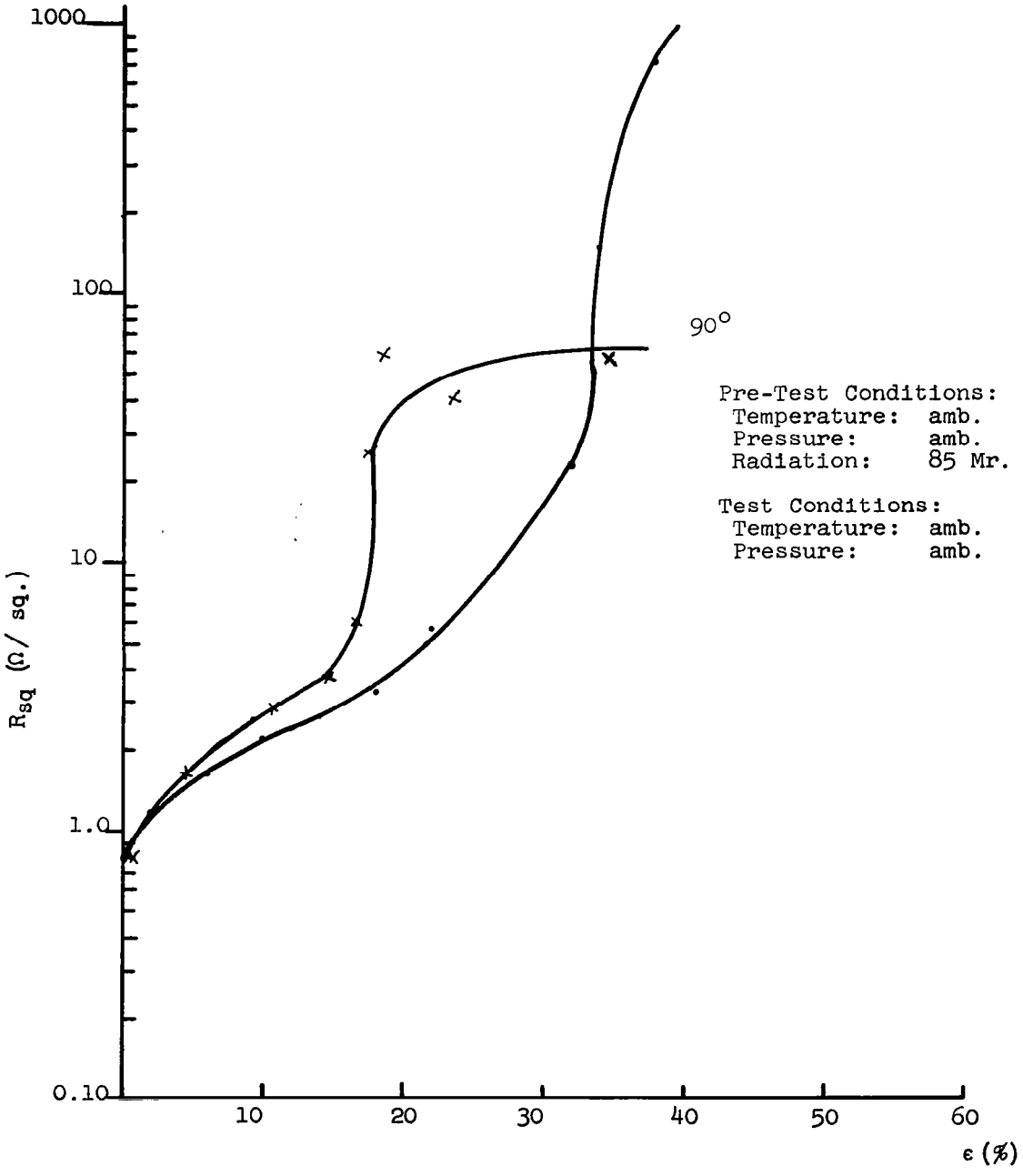

Figure 60 SURFACE RESISTANCE VS. STRAIN FOR COMPLETED MATERIAL (0° Direction)

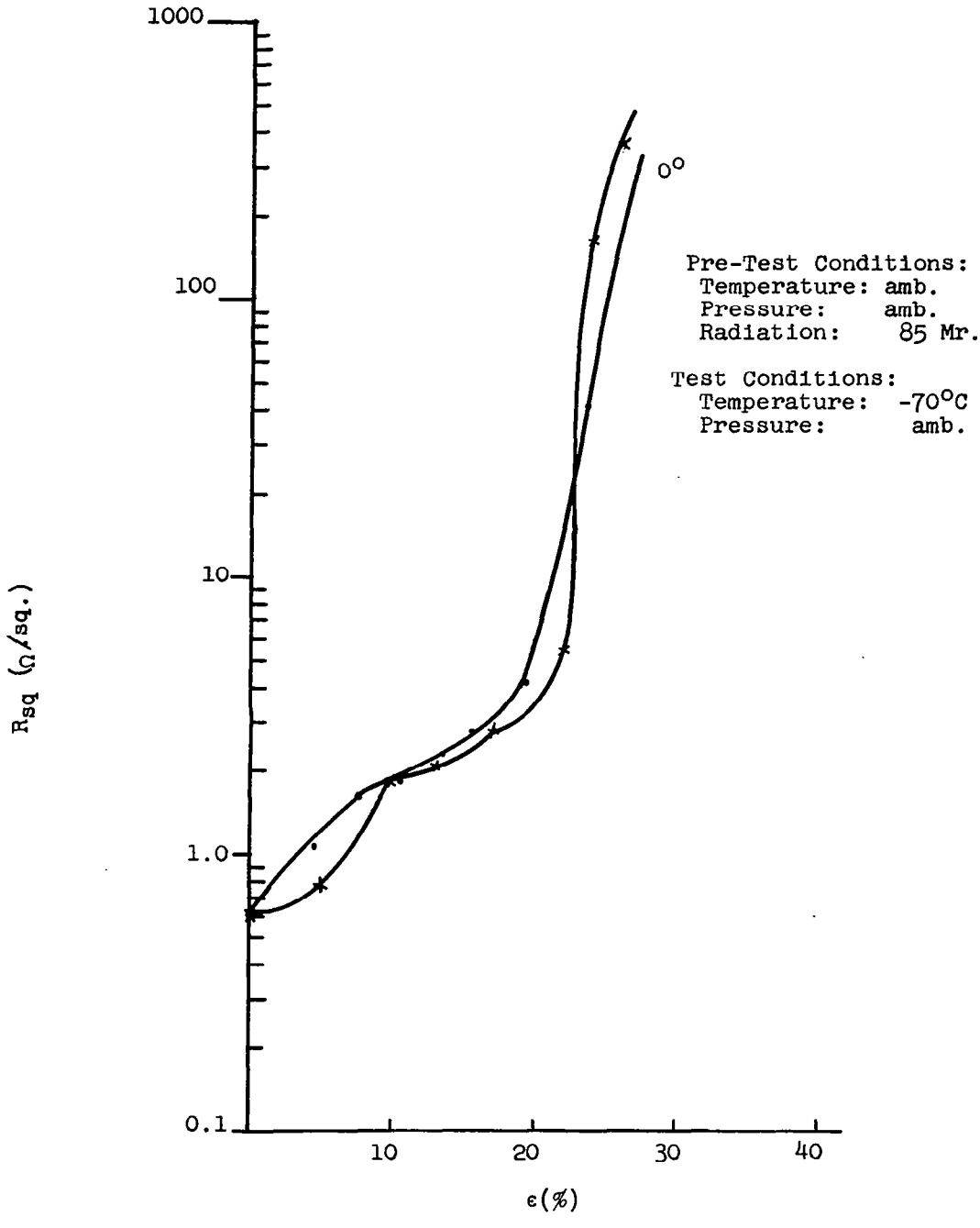

Figure 61 SURFACE RESISTANCE VS. STRAIN FOR COMPLETED MATERIAL (in 45°and 90°Directions)

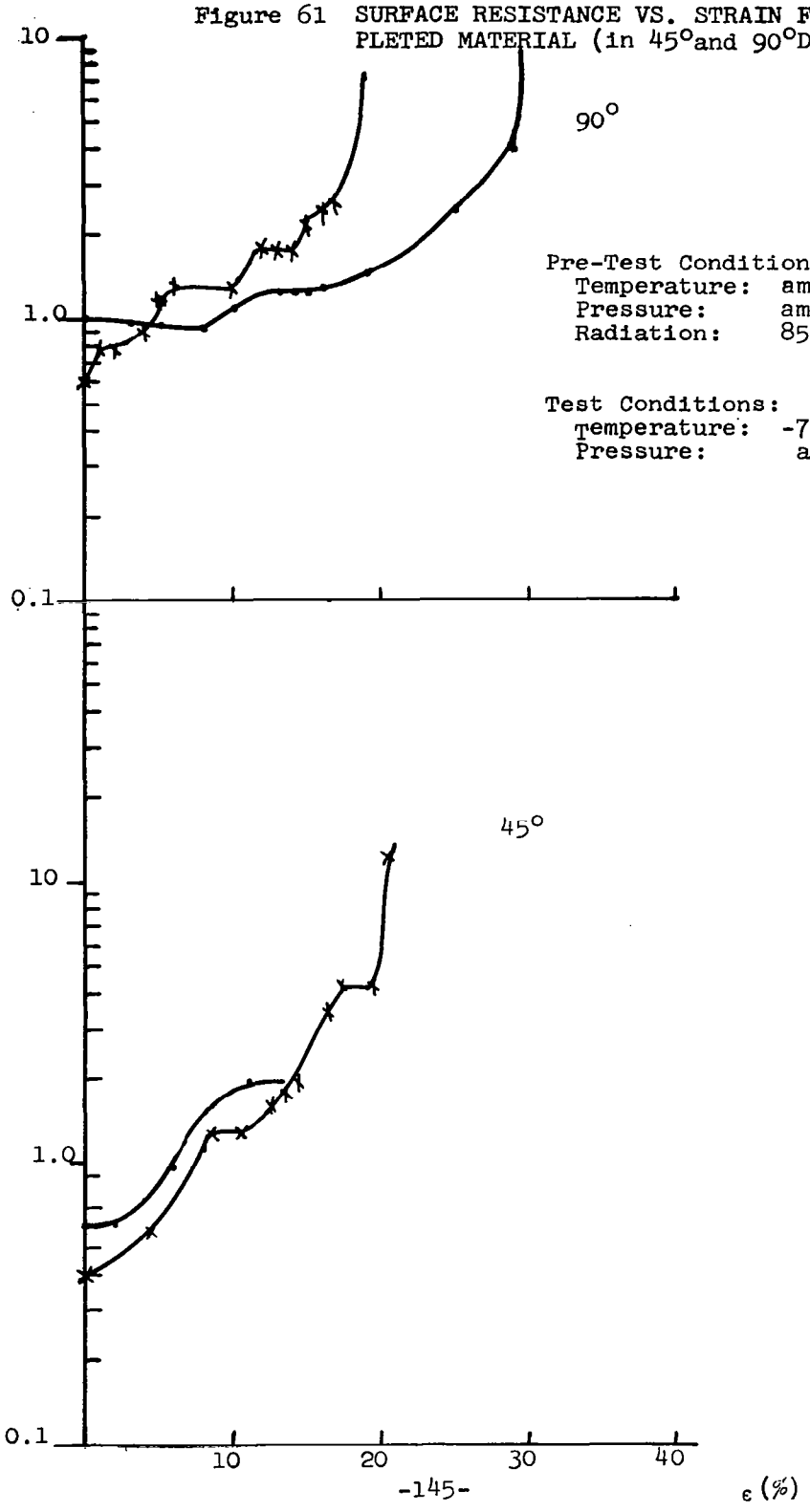

Figure 62 SURFACE RESISTANCE VS. STRAIN FOR COMPLETED MATERIAL (in 0°Direction)

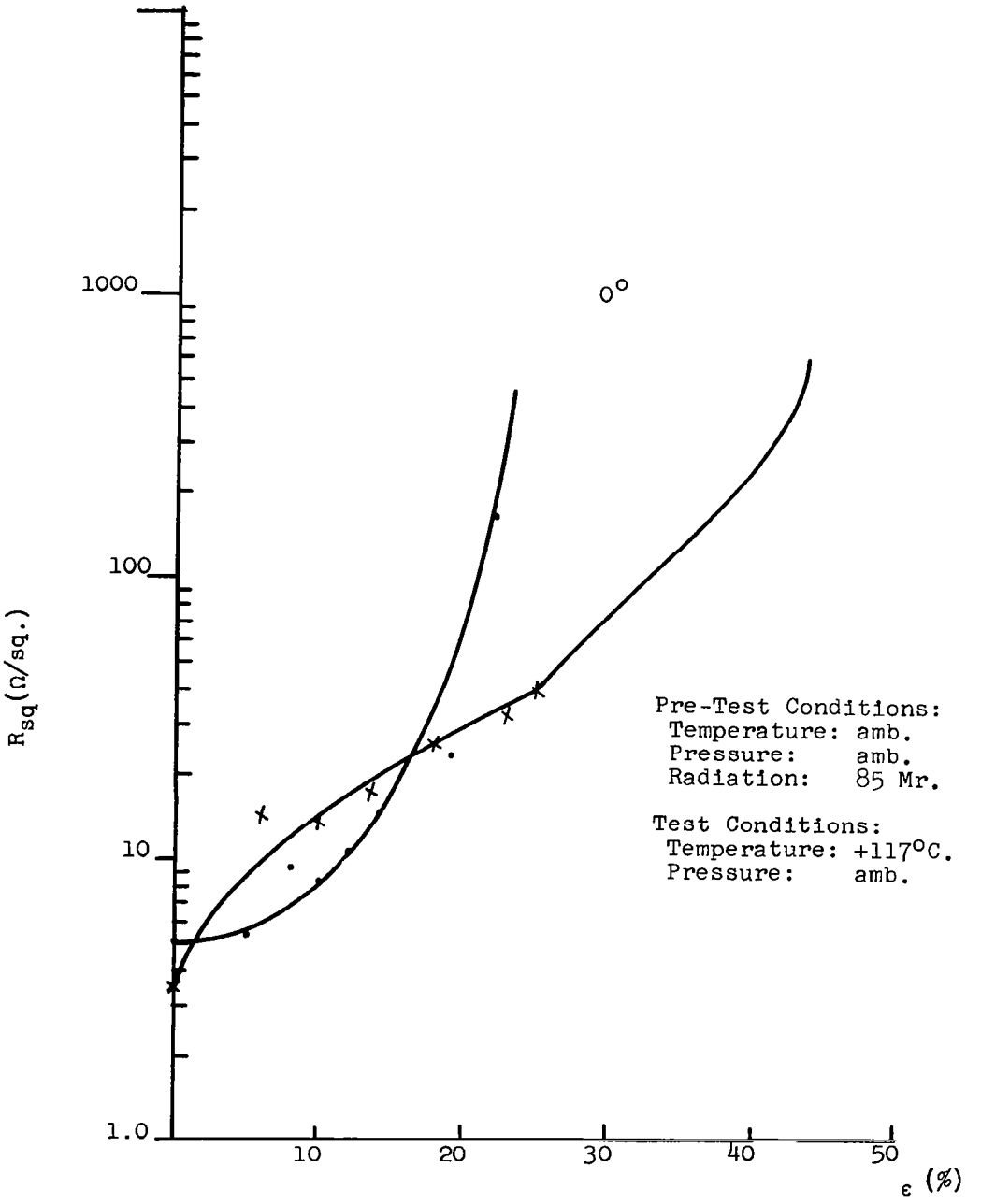

Figure 65 SURFACE RESISTANCE VS. STRAIN FOR COMPLETED MATERIAL(in 0°,45° and 90°Directions)

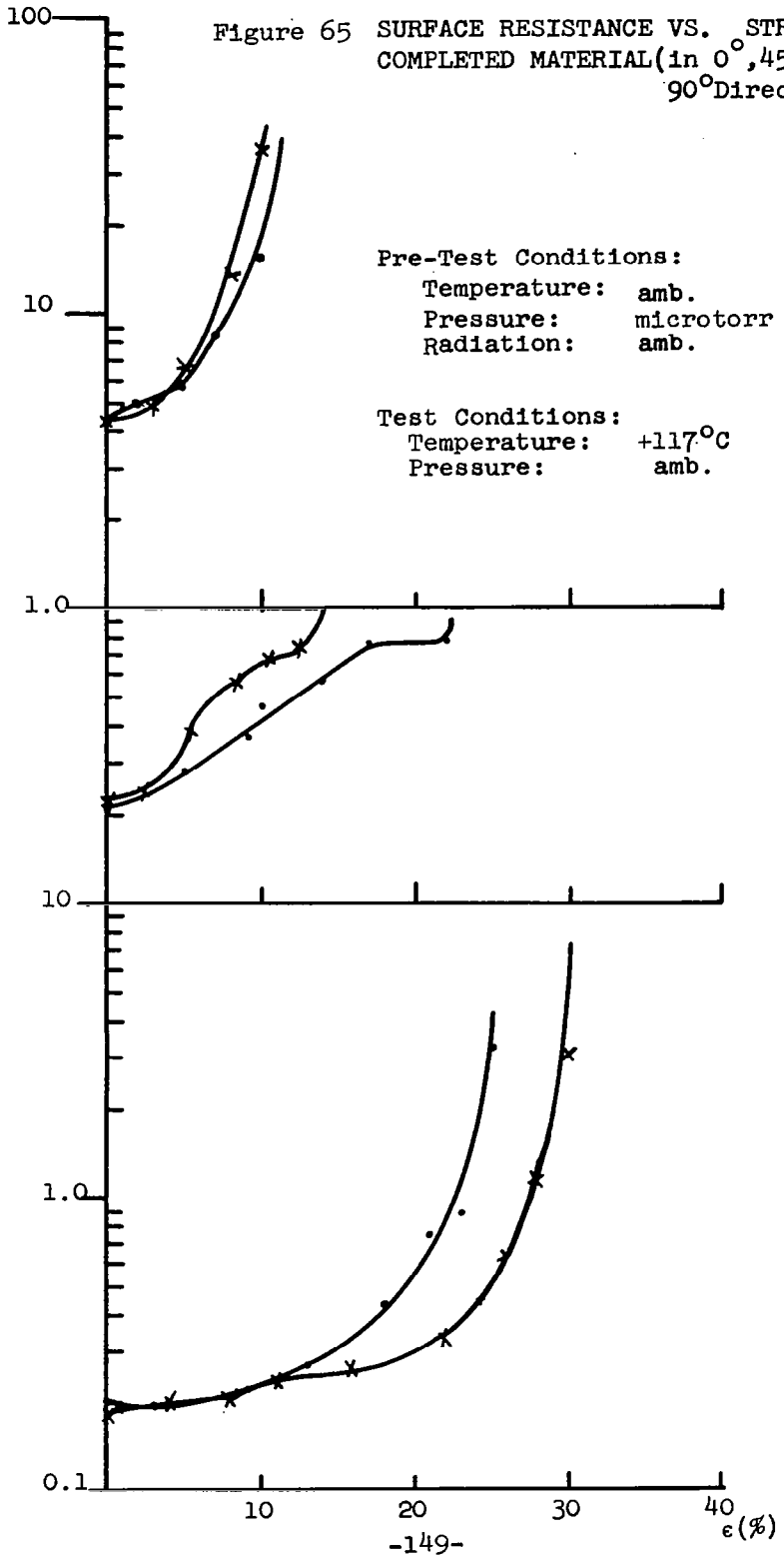

Pre-Test Conditions:
Temperature: amb.
Pressure: microtorr 48 hrs.
Radiation: amb.

Test Conditions:
Temperature: +117°C
Pressure: amb.

Figure 66 SURFACE RESISTANCE VS. STRAIN FOR COMPLETED MATERIAL (in 0°, 45° and 90° Directions)

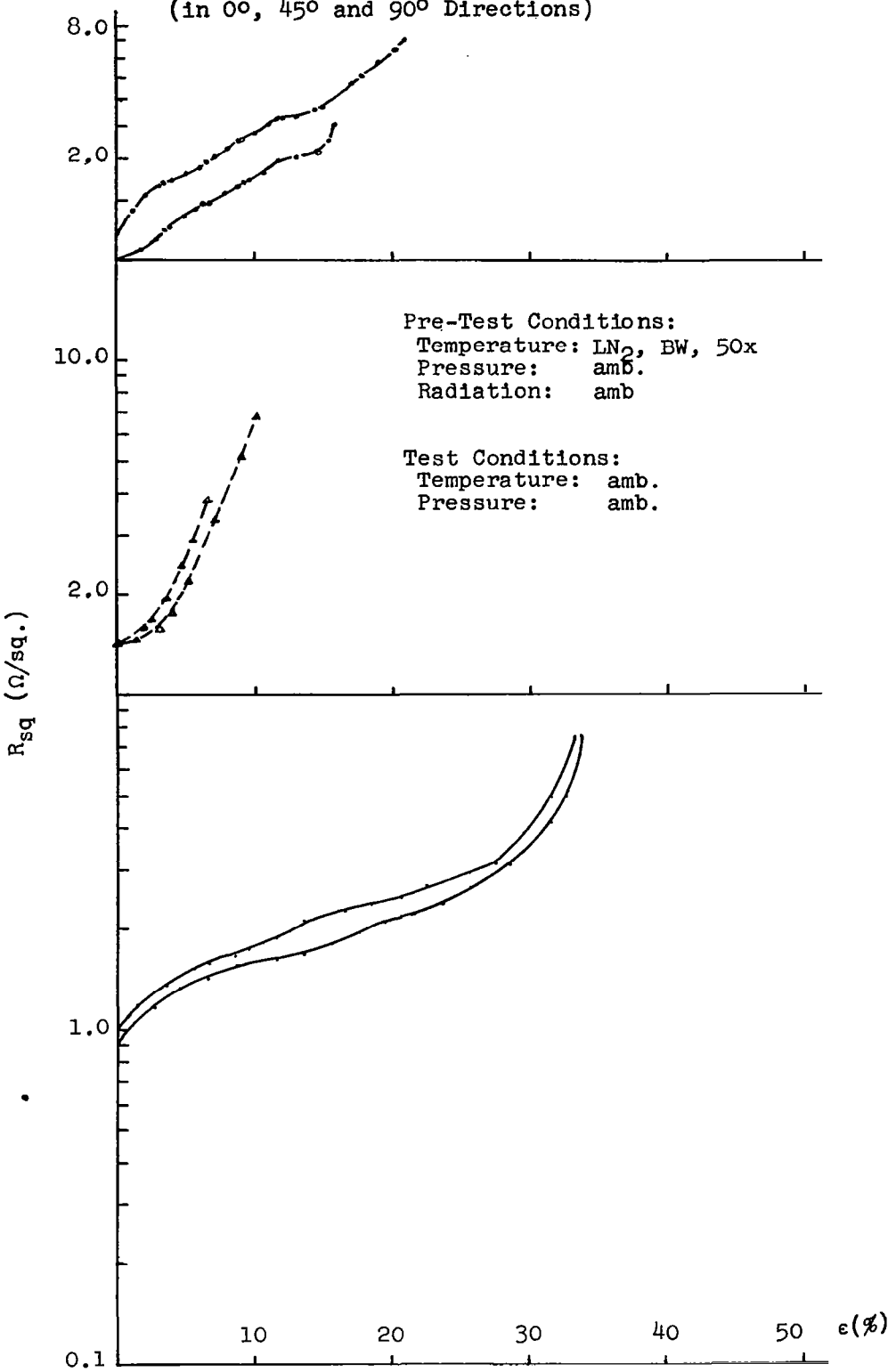

Table 29

Final Qualifications Test: Flexural Rigidity[a]

Pre-Test Condition			Test Condition		G (lb.in.^{2}/in. x 10^{-6})		
Temp.	Press.	Rad.	Temp.	Press.	0°	45°	90°
amb.	amb.	amb.	-70°C.	amb.	59.96±21.18	31.84±7.90	45.40±12.71
amb.	amb.	amb.	117°C.	amb.	16.27±4.37	10.78±3.09	16.64±6.14
amb.	micro-torr[b]	amb.	amb.	amb.	34.14±6.51	36.47±9.13	28.13±7.61
amb.	micro-torr[b]	amb.	-70°C.	amb.	42.46±25.24	48.47±20.35	61.45±12.96
amb.	micro-torr[b]	amb.	117°C.	amb.	9.88±5.28	8.63±2.38	9.85±5.03
LN_2 BW 50X	micro-torr[b]	amb.	amb.	amb.	17.93±1.03	29.87±0.96	41.47±8.15
LN_2 BW 50X	micro-torr[b]	amb.	-70°C.	amb.	31.06±12.64	44.44±18.33	44.92±16.41
LN_2 BW 50X	micro-torr[b]	amb.	117°C.	amb.	3.39±2.05	4.84±2.02	4.44±1.48

[a] Flexural Rigidity Tests performed in accordance with ASTM D 1388-55T as outlined in Appendix IV.

[b] Vacuum applied for 48 hrs.

Table 30

Final Qualifications Test: Cyclic Flexure Endurance

	Pre-Test Condition			Test Condition		R_{sq} after 200 Cycles			Comments
	Temp.	Press.	Rad.	Temp.	Press.	0°	45°	90°	
1	amb.	amb.	amb.	amb.	amb.	0.62±0.26	0.65±0.40	0.66±0.10	
2	LN_2 BW 50X	amb.	amb.	amb.	amb.	0.63±0.04	0.92±0.08	0.96±0	
3	LN_2 BW 50X	micro-torr[a]	amb.	amb.	amb.	1.83±0.80	0.63±0	2.00	90°- above specifications at 50 cycles
4	amb.	amb.	amb.	amb.	amb.	0.82±0.06	0.65±0.19	0.72±0.30	unperforated

[a] Vacuum applied for 48 hrs.

Figure 67 CYCLIC FLEXURE ENDURANCE SCHEMATIC DIAGRAM

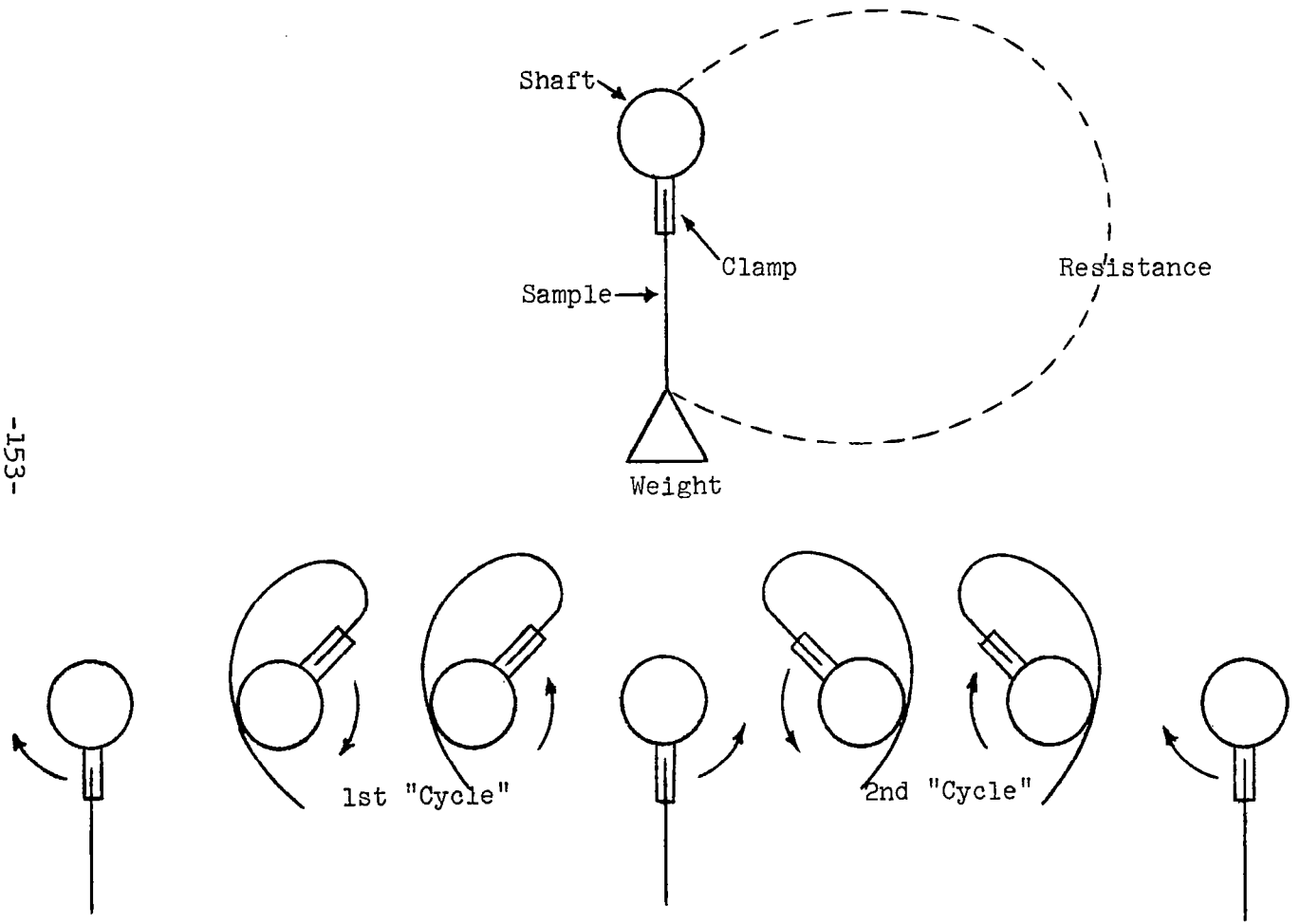

of less than 2 ohms/sq. for 200 cycles of flexure. Additionally the photomicrographs of Figure 68 show that there is minimal cracking of the copper coating in the region of flexure.

6.2.4 Fold Resistance Tests

The fold resistance tests were performed to determine the effect of force folding on the completely processed material and to demonstrate the memory effect. Samples (1 in. x 1 in.) of film were folded under a force of 0.5 lb./in. of length under the pre-test conditions listed in Table 31. The samples were then placed in an oven at 117°C. and allowed to restore. It was found that the samples were not able to restore (see Table 31), on the other hand, electrical continuity was maintained although it was above 2 ohms/sq. The photomicrographs of Figures 68 through 71 show the cracking which occurred at the fold. A perpendicular triple fold test was additionally performed on the completed material. A sample of material was folded three times; one fold perpendicular to the other. The sample was then placed under a force of 0.5 lb./inch of length for 24 hours. It was then pulled apart under the same force. The result is seen in Figure 72 where the sample is magnified 1.9 times. It is seen that the sample tore at the apex of the two folds.

Table 31

Final Qualifications Test: Fold Resistance

Pre-Test Condition				Test Condition		R_{sq} after Test (Ω/sq.)			Opened Set Angle		
Temp.	Press. (lb./in.)	Time	Rad.	Temp.	Press.	0°	45°	90°	0°	45°	90°
amb.	0.5	24 hrs.	amb.	117°C.	amb.	6.0	4.7	7.6	61.3	45.0	77.5
IW* BW 25X	0.5	24 hrs.	amb.	117°C.	amb.	4.4	3.6	3.8	25.0	90.0	60.0
117°C.	0.5	30 min.	amb.	117°C.	amb.	6.0	6.2	7.6	0	20.0	0
amb.	0.5	24 hrs.	amb.	amb.	0.5 lb/in.	11.31	4.56	2.83	-	-	-

*IW = ice water
BW = boiling water
25X = cycled 25 times.

After Test on Unperforated Plated Material

After Test on Perforated Plated Material

Pre-Test and Test Conditions: Ambient

Figure 68 CYCLIC FLEXURAL ENDURANCE TEST (250x)

Before Test
Pre-Test Conditions:
0.5 lb./in. for 24 hrs.

After Test
Test Conditions: 117°C.

Figure 69 FOLD RESISTANCE TEST ON PERFORATED, PLATED MATERIAL (250x)

After Test

Figure 70 FOLD RESISTANCE TEST ON PERFORATED, PLATED MATERIAL (250x)

Pre-Test Condition: 0.5 lb./in. for 24 hrs.
Immersed alternately in boiling water & ice water
Test Condition: 117°C.

Before Test

Figure 71 FOLD RESISTANCE TEST ON PERFORATED, PLATED MATERIAL (250x)

Pre-Test Condition: 0.5 lb./in. for 30 min; 117°C.
Test Condition: 117°C.

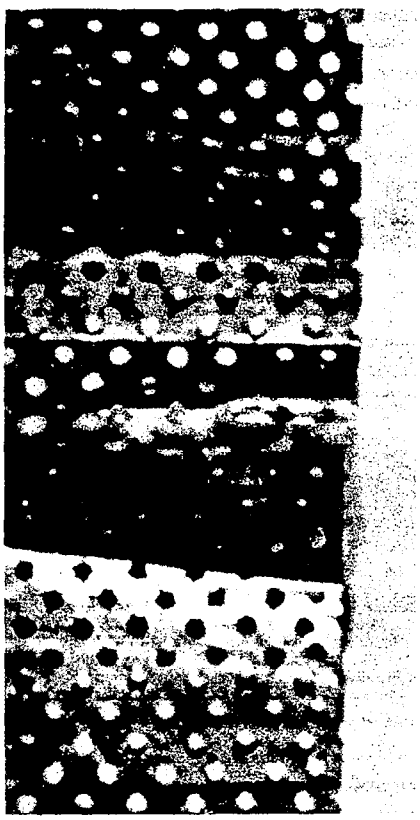

Before Test
Pre-Test Conditions:
0.5 lb./in. for 24 hrs.

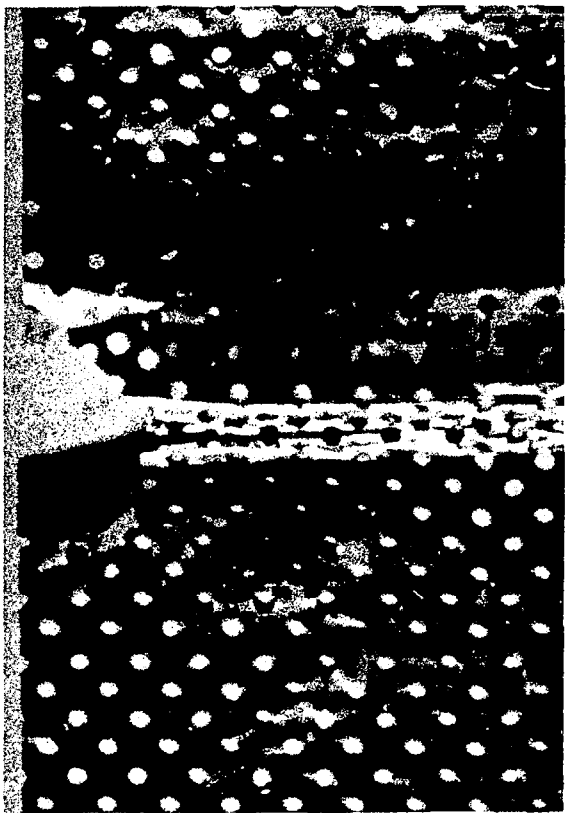

After Test
Test Conditions: 0.5 lb./in.

Figure 72 FOLD RESISTANCE TEST ON PERFORATED PLATED MATERIAL
(Perpendicular Triple Fold)

6.2.5 Final Qualifications Test - Bonded Material

Completed PE 12 material ultrasonically bonded under the conditions summarized in Section 4.1.7.2 was subjected to most of tests under the variety of pre-test and test conditions. The results are listed in Tables 32, 33 and 34 and Figures 73 and 74. Due to the fact that it was difficult to maintain electrical continuity across a welded bond and the near impossibility of creating an adequate bond on or through the copper, the copper was completely removed from all weld areas and hence, no resistance measurements were needed. The results show that the ultrasonic bond is nearly as strong as the unbonded film. It is additionally interesting to note the ultrasonic action on the copper plate. The photomicrograph Figure 73, left, shows the copper coat near an ultrasonic bond. It can be seen that there is a large amount of cracking, nearly as much as if a tensile were pulled on the sample.

6.2.6 Blocking Tests

A limited number of blocking tests were performed on the completely processed polyethylene material as part of the testing program. Two 4 in. x 3 in. samples were placed together face to face between sheets of glass. A 6 lb. weight was then placed upon the top sheet of the glass. The complete setup was then placed in a vacuum chamber operating at 1 microtorr for 48 hours. The samples were then taken from the vacuum chamber, removed from the glass and pulled apart. The difficulty in pulling the samples apart is then considered the degree of blocking. The materials on which blocking tests were performed are listed in Table 35 with the corresponding results. The

Table 32

Final Qualifications Test: Tensiles[a] (Bonded)

Pre-Test Condition			Test Condition		F_y (lbs.)		ϵ_y (%)	
Temp.	Press.	Rad.	Temp.	Press.	0°	90°	0°	90°
amb.	amb.	amb.	amb.	amb.	0.41 ± 0.01[b]	0.42 ± 0.01[b]	0.85 ± 0.11[b]	0.81 ± 0.13[b]
amb.	micro-torr[c]	amb.	amb.	amb.	0.31 ± 0.01	0.38 ± 0.02	0.65 ± 0.01	0.70 ± 0.05
amb.	amb.	85 Mr.	amb.	amb.	0.69 ± 0.01	0.67 ± 0.04	2.43 ± 0.03	2.47 ± 0.12
amb.	amb.	85 Mr.	-20°C.	amb.	0.95 ± 0.05	0.79 ± 0.21	2.10 ± 0.45	1.58 ± 0.38
amb.	amb.	85 Mr.	117°C.	amb.	0.0049 ± 0.0001	0.0031 ± 0.0010	7.55 ± 1.65	4.85 ± 0.85
amb.	amb.	amb.	-70°C.	amb.	1.38 ± 0.33	1.8 ± 0.3	4.0 ± 0.9	2.5 ± 0.9
amb.	micro-torr[c]	amb.	117°C.	amb.	0.0015 ± 0.002	0.012 ± 0.001	32.45 ± 15.25	18.45 ± 4.55
LN_2 BW 50X	amb.	amb.	amb.	amb.	0.46 ± 0.04	0.46 ± 0.06	0.23 ± 0.18	0.98 ± 0.03

[a] All tensile tests performed at 0.2 in./min., as described in Appendix I.

[b] The result of five tests.

[c] Vacuum applied for 48 hours.

Table 33

Final Qualifications Test: Flexural Rigidity (Bonded)[a]

Pre-Test Condition			Test Condition		G (lb.in.^{2}/in. x 10^{-6})	
Temp.	Press.	Rad.	Temp.	Press.	0°	90°
amb.	amb.	amb.	amb.	amb.	17.05 ± 7.38[b]	23.11 ± 4.06[b]
amb.	amb.	amb.	-70°C.	amb.	38.28 ± 9.06	48.87 ± 10.09
amb.	amb.	amb.	117°C.	amb.	1.79 ± 1.13	4.06 ± 0.65
amb.	micro-torr[c]	amb.	amb.	amb.	17.97 ± 4.79	23.04 ± 6.01
amb.	micro-torr[c]	amb.	-70°C.	amb.	43.35 ± 12.78	63.06 ± 14.61
amb.	micro-torr[c]	amb.	117°C.	amb.	2.01 ± 1.03	2.61 ± 1.48
LN_2 BW 50X	micro-torr[c]	amb.	amb.	amb.	11.84 ± 4.8	13.90 ± 4.45
LN_2 BW 50X	micro-torr[c]	amb.	-70°C.	amb.	38.14 ± 17.52	75.58 ± 14.47
LN_2 BW 50X	micro-torr[c]	amb.	117°C.	amb.	1.81 ± 0.78	2.21 ± 1.00

[a] Bond running the length of sample.

[b] The result of five tests.

[c] Vacuum applied for 48 hours.

Table 34

Final Qualifications Test: Cyclic Flexure Endurance (Bonded)[a]

Pre-Test Condition			Test Condition		Result (at Completion of 200 Cycles)
Temp.	Press.	Rad.	Temp.	Press.	0^0
amb.	amb.	amb.	amb.	amb.	one failure at 115th cycle
LN_2 BW 50X	amb.	amb.	amb.	amb.	All
LN_2 BW 50X	micro-torr[b]	amb.	amb.	amb.	All

[a] Bond perpendicular to length of sample.

[b] Vacuum applied for 48 hours.

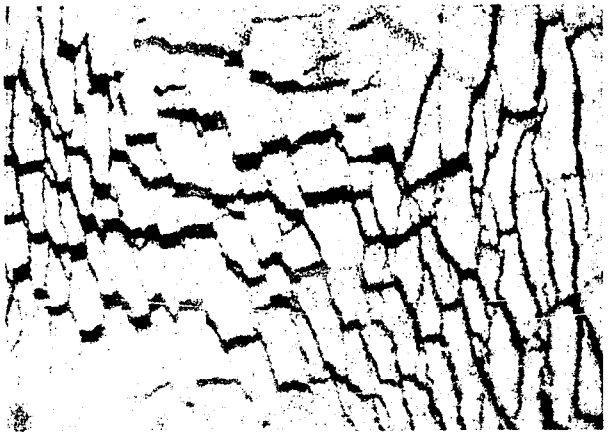

Before Test

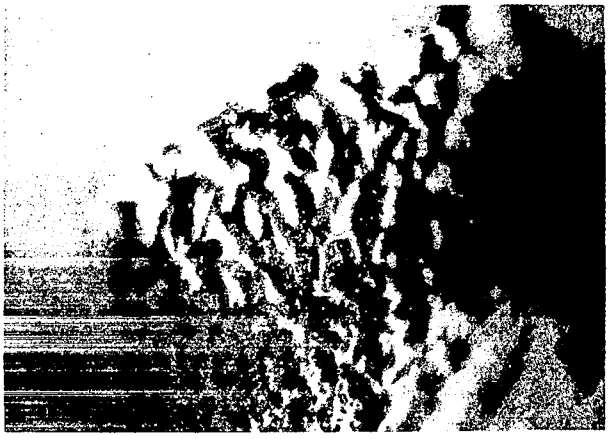

After

Pre-test and test conditions: Ambient

Figure 73 TENSILE TEST ON BONDED PERFORATED, PLATED MATERIAL

After Test
Test Conditions: Ambient

Figure 74 CYCLIC FLEXURAL ENDURANCE ON BONDED, PERFORATED, PLATED MATERIAL

blocking occurred at the polyethylene bond. It is apparent from this test and the deployment tests on the unplated cylinders that polyethylene can be caused to block while the copper does not block.

Table 35

Blocking Tests

Pre-Test Condition: Temp. : amb.
Press.: microtorr
Time : 48 hrs.
Rad. : amb.

Test Condition: Temp. : amb.
Press.: 6 lbs.

	Material Description	Results	Comments
1.	PE 12 non-perforated, plated	degree slight blocking	-
2.	PE 12 perforated, plated	degree slight blocking	-
3.	PE 12 plated, bonded (bonds folded perpendicular to each other)	degree blocking	slight damage at intersection of bonds

7.0 CONCLUSION AND RECOMMENDATIONS

It is concluded that the results obtained from this investigation have yielded sufficient design information to permit construction of a 425-foot diameter sphere weighing less than 1000 pounds.

In addition, the memory phenomenon is now more fully understood and much of the data and procedures developed during the investigation can be used to construct other expandable items besides thin film spheres. Most noteworthy in this area is the work done on polyethylene mesh. The irradiated, plated polyethylene mesh could well be used for other items, such as lenticular components, waveguides, booms, etc. without the critical regard for buckling pressure since the mesh material is much thicker than the thin film used to design the large sphere. Furthermore, the deployment of mesh items can be demonstrated in a 1-g field.[20]

The specific conclusions which follow indicate those areas completed and the specific accomplishments realized. In addition, a listing of work still needed is given.

7.1 Material Properties Development Program and Buckling Pressure Evaluation

A copper laminated polyethylene film has been developed which is light in weight and can withstand five times solar pressure when fabricated as a 425 foot diameter sphere. In the course of the development of the polyethylene-copper laminate it was shown that a general method of increasing the strength to weight ratio of a film is by application of a thin coat of metal to the base film. The metallized material has sufficient copper thickness for adequate radio-frequency characteristics. The results of the testing program additionally show that thin film polyethylene-copper laminates can withstand

the conditions of a space environment and withstand normal handling for packaging. The material successfully withstood vacuum, radiation, low temperature and mechanical handling tests. Laminate peeling, film degradation or weight loss did not occur.

7.2 Test Models and Production

The necessary procedures for the production of the large size satellites were investigated during this program. The following list shows what has been accomplished.

a) Establishment of operating variables and procedures necessary for the production of large deliverable items.

b) The actual production of deliverable items.

c) Design information necessary for scale-up.

d) Design information still needed for scale-up.

The state of the procedures for scale-up are listed below:

1. Production of a plastic film of given gauge and density. Scale-up here is not necessary; sufficient data has been compiled for complete characterization of the film.

2. Irradiation of the extruded plastic film. Sufficient investigation was accomplished in the area of film irradiation to warrant direct scale-up. The effects of depth-dose relationship, irradiation environment, uniformity and film handling have been investigated.

3. Heat Treatment. It was not possible to heat treat the irradiated polyethylene film on a continuous production scale basis during the course of this contract. It was found necessary from experimental tests to heat treat the film above its crystalline melting point; but when it was tried on a continuous basis difficulty was encountered in controlling

the tensioning of the film. It was, therefore, necessary to heat treat the film below its crystalline melting point; fully realizing the film would not completely maintain its dimensional stability if it were heated above its crystalline melting point. In light of this it is then necessary to conduct further heat treating tests on a production scale using continuous equipment to resolve this problem.

4. Electroless Plating. In order for the polyethylene film to have sufficient strength and the necessary radio-frequency characteristics the polyethylene film was metallized with copper using the Enthone electroless plating process. It was found that plating thicknesses between 1-20 x 10^{-6} inches of copper could be readily applied. The testing program showed that this copper coating had excellent adhesion under the environmental conditions that would be encountered in space. The operating conditions and procedures for the electroless plating of polyethylene films to various metal thicknesses have been accomplished and sufficient information has been established to scale-up the metallization for continuous production.

5. Ultrasonic Bonding. The operating variables and procedures for ultrasonic bonding have been adequately established during the course of this contract. It was found that a strong bond could be created by ultrasonic methods which would withstand the environmental conditions of space.

Two problem areas still remain to be solved in conjunction with the ultrasonic bonding of polyethylene.

1. Electrical continuity cannot be maintained across an ultrasonic bond without coating over the bond with a conductive lacquer.*

2. The unplated ultrasonic bond (and any unplated polyethylene) has a tendency to block when packaged.

In light of these two problems it is necessary to insure that the exposed polyethylene is coated with a non-blocking material. This problem will be resolved, incidentally, with the development of the thermal control coating which will consequently be required to be non-blocking.

6. Packaging - In light of the testing program which showed that the film can be force-folded with minimal damage occurring to it, a packaging procedure has been established which permits packaging the 425 ft. sphere into a package of 74.4 $ft.^3$ The development of a canister which is part of the packaging program has not been investigated, since it was not included in the scope of the contract. With the development of the canister the packaging procedure would be complete.

7.3 Memory Effect and Deployment

Although it was possible to characterize and prove that a plastic memory exists in irradiated thin polyethylene film it was not possible to conclusively demonstrate the deployment of test models constructed out of thin film polyethylene. It was found that gravity, air currents and blocking resist restoration thereby hindering full deployment. In order to conclusively demonstrate that the plastic memory effect

*The effect (if any) on the radio-frequency reflectance characteristic of electrical continuity across gores on passive communications satellites is still open to question. In an attempt to answer this question half of the test models produced had their bonded sections coated with a silver lacquer to insure continuity across bonds. At the time of this writing, the radio-frequency reflectance has not as yet been conducted.

works on thin irradiated polyethylene film it is suggested that a number of follow-on tests be conducted. These tests should be run after the thermal control coating is developed since the thermal control coating would have to be non-blocking. The next deployment test should be conducted in a vacuum chamber thereby eliminating the effects of air current. The final test should be a 0-g deployment test (in space) of a small three-dimensional model. The 0-g test would eliminate the effects of gravity which are believed to be the main resistance to restoration of thin film materials. The 0-g deployment test would conclusively substantiate the feasibility of using the plastic memory effect in the deployment of thin film materials.

7.4 Thermal Control Coatings

An area necessary for the completion of this program which was not included in the scope of work is thermal control coatings. The area of thermal control coating is both necessary to initiate deployment and maintain the required equilibrium temperature once the item is deployed.

The utilization of the memory phenomenon is wholly dependent on the application of heat to the packaged article. The heat input must raise the temperature of the structure to be deployed above its T_m. As noted previously, the restoration forces can only operate once the crystalline restraining forces are removed. Therefore, step one in any deployment scheme requires heating the structure above its T_m. Since the predominant source of heat in space is via radiative absorption it necessitates control of the surfaces α/ϵ ratio.

Initially, the α/ϵ of the metallized coating must be

determined and the equilibrium temperature to be expected must be calculated.* The surface of the metallized film must be changed either via the use of selected thermal control coatings or a change in the metallization procedure. In either case, a final α/ϵ must be obtained which permits a $Teq > T_m$ for deployment. Additionally, the thermal control coating must be non-blocking not to interfere with deployment.

Once the sphere is deployed then the following procedure is necessary to increase the rigidity of the sphere.

The large structure would, undoubtedly, require cooling the structure considerably below its T_m to increase its rigidity. To effect this would require the development of a thermal control coating which would

a. have an α/ϵ ratio sufficient to heat the structure above its T_m,
b. subsequently boil off and expose a second surface with an α/ϵ ratio which would result in a final equilibrium temperature sufficiently cool to permit the rigidity to be adequate to withstand solar buckling pressures.

*An initial determination of α/ϵ was conducted at NASA towards the end of the contract; the results are presented in Appendix VIII.

8.0 LIST OF SYMBOLS

$A(F_v)$	The function $\frac{1-F_v}{Q(F_v)}$
D	Cap section diameter (24 ft.)
E	Modulus of elasticity of polyethylene film, psi
$F(\rho)$	The function $\frac{2E}{\pi R^2 k^{\frac{1}{2}}} \left[\frac{10^{-2} k\rho}{4} + \frac{1}{\rho} \right]$
F_{cr}	Critical loading force, lb_f
F_v	Void fraction, dimensionless
F_y	Yield Force, lbs.
$F^c(\rho)$	The function $\frac{24}{\pi R^2 k^{\frac{1}{2}} P_{cr}} \left[\frac{10^{-2} k\rho}{4} + \frac{1}{\rho} \right]$
G	Flexural Rigidity lb.in.^{2}/in.
$\hat{G}^L(t)$	Experimental flexural rigidity of polyethylene film of various thickness laminated with a constant thickness of copper, lb.in.^{2}/in.
$\overline{G}^L_0$	Average flexural rigidity in 0^o direction, lb.in.^{2}/in.
$\overline{G}^L_{90}$	Average flexural rigidity in 90^o direction, lb.in.^{2}/in.
$H(t)$	The function $\frac{t}{\hat{G}^L(t)}$
M_c	Molecular weight between crosslinks
M_n	Number average molecular weight
Mr, Mrad	Megarad
N	Avagadros Number
P_{cr}	Critical buckling pressure = 5 P_s = 6.5 x 10^{-9} psi
$P_{crr}(\rho)$	Reduced critical buckling pressure, dimensionless $= \frac{P_{cr}}{2E\, k^{\frac{1}{2}} (\frac{t}{R})^2}$ see Figure 10, Section 3.0.
P_s	Solar pressure 1.3 x 10^{-9} psi

LIST OF SYMBOLS (Continued)

Q	The latitudinal angle in spherical coordinates
R	Radius of sphere 212.5 ft.
R_{sq}	Experimentally measured resistance, ohms/sq.
$\overline{R}_{sq}$	Average experimentally measured resistance, ohms/sq.
T	Residence Time
T_m	Crystalline melting point
$U(\rho)$	The function $\frac{2Ek^{\frac{1}{2}}}{R^2} P_{crr}(\rho)$
$Q(F_v)$	$\frac{\text{Flexural rigidity after perforation of 0.30 mil laminated film}}{\text{Flexural rigidity before perforation of 0.30 mil laminated film}}$
W_A	Area weight, lb./ft.^{2}
a	Perforator dimension
b	The width of a spherical gore, see Appendix VI
d_f	Final diameter
d_i	Initial diameter
g	gravitational acceleration
k	$\frac{2}{3}(1-v^2)$, dimensionless, and the Boltzmann constant
l	Perforator dimension
l_f	Final length, length of overhang
l_i	Initial length
n_R	Number of rows of holes on perforator die
r	Radius of deformation (inch) see Figure 11, Section 3.0
t	Thickness of polyethylene film, mil, inches
t_{cu}	Thickness of copper plate, inches
v	The number of polymer chains per unit volume, and Poisson's ratio
x, y, z	Perforator dimension

LIST OF SYMBOLS (Continued)

α	Absorptance
ϵ	Strain (dimensionless, or percent) and emittance
ϵ_y	Yield strain, dimensionless
Θ	The longitudinal angle in spherical coordinates
λ	A geometrical parameter for a spherical surface $= \frac{r^4}{t^2 R^2}$, dimensionless
μ	A loading parameter dimensionless $= \frac{R\ F_{cr}}{E\ t^3}$
ρ	A geometrical parameter for a spherical surface $= 2k^{-\frac{1}{2}} \frac{r^2}{R} \frac{1}{t}$
ρ_{cu}	Density of copper, gm./cc.
ρ_F	Density of polyethylene film, gm./cc.
σ	Stress, psi.
σ_u	Ultimate stress, psi.
σ_y	Yield Stress, psi.
Ω	Ohms.

9.0 REFERENCES

1. Charlesby, A., "Atomic Radiation and Polymers," Pergamon Press, London (1960).

2. Bueche, F., "Physical Properties of Polymers," Chapter III, John Wiley & Sons, New York, N.Y. (1962).

3. Flory, P.J., "Principles of Polymer Chemistry," Chapter IV, Cornell University Press, Ithaca, N.Y. (1953).

4. Report NASA CR-274, "Ultra-thin Gauge Polymeric Films for Space Applications," Sea Space Systems, Inc., Torrance, Calif.

5. Report RAI-3333-1, "Upgrading of By-Product Polypropylene by Radiation Techniques," Final Summary Report, Radiation Applications, Inc., Long Island City, N.Y., March 15, 1965.

6. Pezdirtz, G.F., H. Price, "Mechanical Properties of Echo II Laminate," NASA Technical Note TN D-2367, Aug. 1964.

7. Price, H.L., "Techniques for the Measurement of the Flexural Rigidity of Thin Films and Laminates," NASA Technical Note TN D-3270, April 1966.

8. Siebert, Leo, "How to Specify Perforated Metals," Machine Design, Vol. 38, No. 7, pp. 152-158, March 17, 1966.

9. Final Report, NAS5-1190, p. 4.1.

10. Rourk, Raymond, J., "Formulas for Stress and Strain," 3rd Ed., p. 318.

11. Timoshenko, S. and Gere, "Theory of Elastic Stability," 2nd Ed., pp. 512-519, "Buckling of Uniformly Compressed Spherical Shells".

12. Ibid., p. 518.

13. Ibid. ref. 10, p. 303.

14. Reiss, E.L., "On the Non-Linear Buckling of Shallow Spherical Domes," Journal of Aeronautical Sciences, Vol. 23, #10, pp. 973-975, October 1956.

15. Reiss, E.L., H.L. Greenburg, and H.B. Keller, "Non-Linear Deflections of Shallow Spherical Shells," Journal of Aeronautical Sciences, Vol. 24, #7, pp. 533-543, July 1957.

16. Ibid. ref. 14.

17. Carlson, R.L., R.L. Stendelbeck and N.J. Hoff, "An Experimental Study of the Buckling of Complete Spherical Shells," NASA Contractor Report NASA CR-550, Aug. 1966.

18. Biezeno, C.B. and R. Grammel, "Elastic Problems of Single Machine Elements," Engineering Dynamics, Vol. II, pp. 484-496.

19. Chapiro, A., "Radiation Chemistry of Polymeric Systems," Interscience Publishers, N.Y., 1962, p. 19.

20. RAI 308, Final Report, NASr-78, "The Use of Radiation-Induced Plastic Memory to Develop New Space Erectable Structures," pp. 8-11, April 15, 1963.

APPENDIX I - TENSILE TESTS

All tensile tests were performed using a standard table model Instron tester equipped with a Missimers constant temperature chamber, Figure 2. All Tensile tests were run on 1 inch wide samples with a 1 inch grip separation. The strain rates used were 0.2 and 2 in/min for most of the tests. The jaws gripping the sample were pneumatically operated and gave a uniform clamping pressure of 30 psi. In order to measure the electrical surface resistance the plated samples were placed in tensile jaws previously coated with silver oxide. Leads from this surface were connected to an Ohmmeter to give resistance measurements. The set up is given in Figure 3 . In all of the tests very little slippage was observed. Typical stress-strain curves obtained on the biaxially oriented film are shown in the Figure below.

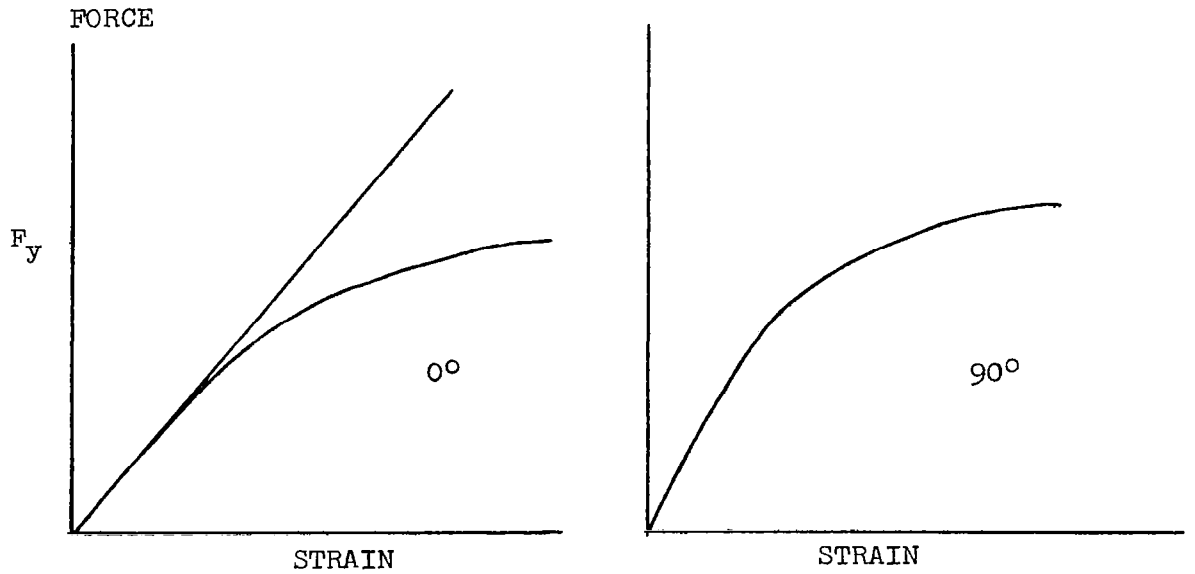

Figure 1 REPRESENTATIVE STRESS-STRAIN CURVES

Figure 2 INSTRON TABLE MODEL TENSILE TESTER
Left: Cross-head and jaw assembly enclosed in Missimers Constant Temperature Oven
Right: Recorder for measurement of stress strain relationship

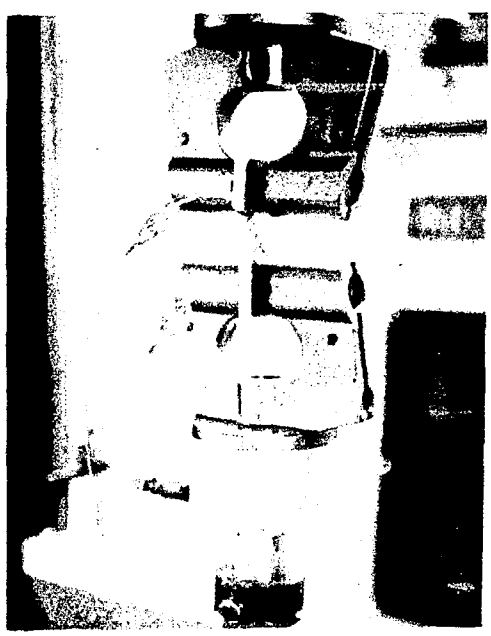

Figure 3 PNEUMATIC JAW DETAIL
Top: Upper Jaw with Silver Oxide Plates for Resistance Tensile measurement
Center: Tensile Sample
Bottom: Lower Jaw

The initial linear slope of the stress-strain curves were taken as the modulus of elasticity

$$E = {}^{F_y}/_{\epsilon_y} \frac{1}{A}$$

where A is the cross-sectional area of the film .

F_y, as shown on the diagram has been taken as the yield force although the actual yield force may be somewhere above this (somewhere between the point where the curve becomes non-linear and where it levels off). The F_y chosen will give a conservative result for design purposes.

APPENDIX II - CRYSTALLINE MELTING POINT (T_m) OF PE 12

The crystalline melting point (T_m) of the Sea Space film was determined in the following three ways:

1. Heating while restrained.
2. Stress relaxation upon increased temperature.
3. Modulus of elasticity changes with temperature.

1. Heating While Restrained

This experiment consisted of restraining 1 mil film with seven 1.8 cm. diameter circles punched in a face-centered hexagonal array, in a steel ring Figures 1 and 2. The restrained sample was then heated slowly from room temperature. As the temperature increased, the circles became elliptical in shape. At 116°C. the elliptical holes became more elongated and began to tear. This temperature, where large deformations begin to occur, is indicative of the T_m (crystalline melting point).

2. Thermal Stress Relaxation

One inch wide samples of Sea Space film were elongated at 75°C. to their yield points on an Instron tensile tester operating at a strain rate of 2 inch/min. The straining was then stopped and heating was begun. The force to keep the film at its constant elongation was then measured as temperature increased. The resulting data points are shown plotted in Figure 3. It can be seen that the force begins to drop to zero at 115°C. This temperature (115°C) is indicative of the crystalline melting point temperature.

3. Modulus of Elasticity Changes With Temperature

The modulus of elasticity, E, of the film was

Figure 1 PERFORATED 0.15 MIL SEA SPACE FILM BEFORE ANNEALING

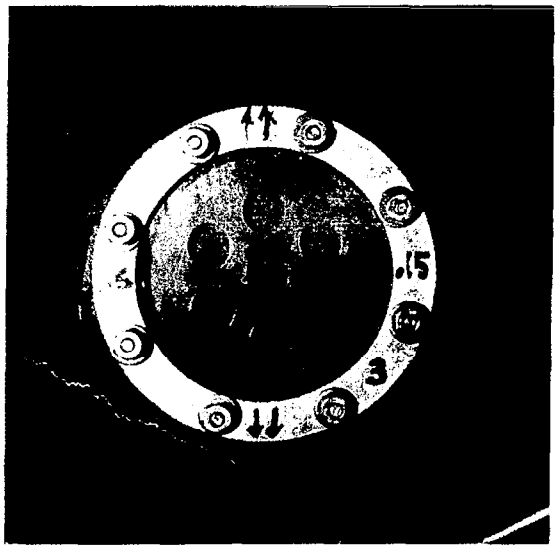

Figure 2 PERFORATED 0.15 MIL SEA SPACE FILM AFTER ANNEALING

Figure 3: THERMAL STRESS RELAXATION TO DETERMINE CRYSTALLINE MELTING POINT OF PE 12

Different symbols indicate different sample runs. Number of runs: 5

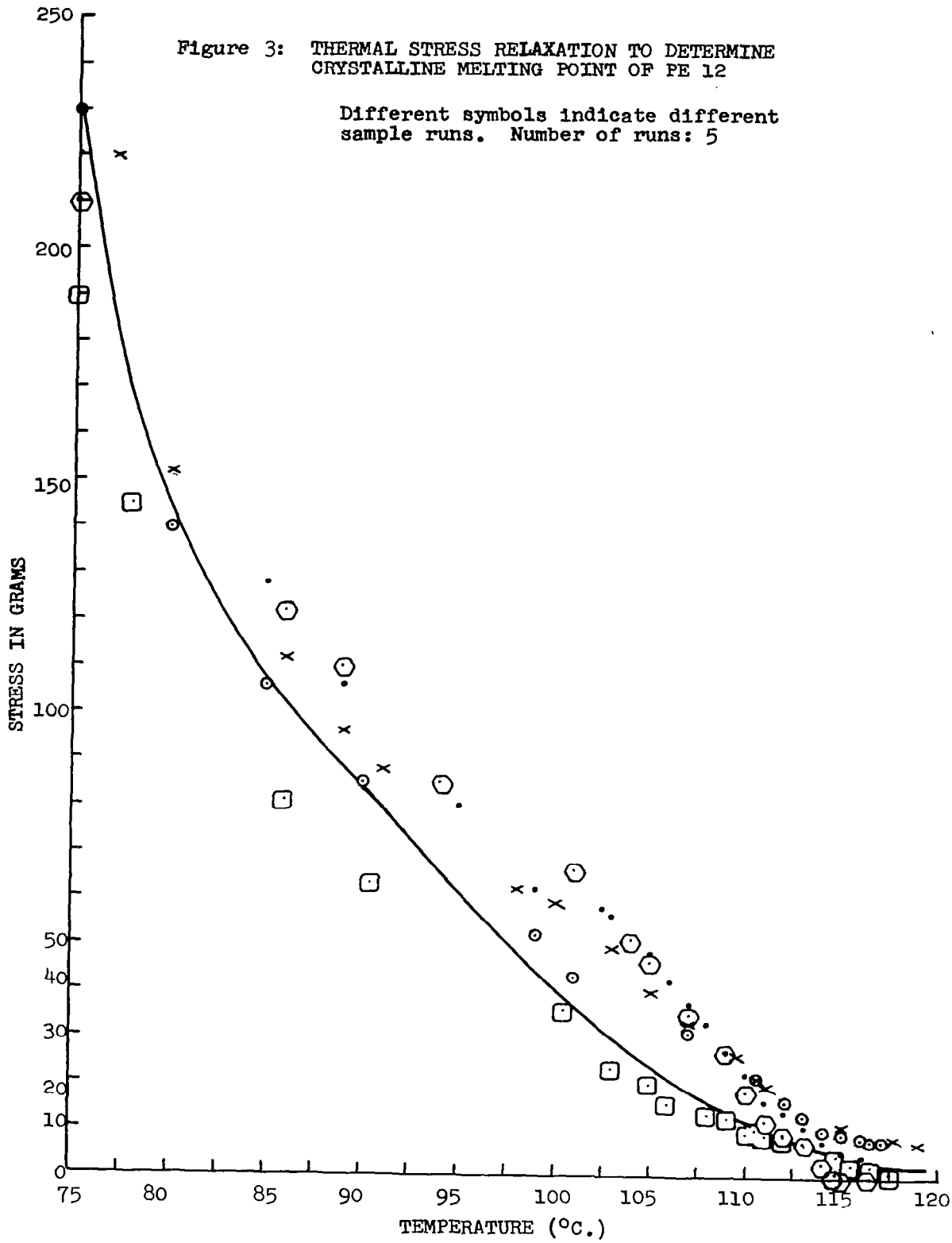

determined from standard tensile tests at temperatures from 28°C. to 116°C. The results are plotted in Figure 4. The temperature where E approaches zero is considered the crystalline melting point, since this is the temperature where the material loses its solid properties and begins to behave as a fluid.

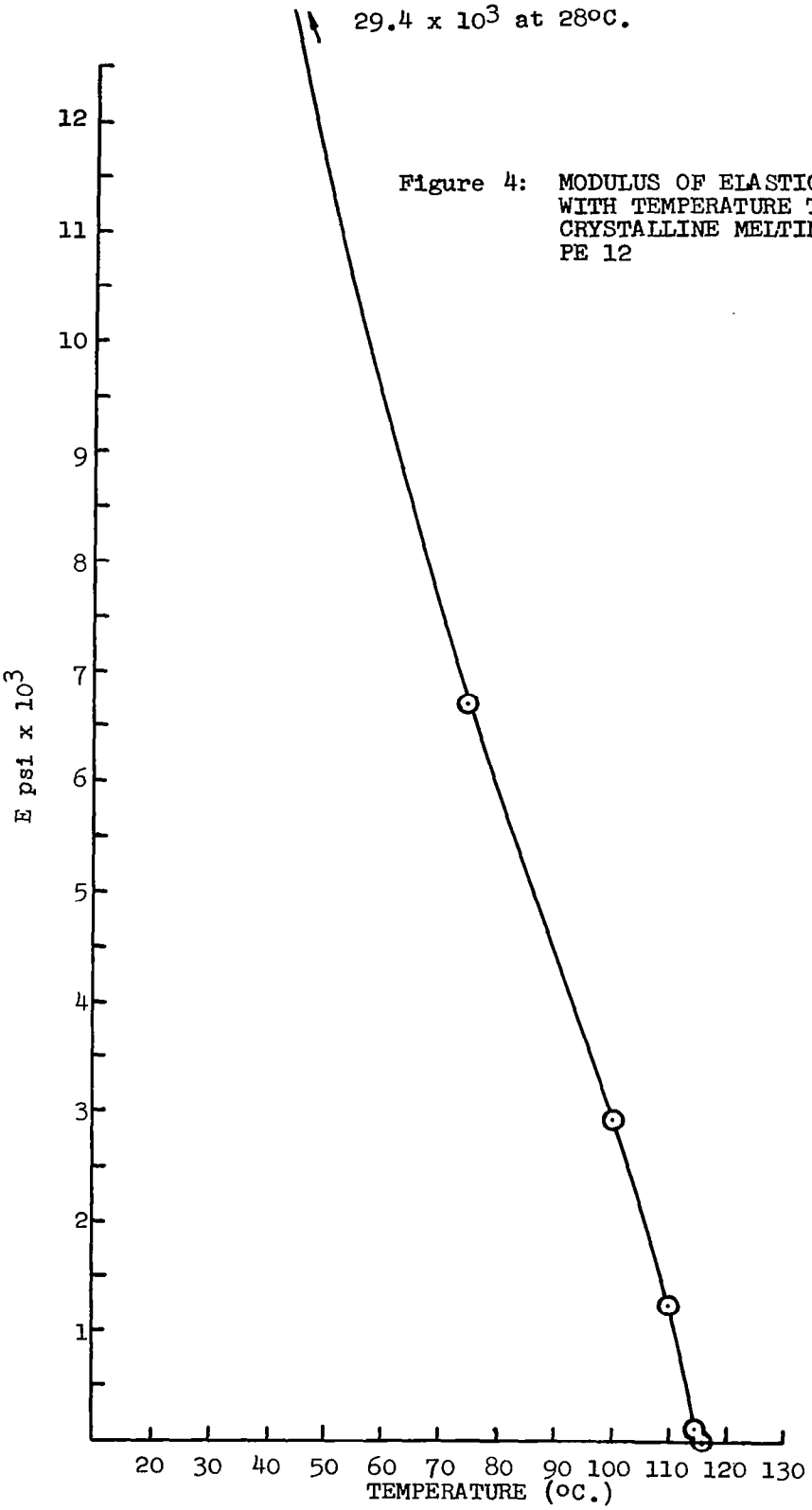

Figure 4: MODULUS OF ELASTICITY CHANGES WITH TEMPERATURE TO DETERMINE CRYSTALLINE MELTING POINT OF PE 12

APPENDIX III - DENSITY GRADIENT COLUMN

The density of PE 12 and the samples in the extraction study were determined using a density gradient column consisting of isopropanol and water operated at 23.3°C. The column, whose dimensions are given in Figure 1, is recommended in an article by G. Oster and M. Yamamoto.[1] Further procedures for constructing, maintaining and operating the density gradient column have been drawn from the ASTM-Standards, "Density of Plastics by the Density Gradient Technique,[2] and the article "Setting up a Density Gradient Laboratory".[3] The density gradient prepared is shown in Figure 2. It is capable of measuring densities between 0.790 gm./cc. and 1.00 gm./cc. at 23.3°C.

Figure 1: DENSITY GRADIENT APPARATUS

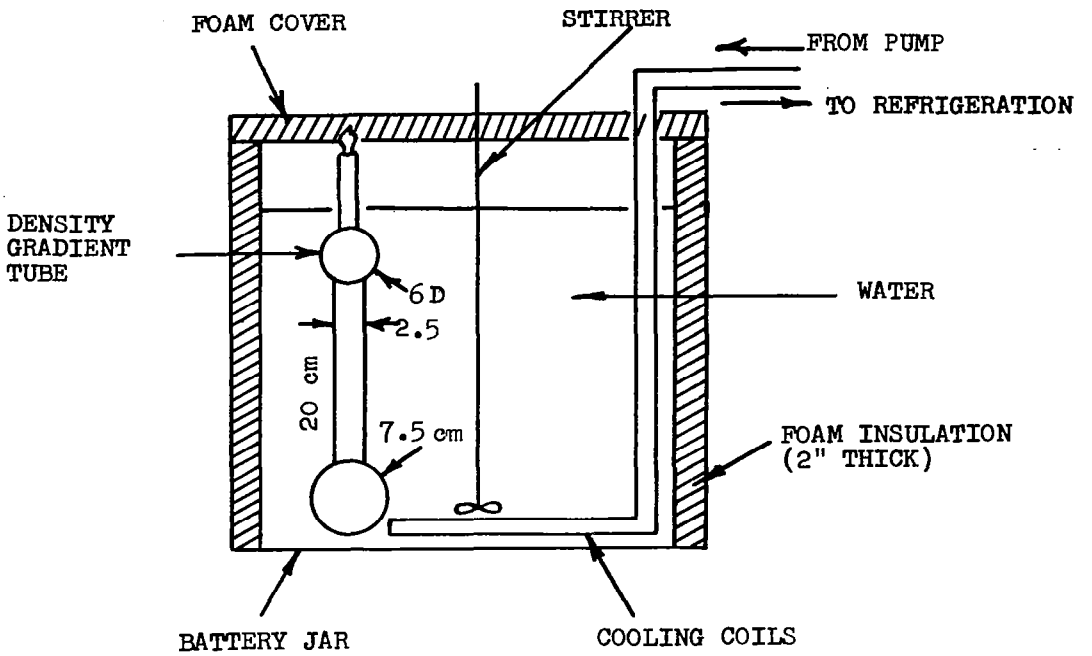

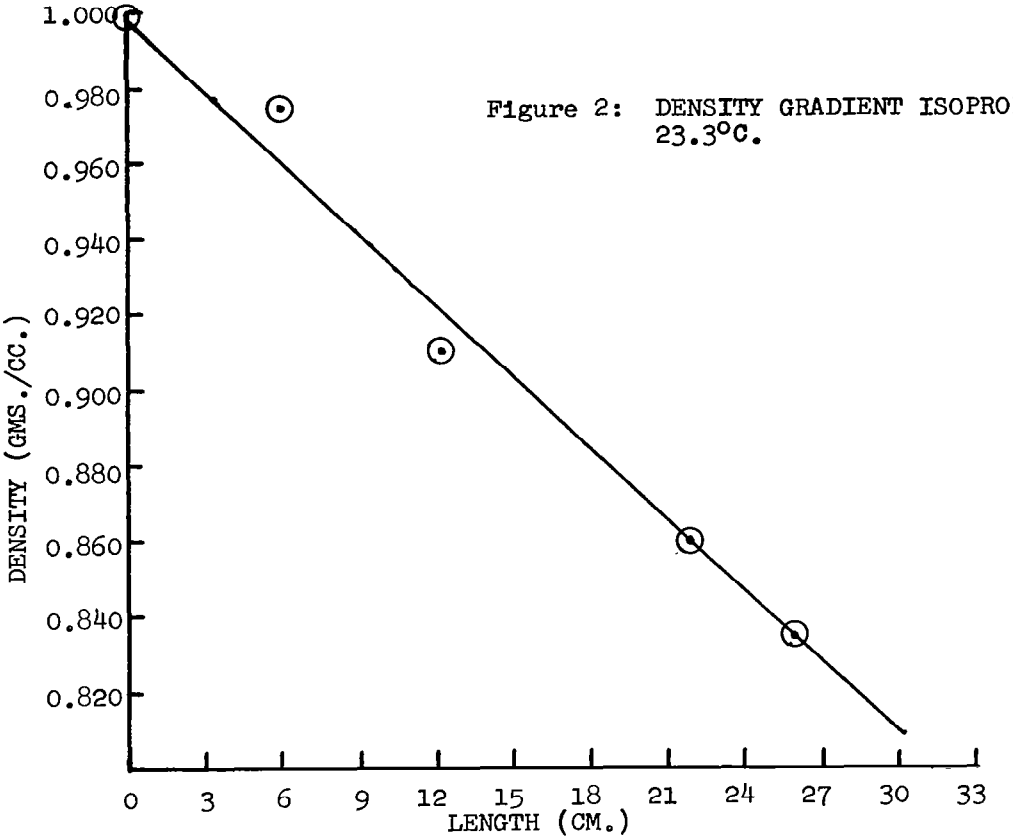

Figure 2: DENSITY GRADIENT ISOPROPANOL-WATER, 23.3°C.

APPENDIX III - References

1. Oster, Gerald, M. Yamamoto, "Density Gradient Techniques," Chemical Review, Vol. 63, #3, pp. 257-268, June 1963.

2. ASTM D 1505-63T, ASTM Standards Plastics-Methods of Testing, Part 27, June 1965, pp. 500-506.

3. Wiley, Richard, E., "Setting up a Density Gradient Laboratory," Plastics Technology, March 1962.

APPENDIX IV - FLEXURAL RIGIDITY TEST

The Flexural Rigidities of all samples measured in this program have been measured by the ASTM D 1388-55T Beam Cantilever Test described as follows:

A 1 inch wide sample is placed on a flat surface and moved out over its edge until the leading edge of the sample falls to an angle of 44.5° with the plane it is slid off. See diagram below:

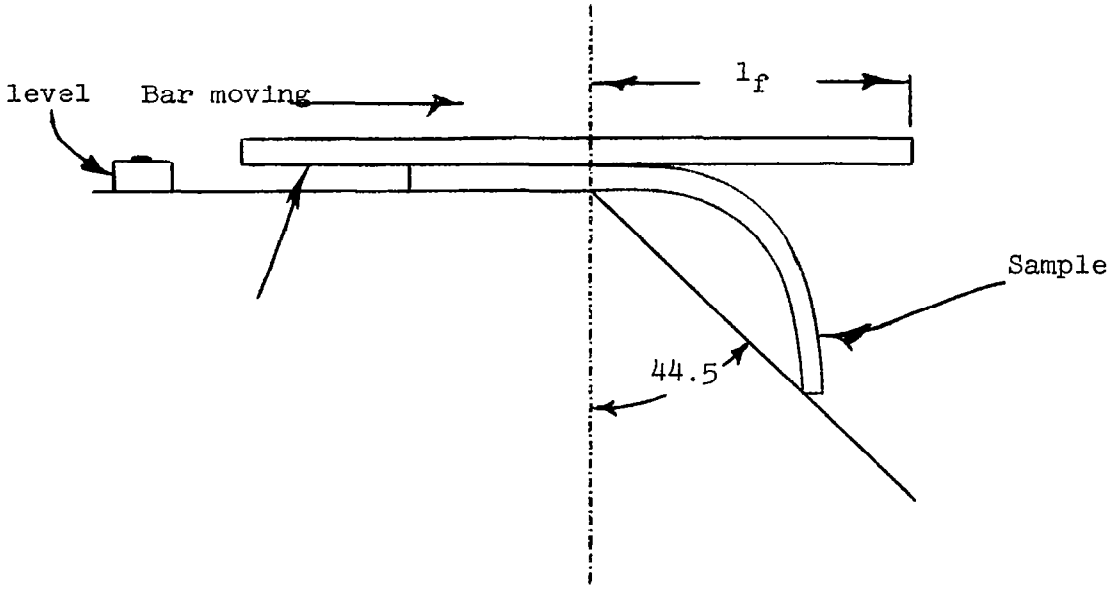

The length of overhang l_f is then read. The test is done, both in the 0 and 90 degree directions, and for each direction it is done four times; on top foward, top back, bottom forward, and bottom back. The flexural rigidity is then measured as follows for each measurement

$$G = W_A \left(\frac{l_f}{2}\right)^3 \qquad (1)$$

An average flexural rigidity is then computed for

each direction (i.e., $\overline{G}_0$, $\overline{G}_{90}$) and the true flexural rigidity is then given as:

$$\hat{G} = \sqrt{\overline{G}_0 \times \overline{G}_{90}} \qquad (2)$$

In running the tests the following precautions were observed:

1. All samples were slid over the edge at a steady, uniform rate.
2. Air currents were kept to a minimum.
3. All samples were brought to ground potential during each test with Static Master 3T125 β source antistatic brushes to eliminate electrostatic forces.

APPENDIX V - ANALYTICAL PROCEDURES FOR PLATING BATHS IN ENTHONE PLATING CYCLE

Plating Bath 5: Analysis for Enplate Conditioner 472

Equipment Required:

1 - 10 ml. graduate

1 - 250 ml. graduate

1 - 1.400 to 1.620 (Specific Gravity) hydrometer

1- 2 ml. pipette

2 - 250 ml. stoppered Erlenmeyer flasks

1 - 50 ml. burette

Solutions Required:

50% HCl (6N)

20% KI (Wt.)

1% Starch solution (Wt.)

0.1N $Na_2S_2O_3$

Procedure:

1. Cool the sample to 75°F.
2. Measure the Specific Gravity of the sample. The Specific Gravity should be 1.590-1.608; if it is lower the solution should be heated and the excess water driven off.
3. Pipette a 2 ml. sample into a 250 ml. flask and dilute with 100 ml. of deionized water.
4. Add 10 ml. of a 20% KI solution.
5. Add 2 ml. of 6N HCl.
6. Stopper the flasks immediately and store in a dark place for 5-10 minutes.
7. Titrate the sample with 0.1N $Na_2S_2O_3$ to a straw color; then add 2 ml. of starch solution and titrate to a clear end point (greenish blue).

Calculation:

$$\frac{\text{ml } 0.1N\ Na_2S_2O_3}{30} \times 100 = \%\ \text{activity of}$$

Conditioner 472.

For each 10% low add 3/4 oz./gal. of Enplate Conditioner 470 Additive.

Plating Bath 7

Analysis of Sensitizer 432 Working Solution

Apparatus Needed:

3 ml. pipette

25 ml. pipette

250 ml. Erlenmeyer Flask

25 ml. graduated cylinder

5 ml. graduated cylinder

Eye dropper

Hot plate

50 ml. burette

Reagents Needed:

EDTA Solution (EDTA Disodium Salt) 0.0575 M

Zinc Solution (Zinc Metal) 0.0575 M

A. R. Hydrochloric acid (HCl)

Ammonium Acetate ($NH_4C_2H_3O_2$) solution 30%

Hydrogen Peroxide (H_2O_2) 30%

Xylenol Orange Indicator Mix (0.1% by weight in sugar) (Fisher-Scientific Xylenol Orange Tetra-sodium Salt)

Procedure:

1. Pipette 3 ml. sample into 250 ml. Erlenmeyer Flask.
2. Add 5 ml. concentrated HCl.
3. Add 5 drops H_2O_2 (30%) of 2.5 ml. H_2O_2 (3%).

4. Heat on hot plate to boiling, remove and allow to cool.

5. Pipette 25 ml. Standard EDTA into cooled solution.

6. While swirling add 25 ml. $NH_4C_2H_3O_2$ solution.

7. Add 1.5 g. indicator mix and dissolve.

8. Titrate with standard 0.0575 M zinc solution. Color changes from yellow to red.

Calculations:

0.55 x (25 -ml. zinc sol.) = % (Vol.) of Enplate Sensitizer 432 in solution.

Replenishment:

Maintain the desired level of sensitizer 432 by adding 38 ml. (1.3 fl. oz.) of concentrate per gallon of solution for each 1% low.

Analytical Procedure for Acidity of Sensitizer 432 Working Solution

Apparatus Needed:

2 ml. pipette

250 ml. Erlenmeyer Flask

Eye-dropper

50 ml. burette

Reagents Needed:

0.1N Sodium Hydroxide (NaOH) solution

Phenolphthalein Indicator

Procedure:

1. Pipette 2 ml. of sample into 250 ml.Erlenmeyer flask.

2. Dilute with approximately 100 ml. distilled water.

3. Add 3 drops of phenolphthalein indicator.

4. Titrate with 0.1N NaOH. Color range is from clear to pink.

Calculations:

0.42 x mls titrated = % (Vol.) Conc. HCl in solution.

Replenishment:

Maintain the desired level of acidity adding:

For each 1% low add 75 ml. (2.2 fl.oz.) of 6N HCl (50% by Vol.) for each gallon of solution.

If necessary, the acidity can be reduced adding for each 1% high, 75 ml. (2.5 fl. oz.) of 6N NaOH (2lb/gal.) for each gallon of solution.

A solution made up using 1 part Sensitizer 432 and 15 parts of water contains approximately an equivalent of 8% (by Vol.) of conc. HCl.

A solution made up using 1 part of Sensitizer 432 and 30 parts of water contains approximately an equivalent of 4% (by Vol.) of conc. HCl.

A solution made up using 1 part of Sensitizer 432, 1 part of conc. HCl and 14 parts of water contains approximately an equivalent of 14% (by Vol.) of HCl.

Plating Bath 9

Analysis of Activator 440 Working Solution - Colorimetric Procedure

Apparatus Needed:

Set of clean dry test tubes (or Nessler tubes)

2 ml. pipette - 0.1 ml. graduations

10 ml. graduate

Procedure:

1. Set up standards ranging from 1% to 10% (Vol.)

by pepetting 0.1 ml. increments of Activator 440 concentrate into the tubes and adding water with the graduate to make 10 ml. of standard. (These standards may be sealed and kept permanently.)

2. Place 10 ml. of filtered sample of Activator 440 working solution into the sample test tube.

3. Obtain concentration versus transmittance curve using colorimeter at set wave length and temperature. (See Figure 1 on page V-6).

Replenishment:

Maintain the desired level of Activator 440 by adding 38 ml. (1.3 fl.oz.) of concnetrate per gallon of solution for each 1% low.

Analytical Procedure for Acidity of Activator 440 Working Solution

Apparatus Needed:

20 ml. pipette

250 ml. Erlenmeyer flask

Eye dropper

Reagents Needed:

0.1N Sodium Hydroxide (NaOH) solution.

Phenolphthalein Indicator

50 ml. burette

Procedure:

1. Pipette 20 ml. of sample of Activator 440 into the Erlenmeyer flask.

2. Dilute with approximately 100 ml. distilled water.

3. Add 2 to 3 drops of phenolphthalein indicator.

4. Titrate with 0.1N NaOH. Color change is from clear to pink.

Calculations:

0.042 x mls. titrated = % of conc. HCl in solution.

Figure 1 ACTIVATOR CONCENTRATION VS. TRANSMITTANCE
at 535 x 10^{-9} cm. and 24°C.
wavelength

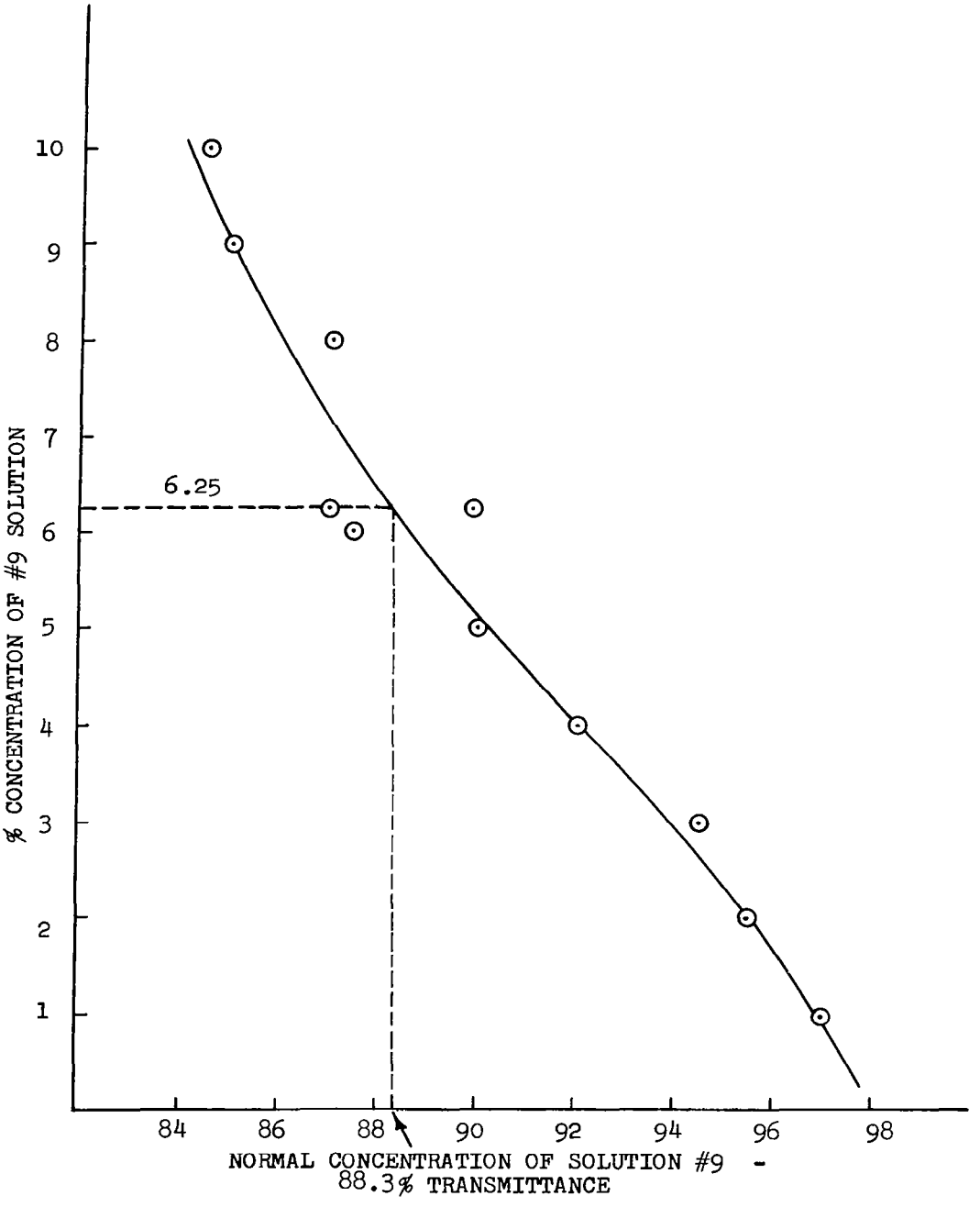

Replenishment:

Maintain the desired level of acidity by adding:

For each 0.1% low, add 7.5 ml. (0.25 fl.oz.) of 6N HCl (50% by Vol.) for each gallon of solution.

For each 0.1% high add 7.5 ml. (0.25 fl.oz.) of 6N NaOH (2 lb./gal.) for each gallon of solution.

A solution made up using 1 part of activator and 15 parts water contains approximately 0.5% (by Vol.) conc. HCl.

A solution made up using 1 part of Activator and 30 parts water contains approximately 0.25% (by Vol.) conc. HCl.

NOTE: The concentration of acid in Activator 440 working solution is always under 1% (by Vol.).

Plating Bath 11

Analysis for Cu-400A Operating Solution

Apparatus Needed:

50 ml. pipette

50 ml. burette

500 ml. Erlenmeyer flask

25 ml. graduated cylinder

Reagents Needed:

Glacial Acetic Acid

Potassium Iodide (KI) reagent grade

Starch solution (10% soluble starch solution)

0.1N Sodium thiosulfate ($Na_2S_2O_3$)

Procedure:

1. Pipette 50 ml. sample into 500 ml. Erlenmeyer flask.

2. Add 100 ml. distilled water.

3. Add 15 ml. glacial acetic acid (Color should change to light blue-green).

4. Add 15 g. KI (about 1 teaspoon), swirl until completely dissolved. (Color changes from light blue-green to dark brown).

   NOTE: It is important to add KI as solid, not as liquid concentrate.

5. Titrate with 0.1N $Na_2S_2O_3$ until color changes from dark brown to light brown or yellow.

6. Add 5 ml. starch indicator solution. (Color will change to dark purple or black).

7. Continue titrating with 0.1N $Na_2S_2O_3$ until color changes to white and remains clear for 1 minute.

   NOTE: With some starch solutions the white may be tinged with a faint pink color which cannot be made to disappear.

8. Record ml. of 0.1N $Na_2S_2O_3$ used.

Calculations:

(0.883)(ml. 0.1N $Na_2S_2O_3$ used) = % (by Vol.)CU-400A present.

Replenishment:

Maintain at desired level of CU-400A by adding 38 ml. (1.3 fl. oz.) of CU-400A per gallon of solution for each 1% low. CU-400B is maintained by adding an equal volume of CU-400B for each volume of CU-400A replenished.

Free Alkalinity Control

The free alkalinity of a 2-5-9 bath should be controlled by the following titration. This test should only be run after proper additions of both CU-400A and B have been made.

Apparatus Needed.

50 ml. pipette

250 ml. Erlenmeyer flask

50 ml burette

Eye dropper

Reagents Needed:

1N sulfuric acid (H_2SO_4) solution.

Phenolphthalein indicator.

Procedure:

1. Pipette 50 ml. sample of CU-400 into a 250 ml. flask.
2. Add 50 ml. deionized water.
3. Add 3-4 drops of phenolphthalein indicator.
4. Titrate with 1N H_2SO_4 until all red color disappears. (Clear blue).

Calculations:

For a bath made-up using 2 parts A, 5 parts B, 9 parts water.

(221-13 x ml. of 1N H_2SO_4 used) = ml. of a 2 lb./gal. (6N) solution of NaOH needed per gallon of made-up CU-400 bath.

(30 ml. = approximately 1 fl. oz.).

APPENDIX VI - CAP SECTION DESIGN CALCULATIONS

The cap section considered has a radius of curvature of R = 212.5 ft. and diameter D = 24 ft.

Maximum Arc Length

From Figure 1 below it can be seen that 1/2 the maximum central angle (Q_{max}) is equal to:

$$Q_{max} = \sin^{-1}\frac{D}{2R} = \sin^{-1}\frac{12.00}{212.50} \qquad (1)$$

$$= 3.237^{\circ}$$

The maximum arc length is then equal to:

$$2(212.50 \text{ ft.})\ (3.237^{\circ})\ (0.017453\ \tfrac{\text{rad}}{\text{deg}}) = 24.01 \text{ ft.}$$

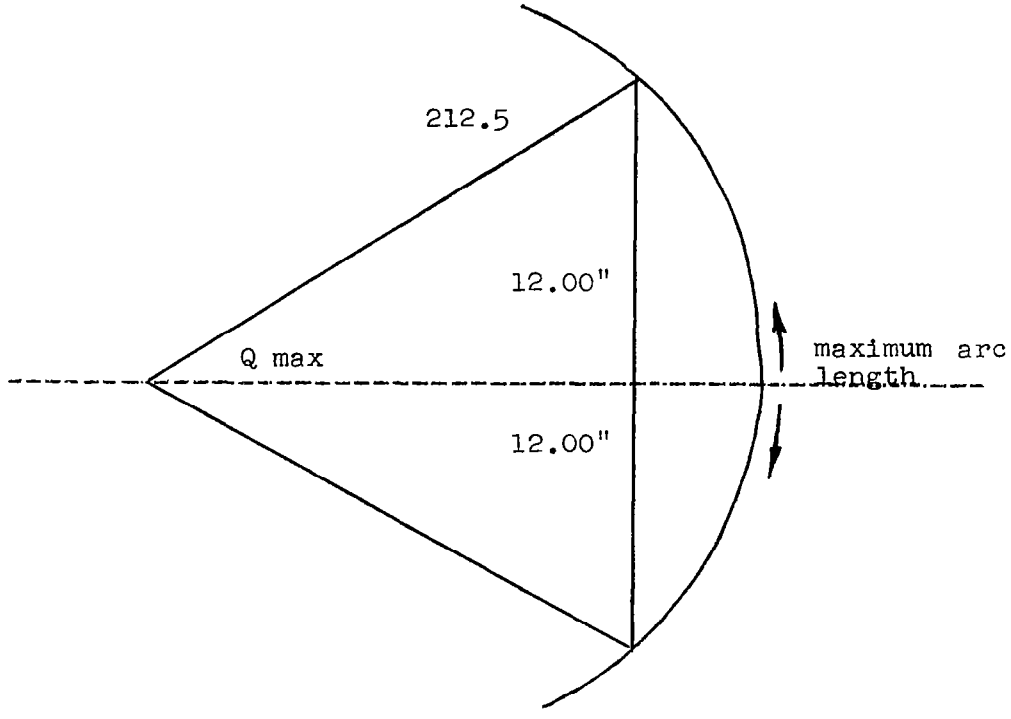

Figure 1: SIDE VIEW OF CAP SECTION

Variations in Gore Width

The maximum variation in the gore width (b) of a gore in the cap section is dependent on the angle Q (see Figure 2) measured from the plane defining the equator of the 212.5 radius sphere. Its dependence can be found as follows:

The length of an arc length b within a gore segment is equal to

$$b = R_1 \theta \qquad (2)$$

with $\theta = \frac{14.5}{212.5\ (12)}$

From right triangle OAC

$$R_1 = R \cos Q \qquad (3)$$

with R = 212.5

Combining equations 2 and 3:

$$b = \frac{14.5}{12} \cos Q \qquad (4)$$

A tabulation of the half gore width ($\frac{1}{2}$b) versus the angle Q from Q=0 at the equator to $Q = Q_{max}$ at the upper boundary is presented in Table 1 . It can be seen from the table that the difference between the maximum gore width at the equator to the minimum gore width near the upper boundary is 0.002 ft., so for all practical purposes the lengths of all the gores can be considered parallel within the cap section. It is for this reason that the flat sections have been used in the construction of the cap section.

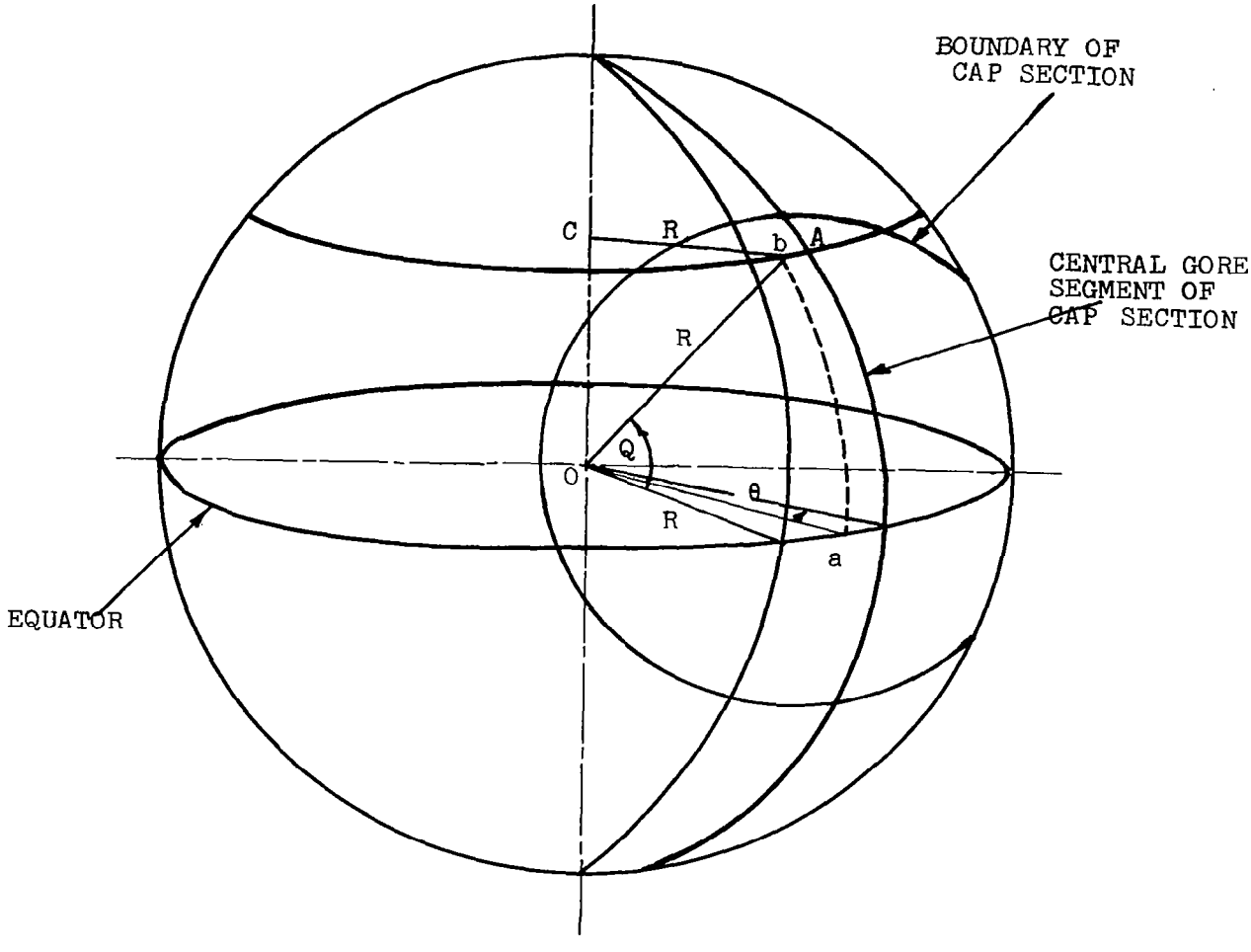

Figure 2 ARC LENGTH WITHIN CAP SECTION

Table 1

Variation of Gore Width with Angle Q in Center of Cap Section

Q (o)	½ Gore Width 0.60416 cos Q (ft.)	½ Gore Height 3.70876 Q (ft.)
0	0.60416	0
0.18	0.60416	0.66757
0.40	0.60415	1.48350
0.60	0.60413	2.22525
0.80	0.60410	2.96700
0.99	0.60407	3.67167
1.08	0.60405	4.00546
1.20	0.60403	4.45051
1.40	0.60398	5.19226
1.62	0.60392	6.00819
1.89	0.60383	7.00956
2.00	0.60377	7.41752
2.20	0.60371	8.15927
2.40	0.60363	8.90102
2.60	0.60354	9.64278
2.80	0.60344	10.38452
2.90	0.60339	10.75540
2.95	0.60336	11.94084
3.00	0.60333	11.12628
3.05	0.60330	11.31177
3.10	0.60327	11.49715
3.15	0.60324	11.68259
3.20	0.60322	11.86803
3.22	0.60321	11.94220
3.23	0.60320	12.0100
3.25	0.60319	12.05347
3.27	0.60318	12.12764
3.29	0.603163	12.20182
3.30	0.603157	12.23890
3.304	0.6031546	12.25374

APPENDIX VII - RESISTANCE DATA ON TEST MODELS

Table 1

Lengths for all Subsegments in Spherical Cap Section

Subsegment*	Actual Maximum Length (in.)	Number
1-3-1	45.88	4
1-3-2	44.10	4
1-3-3	41.42	4
1-3-4	36.83	4
1-3-5	30.44	4
1-3-6	21.97	4
1-3-7	11.19	4
1-2-8	45.48	4
1-2-9	25.59	4
0-1-0	46.00	1
0-6-0	46.00	1
1-1-10**	42.17	4
The remainder are all complete rectangles	49.00	68

* Refer to Figure 1

** The width of these boundary pieces is 6.31 inch.

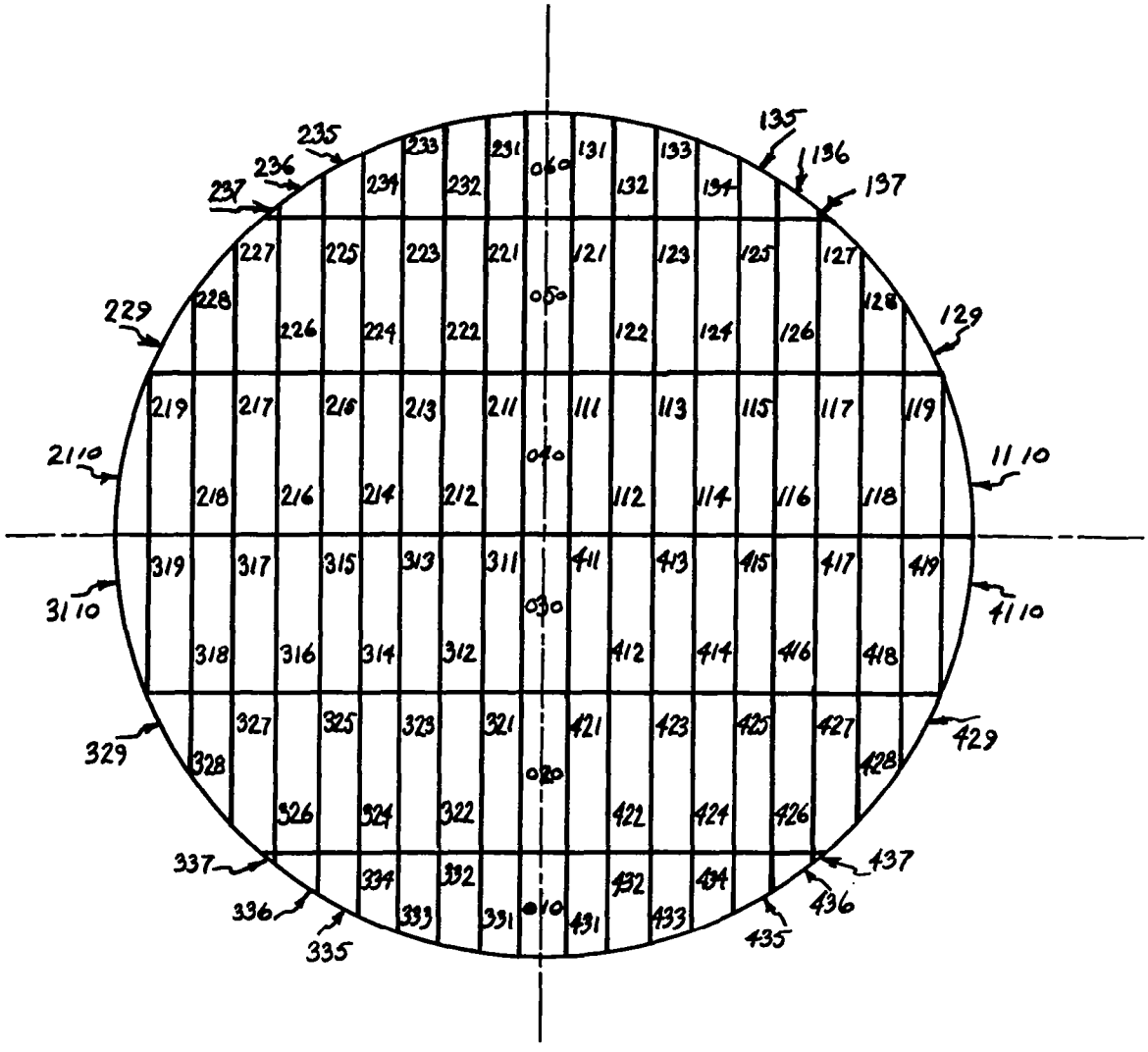

Figure 1

DETAILED ARRANGEMENT OF CAP SECTION SUBSEGMENTS

Table 2

Resistance of Various Subsegments in Spherical Cap Section - Mesh

Subsegment	Resistance (ohms/square)	Subsegment	Resistance (ohms/square)
0-1-0	-	2-2-4	0.18
0-2-0	0.27	2-2-5	0.24
0-3-0	0.24	2-2-6	0.30
0-4-0	0.24	2-2-7	0.30
0-5-0	0.30	2-2-8	-
0-6-0	-	2-2-9	0.96
1-1-1	0.45	2-3-1	-
1-1-2	0.30	2-3-2	0.27
1-1-3	0.63	2-3-3	0.60
1-1-4	0.27	2-3-4	0.20
1-1-5	0.24	2-3-5	0.48
1-1-6	0.30	2-3-6	0.50
1-1-7	0.30	2-3-7	0.90
1-1-8	0.30		
1-1-9	0.27	3-1-1	0.30
1-1-10	0.30	3-1-2	0.24
		3-1-3	0.10
1-2-1	0.30	3-1-4	0.24
1-2-2	0.24	3-1-5	0.30
1-2-3	0.30	3-1-6	0.24
1-2-4	0.2	3-1-7	0.30
1-2-5	0.39	3-1-8	0.30
1-2-6	0.48	3-1-9	0.30
1-2-7	0.30	3-1-10	-
1-2-8	-		
1-2-9	0.8	3-2-1	0.24
		3-2-2	0.24
1-3-1	0.43	3-2-3	0.30
1-3-2	0.30	3-2-4	0.30
1-3-3	0.33	3-2-5	0.18
1-3-4	0.41	3-2-6	0.30
1-3-5	0.24	3-2-7	0.24
1-3-6	0.5	3-2-8	-
1-3-7	0.60	3-2-9	0.60
2-1-1	0.18	3-3-1	0.30
2-1-2	0.30	3-3-2	0.24
2-1-3	0.24	3-3-3	0.30
2-1-4	0.30	3-3-4	0.27
2-1-5	0.30	3-3-5	0.23
2-1-6	0.24	3-3-6	0.31
2-1-7	0.46	3-3-7	0.38
2-1-8	0.18		
2-1-9	0.60	4-1-1	0.24
2-1-10	-	4-1-2	0.30
		4-1-3	0.30
2-2-1	0.20	4-1-4	0.20
2-2-2	0.21	4-1-5	0.61
2-2-3	0.24	4-1-6	0.15

Table 2 (Continued)

Subsegment	Resistance (ohms/square)
4-1-7	0.30
4-1-8	0.60
4-1-9	0.60
4-1-10	-
4-2-1	0.18
4-2-2	0.30
4-2-3	0.24
4-2-4	0.49
4-2-5	0.24
4-2-6	0.48
4-2-7	0.42
4-2-8	0.24
4-2-9	0.23
4-3-1	0.60
4-3-2	0.37
4-3-3	0.60
4-3-4	0.62
4-3-5	0.20
4-3-6	0.30
4-3-7	0.38

Table 3

Resistance of Various Subsegments of Flat Sections - Mesh

Subsegment	Resistance (ohms/square)
1	0.51
2	1.70
3	0.34
4	0.68
5	0.51
6	0.56
7	0.68
8	1.98
9	1.58
10	1.13
11	4.0
12	0.45

Table 4

Resistance of Cylinders - Mesh

Cylinders	Resistance (ohms/square)
1	0.57
2	1.41
3	1.70
4	1.80

Table 5

Resistance of Various Flat Section Subsegments - Film

Flat Section No.	Resistance (Ohms) 0°	90°	Overall (length =6ft)	Overall (width =4 ft)
1 (a)*	1.0	0.66		
(b)	0.8	0.6		
(c)	0.63	0.46		
(d)	1.2	0.9		
(e)	1.0	1.0	no con-	no con-
(f)	1.4	1.4	tinuity	tinuity
(g)	1.4	1.2		
(h)	1.0	0.6		
(i)	1.6	1.4		
2 (a)	1.0	1.0		
(b)	1.8	1.4		
(c)	1.2	0.9		
(d)	1.73	1.6	4.8	4.8
(e)	1.4	0.96		
(f)	1.16	0.83		
(g)	1.8	1.3		
(h)	1.6	1.06		
(i)	1.56	1.1		
3 (a)	1.4	0.8		
(b)	1.03	0.7		
(c)	1.4	1.0		
(d)	1.0	0.7	5.5	3.8
(e)	2.0	1.4		
(f)	1.86	1.4		
(g)	1.9	1.2		
(h)	1.16	0.8		
(i)	2.0	1.6		

Table 5 (Continued)

Flat Section No.	Resistance (Ohms) 0°	90°	Overall (length = 6 ft)	Overall (width =4 ft)
4 (a)	1.46	1.1		
(b)	1.6	1.3		
(c)	1.36	1.2		
(d)	1.33	0.83		
(e)	1.0	0.7	no continuity	no continuity
(f)	1.13	0.93		
(g)	0.57	0.6		
(h)	1.2	0.83		
(i)	1.1	1.0		

* Letters denote various subsegments

Table 6

Resistances of Cylinders - Film

1 ft. length x 7.5 in diameter

Cylinder No.	Resistance of unbonded material for cylinders (Ohms) 0°	90°	
1	1.2	1.4	no continuity
2	1.8	1.0	Silver lacquer*
3	1.8	1.2	Silver lacquer*
4	1.8	1.3	no continuity

* Silver lacquer used.
DuPont Silver prep.
electronic grade 4817
solvent Butyl Acetate

APPENDIX VIII - THERMAL CONTROL PROPERTIES OF METALLIZED FILM

The absorptance over emittance α/ϵ of the metallized film was determined at NASA GSFC. The absorptance measurements were determined by use of a Gier-Dunble Integrating Sphere and a modified Beckmann DK-2A Spectrophotometer. The value of ϵ was determined on a portable Gier-Dunble Emissometer. The results of the tests on three representative completed materials are listed in Table 1.

Table 1

Thermal Surface Properties of Electroless Plated Copper Material*

Material	α	ϵ	α/ϵ
Completed Material	0.47	0.035	13.4
Completed Material (dark in color)	0.55	0.035	15.7
Completed Material (thin coat**)	0.39	0.035	11.1

* All materials tested were unperforated

** Thickness ca. 4×10^{-6} in. Cu